

Cover Page



Universiteit Leiden



The handle <http://hdl.handle.net/1887/30099> holds various files of this Leiden University dissertation.

Author: Moester, Martiene Johanna Catharina

Title: Orchestration of bone remodeling

Issue Date: 2014-12-09

Orchestration of Bone Remodeling

Martiene J. C. Moester

Orchestration of Bone Remodeling

Cover design: Maria Kroon
Cover images: www.ectsoc.org/gallery
www.flickr.com by [wellcomeimages](http://wellcomeimages.commons.wikimedia.org)
commons.wikimedia.org

The research described in this thesis was supported by the Netherlands Enterprise Agency (Rijksdienst voor Ondernemend Nederland; IOP Genomics grant IGE07001A).

Financial support for the printing of this thesis by Greiner Bio-One and NVCB (Nederlandse Vereniging voor Calcium- en Botstofwisseling) is gratefully acknowledged.

Printing: CPI - Koninklijke Wöhrmann
ISBN: 978-94-6203-698-7

© 2014 | M.J.C. Moester

No parts of this thesis may be reproduced, stored in a retrieval system, or transmitted in any form or by any means, electronic or mechanical, without prior permission of the author and the publisher holding the copyright of the articles included in this thesis.

Orchestration of Bone Remodeling

PROEFSCHRIFT

ter verkrijging van
de graad van Doctor aan de Universiteit Leiden,
op gezag van Rector Magnificus prof. mr. C.J.J.M. Stolker,
volgens besluit van het College voor Promoties
te verdedigen op dinsdag 9 december 2014
klokke 13:45 uur

door

Martiene Johanna Catharina Moester
geboren te Leidschendam
in 1983

Promotiecommissie

Promotor: Prof. dr. C. W. G. M. Löwik

Co-promotor: Dr. K. E. de Rooij

Overige leden: Prof. dr. S. E. Papapoulos

Prof. dr. J. Klein-Nulend (ACTA-VU)

Dr. P. A. C. 't Hoen

*Everything will be all right in the end...
if it's not all right then it's not the end.*

Sonny (*Best Exotic Marigold Hotel*, 2011)

Table of contents

Chapter 1	General Introduction	9
Chapter 2	Sclerostin: current knowledge and future perspectives <i>Adapted from: Calcif Tissue Int. 2010 Aug;87(2):99-107</i>	43
Chapter 3	Serum dickkopf 1 levels in sclerostin deficiency <i>J Clin Endocrinol Metab. 2014 Feb;99(2):E252-6</i>	67
Chapter 4	First missense mutation in the <i>SOST</i> gene causing sclerosteosis by loss of sclerostin function <i>Hum Mutat. 2010 Jul;31(7):E1526-43</i>	81
Chapter 5	Regulation of <i>SOST</i> mRNA expression through inhibition of GSK3 β independent of β -catenin	111
Chapter 6	Antisense oligonucleotide-mediated modulation of <i>SOST</i> and <i>Rank</i> expression	125
Chapter 7	Validation of a simple and fast method to quantify <i>in vitro</i> mineralization with fluorescent probes used in molecular imaging of bone <i>Biochem Biophys Res Commun. 2014 Jan 3;443(1):80-5</i>	151
Chapter 8	General discussion	167
	Summary	181
	Nederlandse samenvatting	187
	Curriculum vitae	193



Chapter 1

General Introduction

Bone remodeling

The function of the skeleton is to give structure to the body and provide protection to vital organs such as the heart, lungs and brain. Bones also serve as a reservoir for calcium, phosphorus and magnesium and as an environment for the bone marrow where blood cells are produced. In addition, they provide attachment points for muscles and thereby facilitate movement. While bone appears to be a static tissue, it is actually constantly formed, resorbed and reformed by the different cells in the bone to adapt to changes in metabolic and mechanical requirements. This process is known as remodeling.

There are three main cell types in bone tissue involved in the remodeling of bone: the osteoclasts, osteoblasts and osteocytes (Figure 1). During remodeling, bone is resorbed by osteoclasts. Osteoclasts are large multinucleated cells that are derived from the hematopoietic cell lineage, like monocytes and macrophages. They attach to the mineralized matrix and release protons and proteolytic enzymes, which demineralize and degrade the matrix, into the space between the cell membrane and the bone. After resorption, osteoblasts are recruited to the resorbed surface to form new bone matrix. Osteoblasts originate from mesenchymal stromal cells that also give rise to myoblasts (muscle), fibroblasts (fibrous tissue), chondroblasts (cartilage)

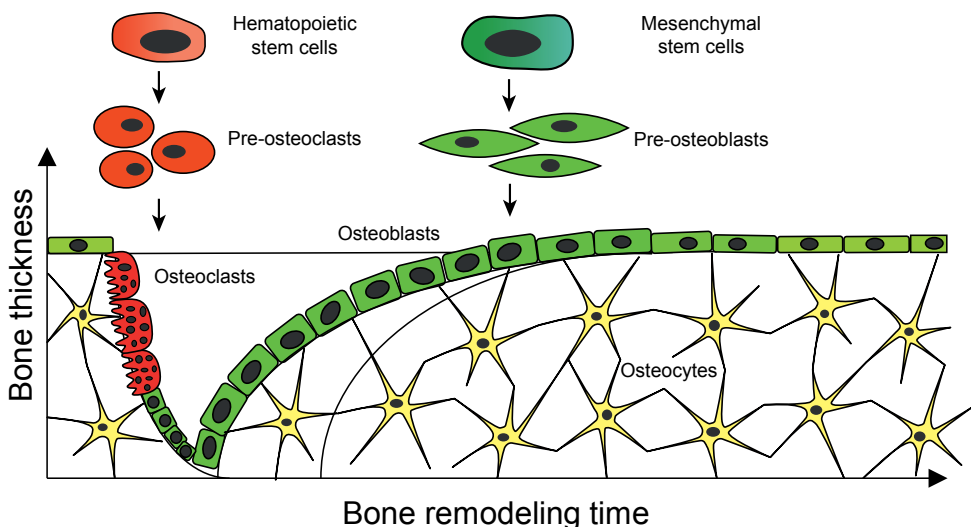


Figure 1. Bone remodeling. Osteoclasts (red) are derived from hematopoietic stem cells and resorb bone. Osteoblasts from the mesenchymal lineage (green) then fill the bone resorption pit with new bone matrix. Some osteoblasts are trapped inside the newly formed matrix and differentiate further into osteocytes (yellow).

and adipocytes (fat). During their differentiation, osteoblasts express different genes in a set order, starting with alkaline phosphatase (ALP). Later the osteoblasts synthesize proteins that form the organic matrix of bone mainly consisting of collagen type I [1]. Osteoblasts are directly involved in the mineralization of bone matrix, secreting vesicles that are rich in calcium, phosphate, alkaline phosphatase and calcium binding molecules. In these vesicles the initial production of hydroxyapatite crystals begins, and when they are released, these crystals support propagation of mineralization on the prepared matrix [2-4].

During bone formation, osteoblasts can become trapped in the matrix and differentiate further into osteocytes. Alternatively, they become quiescent bone lining cells or undergo apoptosis. Osteocytes are the most abundant cell type in bone. They are enclosed in the matrix and communicate with each other and the lining cells on the surface with long cellular processes. Because of this cellular network, osteocytes are implicated as important players in the orchestration of bone remodeling, as they are in a perfect location for sensing mechanical stress on the bone and secrete factors and transfer signals to many other bone cells.

Regulation of bone metabolism

In healthy adults, bone formation and resorption are coupled and balanced so that the total bone mass is maintained. This is tightly regulated by systemic and local factors. Systemic factors such as hormones play an important role in the regulation of bone metabolism. They meet needs of the body for calcium and phosphate by influencing both bone formation and resorption. Factors that are produced locally can affect bone cells independent from systemic hormones. Local factors control changes in metabolism to adapt to the specific requirements of the local environment. In addition, many systemic hormones have been shown to act via the production and/or activation of local factors.

Local factors

Locally produced receptor activator of nuclear factor κ B ligand (RANKL) and macrophage colony stimulating factor (M-CSF) are essential for osteoclast differentiation [5]. M-CSF promotes the survival, proliferation and differentiation of the macrophage lineage. RANKL, a membrane-bound protein produced by

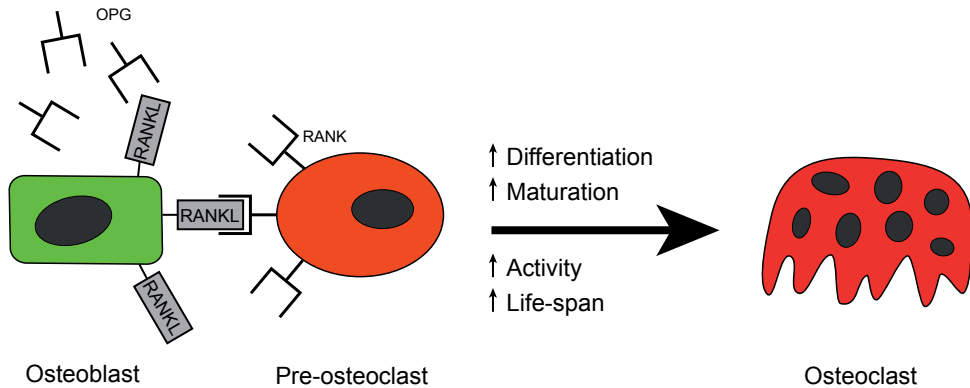


Figure 2. The RANK/RANKL/OPG system. RANKL produced by osteoblasts binds to RANK receptors on the surface of osteoclast precursors, which are then activated to differentiate and mature into osteoclasts. OPG is a protein similar to RANK, but soluble. It competes with RANK for binding to RANKL and therefore inhibits osteoclast differentiation.

osteoblasts, binds to its receptor RANK on osteoclast precursor cells and stimulates the commitment of differentiation to osteoclasts (Figure 2) [6, 7]. Osteoblasts also produce osteoprotegerin (OPG) a soluble protein that acts as a decoy receptor for RANKL and, as the name implies, protects the bone by reducing bone resorption through inhibition of osteoclast formation [8]. The ratio between RANKL and OPG determines the effect on osteoclasts. RANKL is not only essential to osteoclast differentiation and survival, it contributes to activation of mature osteoclast function as well [9]. The importance of the RANK/RANKL/OPG system was demonstrated by the effects of deletion and overexpression of these genes in animal and *in vitro* models [10]. For example, *Rank*^{-/-} as well as *Rankl*^{-/-} mice have a complete absence of osteoclasts with consequent shortened limbs and poorly remodeled structures blocking the marrow cavities [11, 12]. In contrast, *OPG*^{-/-} mice showed a progressive decrease in Bone Mineral Density (BMD) and excessive osteoclast activity [13, 14]. Calcium-regulating hormones such as sex hormones, parathyroid hormone (PTH) and Vitamin D regulate expression of both RANKL and OPG and thereby control osteoclast activity [10, 15].

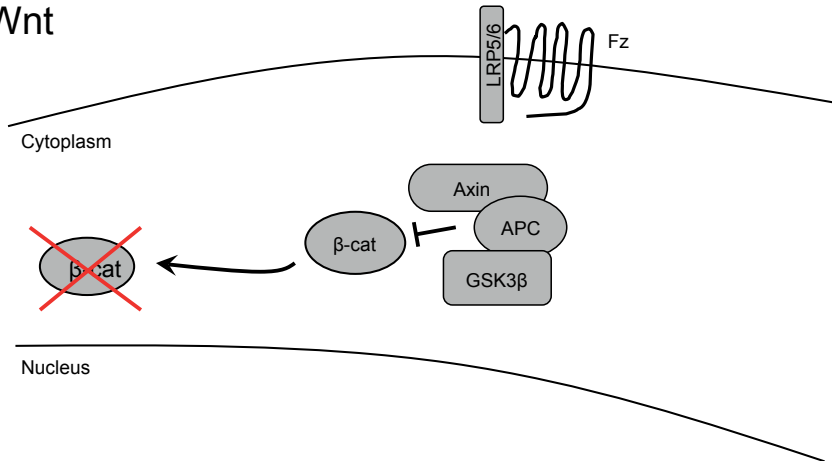
Different cytokines produced by cells of the immune system have an effect on both osteoblasts and osteoclasts, explaining bone effects of inflammation like the bone erosion seen in inflammatory joint disease. Activated T-cells have been shown to promote osteoclastogenesis *in vitro* by upregulation of RANKL [16, 17].

In addition to direct stimulation, T-cells produce many cytokines that stimulate (Tumor Necrosis Factor α (TNF- α), Interleukin (IL) 6 and IL-17) or inhibit (IL-4, IL-13 and IL-10) osteoclast activity and production [18].

Bone morphogenetic proteins (BMPs) were originally identified as proteins capable of induction of ectopic bone formation [19]. BMPs activate the type I and type II receptor complex, leading to initiation of signaling via phosphorylation of intracellular Smad proteins [20]. This can be inhibited by several extracellular inhibitors such as Noggin, Gremlin, Chordin and Cerberus or inhibitory Smads 6 and 7 [21]. BMP signaling has been shown to regulate the differentiation of various cells implicated in cartilage and bone formation during skeletal development and fracture repair [22-24]. Over 20 different BMPs have been identified and of these BMP2, -4, -5, -6 and -7 have been shown to induce osteoblast differentiation. In addition, BMP signaling in bone is closely linked to Wnt signaling, and many reports have shown interactions between these two pathways [25-32].

WNTs are a family of secreted proteins that regulate many developmental processes, for example body axis formation, chondrogenesis and limb development [33, 34] and have an important role in the regulation of osteoblast differentiation [35]. In the absence of Wnt activation, β -catenin is phosphorylated by glycogen synthase kinase 3 beta (GSK3 β) in a complex with axin and adenomatous polyposis coli (APC) and is subsequently degraded. When WNTs bind to the Frizzled receptor and Low-density lipoprotein receptor-related protein 5/6 (LRP5/6) co-receptor, axin is recruited to the membrane. This leads to the disruption of the destruction complex and subsequent inhibition of β -catenin phosphorylation by GSK3 β . Consequently, β -catenin accumulates in the cytoplasm, translocates to the nucleus and activates the transcription of the Wnt target genes with the TCF/LEF transcription factors (Figure 3) [36, 37]. Specific deletion of β -catenin in osteocytes *in vivo* gave rise to dramatically reduced cortical bone thickness and almost absent cancellous bone, indicating the important role of Wnt/ β -catenin signaling in bone formation [38]. Dickkopf-1 (DKK1) and sclerostin inhibit Wnt signaling by binding to the LRP5/6 co-receptor and thereby preventing the interaction with WNTs and the Frizzled receptor [39, 40]. Animal models have emphasized the importance of these Wnt inhibitors in regulation of bone formation. Knockout animals of both *Dkk1* and *Sost* (the gene for sclerostin) display severe gain of bone mass [41, 42], while overexpression

In the absence of Wnt



In the presence of Wnt

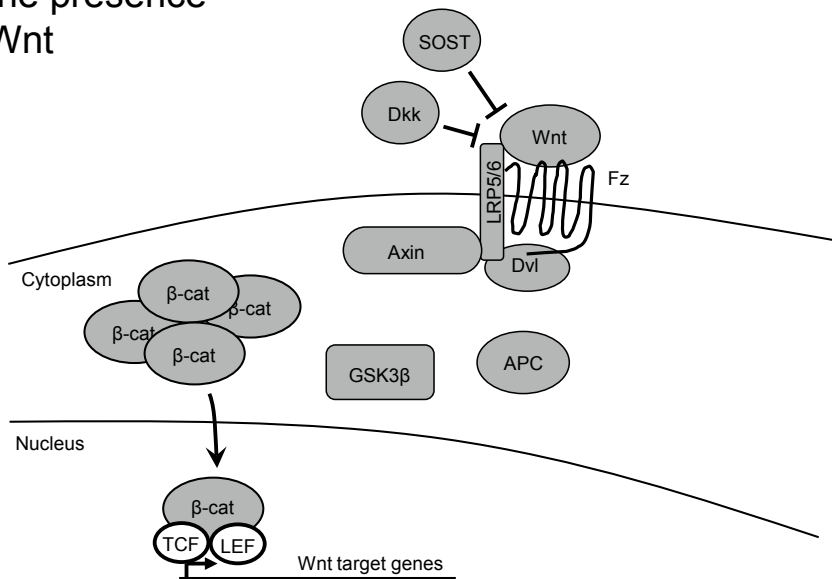


Figure 3. Wnt signaling pathway. In the absence of Wnt, GSK3 β forms a complex with axin and APC to phosphorylate β -catenin, which is subsequently degraded. When Wnts are present, they bind to the Frizzled (Fz) receptor and LRP5/6 co-receptor. Axin is recruited to the membrane and the destruction complex is disrupted. β -catenin is no longer degraded and accumulates in the cytoplasm. It then translocates to the nucleus where it activates transcription of the Wnt target genes by binding to TCF/LEF transcription factors.

models showed very low bone mass [43, 44]. In humans, mutations have been found in different components of the Wnt signaling pathway. Inactivating mutations of LRP5 result in low bone mass and visual impairment (osteoporosis-pseudoglioma syndrome), while a mutation that prevents binding of the Wnt inhibitors sclerostin and DKK1 results in activation of Wnt signaling and a high bone mass phenotype [45-48]. Mutations in sclerostin or the surrounding regulatory region lead to bone overgrowth as seen in sclerosteosis and Van Buchem disease [49, 50].

Finally, bone is remodeled in response to mechanical stimuli to adapt to local loading conditions. Bone mass is lost with disuse *e.g.* in bedrest or microgravity, and gained with increasing levels of activity [51-54]. Osteocytes are thought to regulate this process by altering the production of signaling molecules after mechanical stimulation. The importance of osteocytes was demonstrated by Tatsumi *et al.* [55] who showed that loss of bone mass after hind limb unloading of mice was prevented when the majority (~80%) of osteocytes was ablated. Precisely how osteocytes sense mechanical stimuli is unknown. The current consensus is that mechanical loading induces fluid movements and shear stress in the canaliculi that surround the osteocyte processes, and this leads to changes in cytoskeleton conformation or activates stretch-activated ion channels [56].

The signaling pathways that act in osteocytes upon loading have been thoroughly investigated. Wnt/ β -catenin signaling appears to play an important role as β -catenin activation is increased and *SOST* expression is decreased in bone by mechanical stimulation [57-59]. In addition, deletion of the Wnt co-receptor LRP5 reduced, while a gain-of-function mutation of LRP5 increased the response to mechanical stimulation [60, 61]. Similarly, sclerostin knockout mice are insensitive to unloading-induced bone loss [62]. PTH enhances the effect of mechanical loading, evidenced by a synergistically increased cortical bone volume in adult female mice when loading was combined with intermittent PTH(1-34) [63]. As described below, PTH may also function through modulation of sclerostin expression.

Importantly, a Wnt/LRP5 independent mechanism involving the estrogen receptor α (ER α) has also been observed [64]. The ER α was shown to be important for the response to *in vivo* loading in a study comparing expression of genes in wildtype and ER α knockout mouse bones after loading [65]. In this study, 642 genes were differentially transcribed in the tibiae of wildtype mice 3 hours after loading, while

the expression of only 26 genes was altered in the tibiae of the ER α knockout mice. The ER α was proposed to act together with the insulin growth factor-1 receptor (IGF-1R) to activate protein kinase B (PKB or AKT), which inhibits GSK3 β and causes accumulation of β -catenin [66, 67].

Systemic factors

Parathyroid hormone (PTH) is produced in the parathyroid in response to low serum calcium concentrations sensed by calcium sensing receptors. It increases the reabsorption of calcium in the distal tubules in the kidney and increases production of active vitamin D leading to increased absorption of calcium in the intestine [68]. Interestingly, PTH can have both catabolic and anabolic actions on bone depending on dosage and frequency of administration. Continuous high levels of PTH in the body stimulate the PTH receptors on osteoblasts, leading to increased expression of RANKL and reduced expression of OPG [69-71]. The change in the RANKL/OPG ratio in favor of RANKL leads to increased osteoclast differentiation and bone resorption. As a result, hyperparathyroidism is a cause of secondary osteoporosis [72]. In contrast, when PTH is administered intermittently, it inhibits osteoblast apoptosis extending their matrix-synthesizing function [73]. In addition, expression of *SOST* is decreased [74-76] and this response is blunted in mice lacking the co-receptor LRP5 and in *Sost* overexpressing or deficient mice [77] suggesting an important role for sclerostin in the effect of PTH.

Loss of estrogen has long been implicated as the causative factor for the accelerated bone loss in women after menopause [78]. In women, circulating sclerostin levels are influenced by estrogen [79, 80] and estrogen has been shown to downregulate sclerostin expression in osteocyte-like cells *in vitro* [81]. The fundamental effects of estrogen on bone are to decrease bone turnover by inhibiting the initiation of remodeling and inhibit differentiation and promote apoptosis of osteoclasts. In addition, estrogen promotes osteoblast precursor commitment and differentiation and prevents osteoblast apoptosis. With estrogen withdrawal, this leads to an increase in bone remodeling and a disbalance between formation and resorption [82, 83].

Calcium is required for many functions in the body, including neuromuscular activity, membrane function, hormone secretion, enzyme activity, coagulation of

the blood and skeletal mineralization [84]. It is therefore not surprising that calcium concentrations in the blood are tightly controlled. Bone serves as a calcium store from which minerals can be drawn to maintain calcium levels when calcium intake is not sufficient to compensate for losses in urine and digestive juices [85]. Recommended daily doses differ between experts and countries, leading to wide-ranging results from 15% up to 90% of women that do not meet recommended calcium intake [86, 87]. As calcium uptake in the gut as well as food intake decrease with age, calcium supplementation in combination with vitamin D is recommended for postmenopausal women and elderly men at risk for osteoporosis [88, 89]. Vitamin D is produced in the skin upon exposure to sunlight, which also accounts for shortage in the elderly and less mobile population. It increases calcium uptake in the intestine and also directly stimulates mineralization of bone matrix [90]. In addition, due to its important role in muscle function vitamin D deficiency leads to a higher risk of falling [91, 92].

A relatively new concept was presented by Gerard Karsenty and colleagues in 2008 [93]. They proposed a model in which LRP5 has no direct role in bone metabolism but regulates the production of serotonin in the duodenum, and circulating serotonin inhibits bone formation. This model is actively debated as the significance of LRP5 and Wnt signaling in bone cells has been investigated in detail using (cell specific) knockout models [38, 94-100]. Cui *et al.* [101] could not replicate the results presented by Yadav *et al.* and found no relation between serotonin and bone mass. This discrepancy may be explained by differences in the mouse models that were used. At this point a definitive answer has not been found, and further research may establish whether both models can be integrated.

Osteoporosis

Disregulation of the balance between bone formation and resorption leads to an increase or reduction in bone mass, and subsequent diseases such as osteoporosis. Osteoporosis is the most common skeletal disease and is characterized by low bone mass and the loss of connectivity in the trabecular bone. This leads to decreased bone strength and increased risk of fracture, particularly in the spine, hip and wrist [102]. Osteoporosis is defined on the basis of bone mineral density (BMD) assessment of the femoral neck with dual-energy X-ray absorptiometry (DEXA). According to the

World Health Organisation criteria, osteoporosis is defined as a BMD of 2.5 standard deviations or more below the average value for young healthy women (a T-score of < -2.5 SD) [103, 104]. There are several factors that can lead to osteoporosis: low peak bone mass, accelerated bone loss, impaired bone formation during remodeling, and secondary causes like glucocorticoid use and genetic, inflammatory or nutritional disorders [105]. Peak bone mass is largely determined by genetic background, as evidenced by the large number of genetic loci associated with BMD [106, 107], but can also be influenced by lifestyle [108, 109]. Bone loss due to increased resorption is accelerated after menopause due to the loss of estrogen production and this is the main cause for development of osteoporosis in large groups of elderly females [78]. Changes in bone formation rate are inherent to ageing and may begin shortly after reaching peak bone mass [110]. The lower formation rate is probably due to changes in growth factor production and an increase in reactive oxygen species, but the precise mechanisms are unclear. In addition, inadequate calcium intake or vitamin D production decreases the bone formation rate [90].

An estimated 75 million people in Europe, the United States and Japan have osteoporosis. The disease mostly becomes apparent at a later age so due to increases in life expectancy and changing demographics this number is expected to increase worldwide, and especially in developing countries [111, 112]. In the United States, the incidence of osteoporotic fractures is higher than 1.5 million per year [113] and costs related to these fractures were estimated at 17 billion US dollars [114]. Osteoporosis mainly affects females, with only 30% of fractures occurring in males [114]. The lifetime risk for a wrist, hip, or vertebral fracture in women in the US is estimated to be 30-40% [104].

Osteoporotic fractures are most common in the hip, wrist and vertebral bones. Vertebral fractures often occur unnoticed but cause pain, deformity and long-term debility [102]. Many individuals will not regain mobility and independence after a fracture, and approximately 20% of patients will require long-term care [111, 115]. Hip fractures are known to have a high morbidity and mortality, and 5-25% of patients die within 1 year of the fracture event [102, 115, 116].

Treatment of osteoporosis

There are several established pharmacological approaches for treatment of

osteoporosis, as well as new therapies that have just been approved or are in advanced stages of clinical trials. Bisphosphonates are considered a first-line treatment for osteoporosis, and this is the most common drug class for this purpose [117]. These compounds bind strongly to hydroxyapatite in bone and have two side chains; one that participates in binding of the drug to bone and one that determines the potency and biological properties [118, 119]. During bone resorption bisphosphonates that were bound to the bone are taken up by osteoclasts and inhibit their action. Depending on the side chain the bisphosphonates have a direct toxic effect or disturb the osteoclast cytoskeleton [120, 121]. Because of their high affinity to bone, bisphosphonates are quickly bound and gradually released. They have a long half-life and can be found in plasma and urine for months or even years after the last dose [122, 123]. Most bisphosphonates are administered orally with daily or weekly dosing schedules. Oral formulations are poorly absorbed and adversely affected if taken with food or drinks. In addition they often lead to side effects like esophageal and gastric irritation [111, 117].

Bisphosphonate treatment results in decreased resorption which, through coupling mechanisms, also leads to decreased formation. The overall balance however is positive because of several reasons: 1) bone loss due to reduced bone formation is slowed in a state of decreased remodeling, 2) Slower turnover allows more time for remodeling units to finish the process of bone formation and mineralization before the site is remodeled again, 3) bone formation itself is not affected, only as a result of decreased resorption. Resorption pits that have already been formed will first be filled, leading to a transient netto increase in bone formation. 4) a decrease in resorption depth at individual remodeling sites is not matched by a decrease in local formation, and formation exceeds resorption at that location [119].

As loss of estrogen production is implicated as an important causative factor in development of osteoporosis, it seems logical to use estrogen or estrogen receptor modulators as a therapy. Indeed, hormone replacement therapy and the estrogen receptor agonist/antagonist raloxifen decreased fracture risk at both vertebral and non-vertebral sites. However, the Women's Health Initiative reported increased risk of myocardial infarction, stroke, breast cancer and deep vein thrombosis after use of these drugs. Even though a protective effect was found on endometrial cancer, these therapies are not recommended for long periods of time [124, 125].

The bioactive *N*-terminal 34-amino acid fragment of PTH (rhPTH 1-34, teriparatide) is the only bone anabolic drug currently on the market. As described above, intermittent doses of PTH stimulate osteoblast function and therefore lead to increased bone formation. The intermittent nature of administration seems to limit the effects of PTH on RANKL expression and bone resorption [126]. rhPTH affects trabecular bone more than cortical bone and therefore reduces the fracture risk of the spine much greater than that of nonvertebral bones [127]. However, it can only be used for a maximum of 2 years as after that, bone resorption catches up with formation and the drug is no longer effective. In addition, teriparatide is administered in daily subcutaneous injections and is therefore reserved for severe osteoporosis [126].

Recently, a human monoclonal antibody against RANKL (denosumab, Amgen) was approved for treatment of osteoporosis and bone destruction by bone metastases or rheumatoid arthritis [128]. Binding to RANKL, denosumab inhibits the formation, function and survival of osteoclasts and thereby inhibits bone resorption. Preclinical studies comparing denosumab to the bisphosphonate alendronate in ovariectomized mice showed that denosumab was more effective in preserving trabecular architecture and cortical thickness [129]. Clinical trials revealed marked reduction of bone turnover markers and a BMD gain at all measured sites after 1 year of treatment and a reduction in fracture risk after 3 years similar to that of the most common bisphosphonates [130]. Few specific side-effects have been reported even though RANK/RANKL also has functions in the immune system and vascular system [131]. Other than bisphosphonates, which are usually prescribed in daily or weekly tablets, denosumab is administered every 6 months by subcutaneous injections and is therefore less sensitive to adherence problems.

Neutralizing antibodies against sclerostin have been developed and are currently in phase III clinical trials (AMG 785, NCT01575834 and NCT01631214 on www.clinicaltrials.gov). Due to the restricted expression pattern of sclerostin and the good quality bone and absence of extra-skeletal complications in patients with sclerostin deficiency, sclerostin is considered a good target for bone anabolic therapy [126, 132]. Preclinical studies showed great promise increasing bone mass and strength in animal models of ovariectomized and aging animals as well as in secondary causes of osteoporosis [133-137]. In a phase I randomized double-blind

placebo-controlled study in healthy volunteers substantial and dose-dependent increases in bone formation markers and reduction of bone resorption markers were found [138]. Results from the phase II clinical trial have recently been published and reported significant increases in lumbar spine BMD at 12 months compared to placebo and, importantly, compared to the other active drugs teriparatide and alendronate [139].

Compliance is a major issue in all osteoporosis treatments. Up to 75% of patients have been reported non-compliant, and this significantly decreased therapy effectiveness [140, 141]. Determinants of compliance appear to be concerns about adverse side effects, belief in the need for medication, the relationship with the prescribing physician, administration requirements, dosing schedules and follow-up or feedback on effectiveness [142, 143].

In addition to pharmacological therapies, patients are advised to stop smoking to increase overall health, and regularly exercise to increase mechanical loading on the bones and improve muscle strength, posture and balance. This will help reduce the risk of falling and consequently fractures. Supplementation of calcium and vitamin D is also advised to achieve adequate serum levels to maintain the skeletal homeostasis [125].

Antisense oligonucleotides

Antisense oligonucleotides (AONs) are small (usually 13-25 nucleotides) RNA or DNA molecules that hybridize to a target sequence on the messenger RNA (mRNA) or pre-mRNA. AONs are well-known for their ability to induce RNase H cleavage of the target RNA [144]. RNase H is a ubiquitous enzyme that hydrolyzes the RNA strand of an RNA:DNA duplex. This method has been used to knock down gene expression in both experimental and clinical applications [145-148]. A 5-bp stretch of homology appears to be sufficient to induce RNase H activity, and is therefore sensitive to off-target effects in longer AONs [149-151]. The only AON-based therapy currently approved is fomivirsen (Isis Pharmaceuticals), an RNase H-inducing AON for treatment of cytomegaloviral-induced retinitis [152]. In addition, mipomersen (Genzyme) reduces APOB100 in familial hypercholesterolaemia and is under review by the European and American authorities, but there are significant side effects [153]. Custirsen (OncogeneX) inhibits clusterin, an anti-apoptotic chaperone protein

in cancer cells and is currently in phase III clinical trials [154].

While RNase H cleavage and knockdown of genes was already a known effect of AONs in the 1980s, certain classes of AONs can have non-RNase H mediated effects as well. For example, modulation of pre-mRNA splicing using 2'-O-methyl AONs was pioneered by Ryszard Kole in the 1990s [155]. His goal was to block a mutation that introduced a 'cryptic' splice site in the β -globin (HBB) and cystic fibrosis transmembrane conductance regulator (CFTR) genes and thereby restore normal splicing in patients with β -thalassemia and cystic fibrosis [155-157]. Splicing is a process in which non-coding regions (introns) are removed from the pre-mRNA to generate the messenger RNA (mRNA) with the coding regions (exons) before an RNA transcript can be translated into protein (Figure 4) [158]. Depending on for example developmental state, type of tissue or activation of cells, different (parts of) exons can be included or excluded, producing different proteins from the same gene (alternative splicing) [159, 160]. This process is controlled by sequence motifs in introns and exons that are recognized by splicing factors and can be modulated by blocking these motifs with antisense oligonucleotides (AONs).

Since this was first discovered, knowledge on the application of AONs to

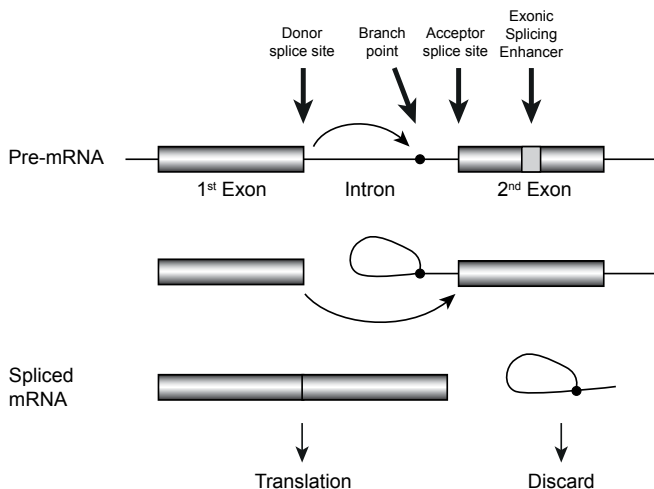


Figure 4. The process of splicing. The pre-mRNA consists of exons and introns. The end of an exon is called the donor splice site, and the beginning the acceptor splice site. A branch point sequence is located inside the intron. During splicing the branch point reacts with the donor splice site, splicing off the intron. Secondly, the donor splice site binds to the acceptor splice site and the intron is discarded. Exonic splicing enhancers (ESEs) are exon-internal sequences where proteins can bind to induce or facilitate splicing.

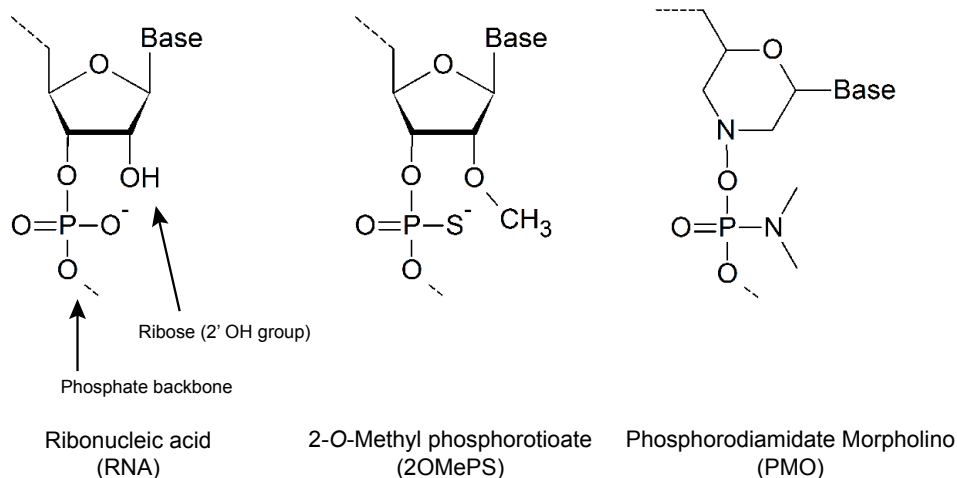


Figure 5. Frequently used AON modifications. Unmodified AONs are quickly degraded by nucleases in biological fluids. To decrease nuclease action different modifications have been developed. The 2'-O-Methyl phosphorothioate modification consists of a methyl group at the 2'-O location of the ribose, and a oxygen to sulphur substitution in the phosphate backbone. Phosphoroamidate morpholino's consist of a backbone without ribose, making them resistant to nucleases.

modulate splicing of different genes for different diseases has quickly expanded. Depending on the target, exon skipping has now also been shown to induce isoform switching, secretion of a membrane-bound protein by skipping of the membrane anchor or inactivation of a protein by removal of the active domain or disruption of the reading frame (reviewed in [161] and [148]). In addition, another class of AONs can arrest translation by steric hindrance of the ribosomal complex and consequently inhibit expression of a protein [162].

Unmodified AONs are rapidly degraded by intracellular endonucleases and exonucleases and have a short half-life [163]. Therefore, several backbone modifications have been designed to increase stability and specificity (Figure 5). The most widely used modifications for non-RNase H mediated approaches are 1) the 2'-O-methyl RNA phosphorothioate (2OMePS) backbone, in which a methyl group is added to the 2'-O position in the ribose and one of the nonbridging oxygens is replaced by sulfur in the phosphate backbone of the oligonucleotide chain [144, 164] and 2) the phosphorodiamidate morpholino oligomers (PMOs), containing a morpholine ring and a nitrogen-based backbone [161, 165]. Phosphorothioate AONs are resistant to nucleases, easily synthesized and capable of inducing RNase H activity for gene knockdown. The 2'-O-methyl modification eliminates the latter property, but further

increases stability and improves affinity for the target sequence [164]. PMOs are extremely stable, do not induce RNase H cleavage and are thus suitable for splicing modulation. Because they are uncharged molecules, delivery of PMOs into cells in *in vitro* experiments is more difficult than 2OMePS [166]. Chimeric AONs that consist of a central region with phosphorothioate backbone and a 2'-O-methyl backbone at the 3' and 5' ends (gapmers) can be used to induce RNase H cleavage while retaining the favorable characteristics of the 2OMePS AONs [150, 167].

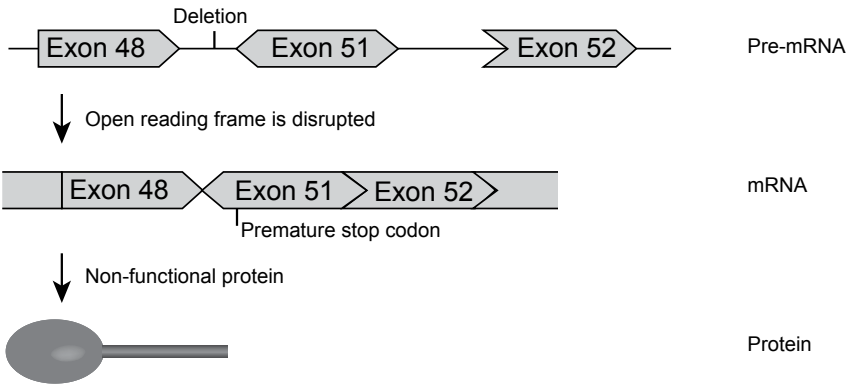
One of the most clinically advanced applications of exon skipping is practiced in treatment for boys with the severe progressive muscular disorder Duchenne muscular dystrophy (DMD). Patients are usually wheelchair-bound by the age of twelve, often require assisted ventilation later in life and generally die in their twenties [168]. The disease is caused by mutations or deletions in the DMD gene that lead to disruption of the reading frame, truncation, and loss of function of dystrophin (Figure 6) [169]. Dystrophin is required for muscle fibre stability and anchors the cytoskeleton to the extracellular matrix with two functional domains linked by a central rod domain [170, 171]. It has been demonstrated in patient cell cultures that exon skipping can be used to skip the mutated or an adjacent exon to restore the reading frame (Figure 6) [172-175]. This allows the production of dystrophins for which the central domain is shortened but both anchor domains are present, leaving it largely functional and resembling the dystrophin protein found in patients with the much milder Becker muscular dystrophy [172]. After local administration and successful dose-escalation and safety studies [176, 177], a 2OMePS AON targeted to exon 51 of DMD (GlaxoSmithKline; originally developed by the Dutch company Prosensa) is currently in Phase III clinical trials [178] (www.clinicaltrials.gov NCT01480245, NCT01462292, NCT01254019). A competing PMO AON (Sarepta (previously AVI BioPharma)) is following closely [179, 180]. Other applications of splicing-modulating AONs in early pre-clinical stages include frontotemporal dementia [181], prostate cancer [182], spinal muscular atrophy [183] and inflammatory diseases such as rheumatoid arthritis [184, 185].

Because of sequence-specificity AONs have to be designed for each new target. The first places to target for the induction of exon skipping are the donor and acceptor splice sites. However, these sites consist of consensus sequences that are shared with many different genes and therefore have a high risk of mistargeting

A Normal dystrophin protein



B Duchenne: deletion of exon 48-50



C Exon skipping of exon 51

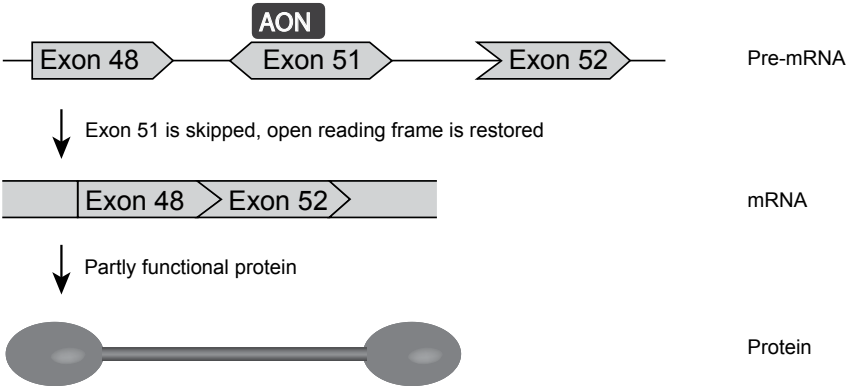


Figure 6. Exon skipping in Duchenne muscular dystrophy (DMD). Dystrophin is a large protein that contains two binding domains to link the actin in the cytoskeleton to the extracellular matrix in muscle cells and is thereby essential for muscle function (A). In DMD patients, the reading frame of the RNA is disrupted by a mutation (B). This results in a premature stop codon and loss of the linker function. In Becker dystrophy, the protein is shortened, but contains both binding domains and can partly fulfill its function. The reading frame of dystrophin in DMD patients can be restored by using AONs to induce skipping of an exon (in this case exon 51), allowing the production of Becker-like dystrophin instead of a non-functional protein (C). Figure adapted from Aartsma-Rus and van Ommen, RNA 2007 [159].

[161, 186]. In addition to the splice site sequences, many exons contain splicing regulatory sequences such as exonic splicing enhancers (ESEs), which facilitate the inclusion of exons [187]. A subfamily of splicing factors, the serine and arginine rich proteins (SR proteins), bind to these ESEs and recruit other splicing factors to the splice sites [188]. ESE motifs are loosely defined because the main task of the exon is encoding protein information, and strict motifs would interfere with this. Putative ESE sites can be predicted with software packages like RESCUE-ESE (<http://genes.mit.edu/burgelab/rescue-ese/>) or ESEfinder (<http://rulai.cshl.edu/cgi-bin/tools/ESE3/esefinder.cgi?process=home>), to help in choosing favorable sites. Based on analysis of 156 AONs that were designed for the DMD gene, several characteristics have been revealed that increase the likelihood of designing effective AONs to 65-70% [189, 190]. Around 20 nucleotides appears to be an optimal length for 2OMePS AONs, although some longer AONs can be more effective [191]. A high percentage of guanines (Gs) and cytosines (Cs) increases affinity of the AON to the target sequence, and therefore this percentage should preferably not be below 40%. However, stretches of three or more Gs or Cs or a GC percentage of >60% should be avoided as this makes self-hybridization of the AON by dimerization or folding more likely. The T_m should be above 48°C as this greatly increased efficacy in the tested DMD AONs [190]. In addition, the secondary structure of the targeted RNA sequence should be accessible for hybridization with the AON [192]. Possible secondary structures can be predicted by m-fold (<http://mfold.rna.albany.edu/?q=mfold> [193]). This program can also calculate the SS count for each nucleotide, indicating in how many of the predicted structures the nucleotide is single stranded. The AON should then be designed to cover partly open and partly closed structures to allow for binding to the target sequence and disruption of the secondary structure [189].

Outline of this thesis

This thesis describes different aspects of bone metabolism, mainly focused on sclerostin, Wnt signaling and bone formation. In **Chapter 2**, the current knowledge on sclerostin is reviewed and its potential as a therapeutic target for osteoporosis is highlighted. The discovery of sclerostin in patients with sclerosteosis and related mutations in Van Buchem disease have greatly improved insight in the function of sclerostin in regulation of bone metabolism. In **Chapter 3** Dkk1 levels were measured

in patients with sclerosteosis and Van Buchem disease. As this inhibitor has a similar action to sclerostin, there may be a mechanism by which Dkk1 compensates for lack of sclerostin. Further advancing knowledge is the discovery of new mutations that result in bone phenotypes. **Chapter 4** describes a novel mutation in sclerostin that results in impaired folding and secretion of the protein, and a phenotype that closely resembles sclerosteosis.

The characteristics of patients with sclerosteosis or Van Buchem disease and carriers of these diseases indicate that sclerostin would be a good target for increasing bone formation in future osteoporosis therapies. For this, sclerostin levels in osteoporosis patients will need to be persistently decreased, for example by interfering with endogenous regulatory pathways. **Chapter 5** therefore investigates the regulation of *SOST*, the gene that codes for sclerostin, and the role of GSK3 β . In **Chapter 6** AONs are investigated as a method for inhibition of sclerostin expression and consequently stimulation of bone formation. In addition, bone resorption is targeted by using AONs to interfere with the function of RANK.

Further research into new therapies for osteoporosis would be aided by suitable high-throughput research methods. Since mineralization is the last and therefore a very important step in osteoblast differentiation, this is a relevant read-out. **Chapter 7** describes a new method to quantify mineralization in bone cell cultures using fluorescent probes. Finally, **Chapter 8** concludes this thesis with a general discussion.

References

1. Herring GM. The chemical structure of tendon, cartilage, dentin and bone matrix. *Clin Orthop Relat Res* 1968;60:261-99.
2. Wuthier RE. A review of the primary mechanism of endochondral calcification with special emphasis on the role of cells, mitochondria and matrix vesicles. *Clin Orthop Relat Res* 1982;219:42.
3. Anderson HC. Molecular biology of matrix vesicles. *Clin Orthop Relat Res* 1995;266:80.
4. Anderson HC. Matrix vesicles and calcification. *Curr Rheumatol Rep* 2003;5:222-6.
5. Wada T, Nakashima T, Hiroshi N, Penninger JM. RANKL-RANK signaling in osteoclastogenesis and bone disease. *Trends Mol Med* 2006;12:17-25.
6. Lacey DL, Timms E, Tan HL, Kelley MJ, Dunstan CR, Burgess T et al. Osteoprotegerin ligand is a cytokine that regulates osteoclast differentiation and activation. *Cell* 1998;93:165-76.
7. Chambers TJ. Regulation of the differentiation and function of osteoclasts. *J Pathol* 2000;192:4-13.
8. Leibbrandt A, Penninger JM. RANK/RANKL: regulators of immune responses and bone physiology. *Ann N Y Acad Sci* 2008;1143:123-50.
9. Burgess TL, Qian Y, Kaufman S, Ring BD, Van G, Capparelli C et al. The ligand for osteoprotegerin (OPGL) directly activates mature osteoclasts. *J Cell Biol* 1999;145:527-38.
10. Wright HL, McCarthy HS, Middleton J, Marshall MJ. RANK, RANKL and osteoprotegerin in bone biology and disease. *Curr Rev Musculoskelet Med* 2009;2:56-64.
11. Dougall WC, Glaccum M, Charrier K, Rohrbach K, Brasel K, De ST et al. RANK is essential for osteoclast and lymph node development. *Genes Dev* 1999;13:2412-24.
12. Kong YY, Yoshida H, Sarosi I, Tan HL, Timms E, Capparelli C et al. OPGL is a key regulator of osteoclastogenesis, lymphocyte development and lymph-node organogenesis. *Nature* 1999;397:315-23.
13. Bucay N, Sarosi I, Dunstan CR, Morony S, Tarpley J, Capparelli C et al. osteoprotegerin-deficient mice develop early onset osteoporosis and arterial calcification. *Genes Dev* 1998;12:1260-8.
14. Amizuka N, Shimomura J, Li M, Seki Y, Oda K, Henderson JE et al. Defective bone remodelling in osteoprotegerin-deficient mice. *J Electron Microsc (Tokyo)* 2003;52:503-13.
15. Theoleyre S, Wittrant Y, Tat SK, Fortun Y, Redini F, Heymann D. The molecular triad OPG/RANK/RANKL: involvement in the orchestration of pathophysiological bone remodeling. *Cytokine Growth Factor Rev* 2004;15:457-75.
16. Kong YY, Feige U, Sarosi I, Bolon B, Tafuri A, Morony S et al. Activated T cells regulate bone loss and joint destruction in adjuvant arthritis through osteoprotegerin ligand. *Nature* 1999;402:304-9.
17. Kotake S, Udagawa N, Hakoda M, Mogi M, Yano K, Tsuda E et al. Activated human T cells directly induce osteoclastogenesis from human monocytes: possible role of T cells in bone destruction in rheumatoid arthritis patients. *Arthritis Rheum* 2001;44:1003-12.
18. Gillespie MT. Impact of cytokines and T lymphocytes upon osteoclast differentiation and function. *Arthritis Res Ther* 2007;9:103.

19. Kingsley DM. What do BMPs do in mammals? Clues from the mouse short-ear mutation. *Trends Genet* 1994;10:16-21.
20. Miyazono K, Maeda S, Imamura T. BMP receptor signaling: transcriptional targets, regulation of signals, and signaling cross-talk. *Cytokine Growth Factor Rev* 2005;16:251-63.
21. Balemans W, Van Hul W. Extracellular regulation of BMP signaling in vertebrates: a cocktail of modulators. *Dev Biol* 2002;250:231-50.
22. Ducy P, Karsenty G. The family of bone morphogenetic proteins. *Kidney Int* 2000;57:2207-14.
23. Groeneveld EH, Burger EH. Bone morphogenetic proteins in human bone regeneration. *Eur J Endocrinol* 2000;142:9-21.
24. ten Dijke P, Korchynski O, Valdimarsdottir G, Goumans MJ. Controlling cell fate by bone morphogenetic protein receptors. *Mol Cell Endocrinol* 2003;211:105-13.
25. Rawadi G, Vayssiere B, Dunn F, Baron R, Roman-Roman S. BMP-2 controls alkaline phosphatase expression and osteoblast mineralization by a Wnt autocrine loop. *J Bone Miner Res* 2003;18:1842-53.
26. Winkler DG, Sutherland MS, Ojala E, Turcott E, Geoghegan JC, Shpektor D et al. Sclerostin inhibition of Wnt-3a-induced C3H10T1/2 cell differentiation is indirect and mediated by bone morphogenetic proteins. *J Biol Chem* 2005;280:2498-502.
27. Mbalaviele G, Sheikh S, Stains JP, Salazar VS, Cheng SL, Chen D et al. Beta-catenin and BMP-2 synergize to promote osteoblast differentiation and new bone formation. *J Cell Biochem* 2005;94:403-18.
28. Chen Y, Whetstone HC, Youn A, Nadesan P, Chow EC, Lin AC et al. Beta-catenin signaling pathway is crucial for bone morphogenetic protein 2 to induce new bone formation. *J Biol Chem* 2007;282:526-33.
29. Kamiya N, Kobayashi T, Mochida Y, Yu PB, Yamauchi M, Kronenberg HM et al. Wnt inhibitors Dkk1 and Sost are downstream targets of BMP signaling through the type IA receptor (BMPRIA) in osteoblasts. *J Bone Miner Res* 2010;25:200-10.
30. Fukuda T, Kokabu S, Ohte S, Sasanuma H, Kanomata K, Yoneyama K et al. Canonical Wnts and BMPs cooperatively induce osteoblastic differentiation through a GSK3beta-dependent and beta-catenin-independent mechanism. *Differentiation* 2010;80:46-52.
31. Miclea RL, van der Horst G, Robanus-Maandag EC, Löwik CWGM, Oostdijk W, Wit JM et al. Apc bridges Wnt/beta-catenin and BMP signaling during osteoblast differentiation of KS483 cells. *Exp Cell Res* 2011;317:1411-21.
32. Zhang R, Oyajobi BO, Harris SE, Chen D, Tsao C, Deng HW et al. Wnt/beta-catenin signaling activates bone morphogenetic protein 2 expression in osteoblasts. *Bone* 2013;52:145-56.
33. Cadigan KM, Nusse R. Wnt signaling: a common theme in animal development. *Genes Dev* 1997;11:3286-305.
34. Yang Y. Wnts and wing: Wnt signaling in vertebrate limb development and musculoskeletal morphogenesis. *Birth Defects Res C Embryo Today* 2003;69:305-17.
35. Johnson ML, Kamel MA. The Wnt signaling pathway and bone metabolism. *Curr Opin Rheumatol* 2007;19:376-82.

36. Logan CY, Nusse R. The Wnt signaling pathway in development and disease. *Annu Rev Cell Dev Biol* 2004;20:781-810.
37. Nusse R, Varmus H. Three decades of Wnts: a personal perspective on how a scientific field developed. *EMBO J* 2012;31:2670-84.
38. Kramer I, Halleux C, Keller H, Pegurri M, Gooi JH, Weber PB et al. Osteocyte Wnt/beta-catenin signaling is required for normal bone homeostasis. *Mol Cell Biol* 2010;30:3071-85.
39. Li X, Zhang Y, Kang H, Liu W, Liu P, Zhang J et al. Sclerostin binds to LRP5/6 and antagonizes canonical Wnt signaling. *J Biol Chem* 2005;280:19883-7.
40. Semenov MV, Tamai K, Brott BK, Kuhl M, Sokol S, He X. Head inducer Dickkopf-1 is a ligand for Wnt coreceptor LRP6. *Curr Biol* 2001;11:951-61.
41. Morvan F, Boulukos K, Clement-Lacroix P, Roman RS, Suc-Royer I, Vayssiere B et al. Deletion of a single allele of the *Dkk1* gene leads to an increase in bone formation and bone mass. *J Bone Miner Res* 2006;21:934-45.
42. Li X, Ominsky MS, Niu QT, Sun N, Daugherty B, D'Agostin D et al. Targeted deletion of the sclerostin gene in mice results in increased bone formation and bone strength. *J Bone Miner Res* 2008;23:860-9.
43. Li J, Sarosi I, Cattley RC, Pretorius J, Asuncion F, Grisanti M et al. *Dkk1*-mediated inhibition of Wnt signaling in bone results in osteopenia. *Bone* 2006;39:754-66.
44. Loots GG, Kneissel M, Keller H, Baptist M, Chang J, Collette NM et al. Genomic deletion of a long-range bone enhancer misregulates sclerostin in Van Buchem disease. *Genome Res* 2005;15:928-35.
45. Gong Y, Slee RB, Fukai N, Rawadi G, Roman-Roman S, Reginato AM et al. LDL receptor-related protein 5 (LRP5) affects bone accrual and eye development. *Cell* 2001;107:513-23.
46. Little RD, Carulli JP, Del Mastro RG, Dupuis J, Osborne M, Folz C et al. A mutation in the LDL receptor-related protein 5 gene results in the autosomal dominant high-bone-mass trait. *Am J Hum Genet* 2002;70:11-9.
47. Boyden LM, Mao J, Belsky J, Mitzner L, Farhi A, Mitnick MA et al. High bone density due to a mutation in LDL-receptor-related protein 5. *N Engl J Med* 2002;346:1513-21.
48. Ai M, Holmen SL, Van HW, Williams BO, Warman ML. Reduced affinity to and inhibition by DKK1 form a common mechanism by which high bone mass-associated missense mutations in LRP5 affect canonical Wnt signaling. *Mol Cell Biol* 2005;25:4946-55.
49. Brunkow ME, Gardner JC, van Ness J, Paeper BW, Kovacevich BR, Proll S et al. Bone dysplasia scleroosteosis results from loss of the *SOST* gene product, a novel cystine knot-containing protein. *Am J Hum Genet* 2001;68:577-89.
50. Balemans W, Patel N, Ebeling M, Van Hul E, Wuyts W, Lacza C et al. Identification of a 52 kb deletion downstream of the *SOST* gene in patients with Van Buchem disease. *J Med Genet* 2002;39:91-7.
51. Bikle DD, Halloran BP. The response of bone to unloading. *J Bone Miner Metab* 1999;17:233-44.
52. Mosley JR. Strain magnitude related changes in whole bone architecture in growing rats. *Bone* 1997;20:191-8.
53. Sugiyama T, Price JS, Lanyon LE. Functional adaptation to mechanical loading in both cortical and cancellous bone is controlled locally and is confined to the loaded bones. *Bone* 2010;46:314-21.

54. Price JS, Sugiyama T, Galea GL, Meakin LB, Sunter A, Lanyon LE. Role of endocrine and paracrine factors in the adaptation of bone to mechanical loading. *Curr Osteoporos Rep* 2011;9:76-82.
55. Tatsumi S, Ishii K, Amizuka N, Li M, Kobayashi T, Kohno K et al. Targeted ablation of osteocytes induces osteoporosis with defective mechanotransduction. *Cell Metab* 2007;5:464-75.
56. Klein-Nulend J, Bacabac RG, Bakker AD. Mechanical loading and how it affects bone cells: the role of the osteocyte cytoskeleton in maintaining our skeleton. *Eur Cell Mater* 2012;24:278-91.
57. Case N, Ma M, Sen B, Xie Z, Gross TS, Rubin J. Beta-catenin levels influence rapid mechanical responses in osteoblasts. *J Biol Chem* 2008;283:29196-205.
58. Hens JR, Wilson KM, Dann P, Chen X, Horowitz MC, Wysolmerski JJ. TOPGAL mice show that the canonical Wnt signaling pathway is active during bone development and growth and is activated by mechanical loading in vitro. *J Bone Miner Res* 2005;20:1103-13.
59. Robling AG, Niziolek PJ, Baldrige LA, Condon KW, Allen MR, Alam I et al. Mechanical stimulation of bone in vivo reduces osteocyte expression of Sost/sclerostin. *J Biol Chem* 2008;283:5866-75.
60. Sawakami K, Robling AG, Ai M, Pitner ND, Liu D, Warden SJ et al. The Wnt co-receptor LRP5 is essential for skeletal mechanotransduction but not for the anabolic bone response to parathyroid hormone treatment. *J Biol Chem* 2006;281:23698-711.
61. Saxon LK, Jackson BF, Sugiyama T, Lanyon LE, Price JS. Analysis of multiple bone responses to graded strains above functional levels, and to disuse, in mice in vivo show that the human Lrp5 G171V High Bone Mass mutation increases the osteogenic response to loading but that lack of Lrp5 activity reduces it. *Bone* 2011;49:184-93.
62. Lin C, Jiang X, Dai Z, Guo X, Weng T, Wang J et al. Sclerostin mediates bone response to mechanical unloading through antagonizing Wnt/beta-catenin signaling. *J Bone Miner Res* 2009;24:1651-61.
63. Sugiyama T, Saxon LK, Zaman G, Moustafa A, Sunter A, Price JS et al. Mechanical loading enhances the anabolic effects of intermittent parathyroid hormone (1-34) on trabecular and cortical bone in mice. *Bone* 2008;43:238-48.
64. Lanyon LE, Armstrong VJ, Saxon LK, Sunter A, Sugiyama T, Zaman G et al. Estrogen Receptors Critically Regulate Bones Adaptive Responses to Loading. *Clinic Rev Bone Miner Metab* 2007;5:234-48.
65. Zaman G, Saxon LK, Sunter A, Hilton H, Underhill P, Williams D et al. Loading-related regulation of gene expression in bone in the contexts of estrogen deficiency, lack of estrogen receptor alpha and disuse. *Bone* 2010;46:628-42.
66. Armstrong VJ, Muzylak M, Sunter A, Zaman G, Saxon LK, Price JS et al. Wnt/beta-catenin signaling is a component of osteoblastic bone cell early responses to load-bearing and requires estrogen receptor alpha. *J Biol Chem* 2007;282:20715-27.
67. Sunter A, Armstrong VJ, Zaman G, Kypta RM, Kawano Y, Lanyon LE et al. Mechanotransduction in osteoblastic cells involves strain-regulated estrogen receptor alpha-mediated control of insulin-like growth factor (IGF) I receptor sensitivity to Ambient IGF, leading to phosphatidylinositol 3-kinase/AKT-dependent Wnt/LRP5 receptor-independent activation of beta-catenin signaling. *J Biol Chem* 2010;285:8743-58.
68. Lombardi G, Di SC, Rubino M, Faggiano A, Vuolo L, Guerra E et al. The roles of parathyroid hormone in bone remodeling: prospects for novel therapeutics. *J Endocrinol Invest* 2011;34:18-22.

69. Huang JC, Sakata T, Pflieger LL, Bencsik M, Halloran BP, Bikle DD et al. PTH differentially regulates expression of RANKL and OPG. *J Bone Miner Res* 2004;19:235-44.
70. Fu Q, Jilka RL, Manolagas SC, O'Brien CA. Parathyroid hormone stimulates receptor activator of NFkappa B ligand and inhibits osteoprotegerin expression via protein kinase A activation of cAMP-response element-binding protein. *J Biol Chem* 2002;277:48868-75.
71. Lee SK, Lorenzo JA. Parathyroid hormone stimulates TRANCE and inhibits osteoprotegerin messenger ribonucleic acid expression in murine bone marrow cultures: correlation with osteoclast-like cell formation. *Endocrinology* 1999;140:3552-61.
72. Fitzpatrick LA. Secondary causes of osteoporosis. *Mayo Clin Proc* 2002;77:453-68.
73. Jilka RL, Weinstein RS, Bellido T, Roberson P, Parfitt AM, Manolagas SC. Increased bone formation by prevention of osteoblast apoptosis with parathyroid hormone. *J Clin Invest* 1999;104:439-46.
74. Keller H, Kneissel M. SOST is a target gene for PTH in bone. *Bone* 2005;37:148-58.
75. Leupin O, Kramer I, Collette NM, Loots GG, Natt F, Kneissel M et al. Control of the SOST bone enhancer by PTH using MEF2 transcription factors. *J Bone Miner Res* 2007;22:1957-67.
76. Silvestrini G, Ballanti P, Leopizzi M, Sebastiani M, Berni S, Di VM et al. Effects of intermittent parathyroid hormone (PTH) administration on SOST mRNA and protein in rat bone. *J Mol Histol* 2007;38:261-9.
77. Kramer I, Loots GG, Studer A, Keller H, Kneissel M. Parathyroid hormone (PTH)-induced bone gain is blunted in SOST overexpressing and deficient mice. *J Bone Miner Res* 2010;25:178-89.
78. Khosla S, Melton LJ, III, Riggs BL. The unitary model for estrogen deficiency and the pathogenesis of osteoporosis: is a revision needed? *J Bone Miner Res* 2011;26:441-51.
79. Modder UI, Clowes JA, Hoey K, Peterson JM, McCready L, Oursler MJ et al. Regulation of circulating sclerostin levels by sex steroids in women and in men. *J Bone Miner Res* 2011;26:27-34.
80. Mirza FS, Padhi ID, Raisz LG, Lorenzo JA. Serum sclerostin levels negatively correlate with parathyroid hormone levels and free estrogen index in postmenopausal women. *J Clin Endocrinol Metab* 2010;95:1991-7.
81. Mabileau G, Mieczkowska A, Edmonds ME. Thiazolidinediones induce osteocyte apoptosis and increase sclerostin expression. *Diabet Med* 2010;27:925-32.
82. Syed F, Khosla S. Mechanisms of sex steroid effects on bone. *Biochem Biophys Res Commun* 2005;328:688-96.
83. Khosla S. Update on estrogens and the skeleton. *J Clin Endocrinol Metab* 2010;95:3569-77.
84. Francis RM. Prevention and treatment of osteoporosis: calcium and vitamin D. In: Compston JE, editor. *Osteoporosis. New perspectives on causes, prevention and treatment*. London: Royal College of Physicians of London; 1996; p. 123-34.
85. Francis RM, Anderson FH, Patel S, Sahota O, van Staa TP. Calcium and vitamin D in the prevention of osteoporotic fractures. *QJM* 2006;99:355-63.
86. Bates CJ, Prentice A, van der Pols JC, Walmsley C, Pentieva KD, Finch S et al. Estimation of the use of dietary supplements in the National Diet and Nutrition Survey: people aged 65 years and Over. An observed paradox and a recommendation. *Eur J Clin Nutr* 1998;52:917-23.

87. Zhu K, Devine A, Suleska A, Tan CY, Toh CZ, Kerr D et al. Adequacy and change in nutrient and food intakes with aging in a seven-year cohort study in elderly women. *J Nutr Health Aging* 2010;14:723-9.
88. Rizzoli R, Boonen S, Brandi ML, Bruyere O, Cooper C, Kanis JA et al. Vitamin D supplementation in elderly or postmenopausal women: A 2013 update of the 2008 recommendations from the European Society for Clinical and Economic Aspects of Osteoporosis and Osteoarthritis (ESCEO). *Curr Med Res Opin* 2013.
89. Verbrugge FH, Gielen E, Milisen K, Boonen S. Who should receive calcium and vitamin D supplementation? *Age Ageing* 2012;41:576-80.
90. Holick MF. Vitamin D: a d-lightful solution for health. *J Investig Med* 2011;59:872-80.
91. Bischoff-Ferrari HA, Dawson-Hughes B, Staehelin HB, Orav JE, Stuck AE, Theiler R et al. Fall prevention with supplemental and active forms of vitamin D: a meta-analysis of randomised controlled trials. *BMJ* 2009;339:b3692.
92. Girgis CM, Clifton-Bligh RJ, Hamrick MW, Holick MF, Gunton JE. The Roles of Vitamin D in Skeletal Muscle: Form, Function, and Metabolism. *Endocr Rev* 2012.
93. Yadav VK, Ryu JH, Suda N, Tanaka KF, Gingrich JA, Schutz G et al. Lrp5 controls bone formation by inhibiting serotonin synthesis in the duodenum. *Cell* 2008;135:825-37.
94. Babij P, Zhao W, Small C, Kharode Y, Yaworsky PJ, Bouxsein ML et al. High bone mass in mice expressing a mutant LRP5 gene. *J Bone Miner Res* 2003;18:960-74.
95. Kato M, Patel MS, Levasseur R, Lobov I, Chang BH, Glass DA et al. Cbfa1-independent decrease in osteoblast proliferation, osteopenia, and persistent embryonic eye vascularization in mice deficient in Lrp5, a Wnt coreceptor. *J Cell Biol* 2002;157:303-14.
96. Hu H, Hilton MJ, Tu X, Yu K, Ornitz DM, Long F. Sequential roles of Hedgehog and Wnt signaling in osteoblast development. *Development* 2005;132:49-60.
97. Hill TP, Spater D, Taketo MM, Birchmeier W, Hartmann C. Canonical Wnt/beta-catenin signaling prevents osteoblasts from differentiating into chondrocytes. *Dev Cell* 2005;8:727-38.
98. Day TF, Guo X, Garrett-Beal L, Yang Y. Wnt/beta-catenin signaling in mesenchymal progenitors controls osteoblast and chondrocyte differentiation during vertebrate skeletogenesis. *Dev Cell* 2005;8:739-50.
99. Holmen SL, Zylstra CR, Mukherjee A, Sigler RE, Faugere MC, Bouxsein ML et al. Essential role of beta-catenin in postnatal bone acquisition. *J Biol Chem* 2005;280:21162-8.
100. Glass DA, Bialek P, Ahn JD, Starbuck M, Patel MS, Clevers H et al. Canonical Wnt signaling in differentiated osteoblasts controls osteoclast differentiation. *Dev Cell* 2005;8:751-64.
101. Cui Y, Niziolek PJ, MacDonald BT, Zylstra CR, Alenina N, Robinson DR et al. Lrp5 functions in bone to regulate bone mass. *Nat Med* 2011;17:684-91.
102. Consensus development conference: diagnosis, prophylaxis, and treatment of osteoporosis. *Am J Med* 1993;94:646-50.
103. Kanis JA, McCloskey EV, Johansson H, Oden A, Melton LJ, III, Khaltav N. A reference standard for the description of osteoporosis. *Bone* 2008;42:467-75.
104. World Health Organization. WHO scientific group on the assessment of osteoporosis at primary health care level. 2007. 5-5-2004.

105. Raisz LG, Bilezikian JP, Martin TJ. Pathophysiology of Osteoporosis. In: Bilezikian JP, Raisz LG, Martin TJ, editors. *Principles of Bone Biology*: Academic Press; 2008; p. 1635-47.
106. Estrada K, Styrkarsdottir U, Evangelou E, Hsu YH, Duncan EL, Ntzani EE et al. Genome-wide meta-analysis identifies 56 bone mineral density loci and reveals 14 loci associated with risk of fracture. *Nat Genet* 2012;44:491-501.
107. Hsu YH, Kiel DP. Clinical review: Genome-wide association studies of skeletal phenotypes: what we have learned and where we are headed. *J Clin Endocrinol Metab* 2012;97:E1958-E1977.
108. Albagha OM, Ralston SH. Genetics and osteoporosis. *Rheum Dis Clin North Am* 2006;32:659-80.
109. Lock CA, Lecouturier J, Mason JM, Dickinson HO. Lifestyle interventions to prevent osteoporotic fractures: a systematic review. *Osteoporos Int* 2006;17:20-8.
110. Lips P, Courpron P, Meunier PJ. Mean wall thickness of trabecular bone packets in the human iliac crest: changes with age. *Calcif Tissue Res* 1978;26:13-7.
111. Schuiling KD, Robinia K, Nye R. Osteoporosis update. *J Midwifery Womens Health* 2011;56:615-27.
112. Genant HK, Cooper C, Poor G, Reid I, Ehrlich G, Kanis J et al. Interim report and recommendations of the World Health Organization Task-Force for Osteoporosis. *Osteoporos Int* 1999;10:259-64.
113. Lane NE. Epidemiology, etiology, and diagnosis of osteoporosis. *Am J Obstet Gynecol* 2006;194:S3-11.
114. Burge R, Dawson-Hughes B, Solomon DH, Wong JB, King A, Tosteson A. Incidence and economic burden of osteoporosis-related fractures in the United States, 2005-2025. *J Bone Miner Res* 2007;22:465-75.
115. Cooper C. The crippling consequences of fractures and their impact on quality of life. *Am J Med* 1997;103:12S-7S.
116. Braithwaite RS, Col NF, Wong JB. Estimating hip fracture morbidity, mortality and costs. *J Am Geriatr Soc* 2003;51:364-70.
117. Qaseem A, Snow V, Shekelle P, Hopkins R Jr., Forciea MA, Owens DK. Pharmacologic treatment of low bone density or osteoporosis to prevent fractures: a clinical practice guideline from the American College of Physicians. *Ann Intern Med* 2008;149:404-15.
118. Papapoulos SE. Bisphosphonates: how do they work? *Best Pract Res Clin Endocrinol Metab* 2008;22:831-47.
119. Fleisch H. Bisphosphonates: mechanisms of action. *Endocr Rev* 1998;19:80-100.
120. Rogers MJ. New insights into the molecular mechanisms of action of bisphosphonates. *Curr Pharm Des* 2003;9:2643-58.
121. Reszka AA, Rodan GA. Nitrogen-containing bisphosphonate mechanism of action. *Mini Rev Med Chem* 2004;4:711-9.
122. Papapoulos SE, Cremers SC. Prolonged bisphosphonate release after treatment in children. *N Engl J Med* 2007;356:1075-6.
123. Russell RG. Bisphosphonates: from bench to bedside. *Ann N Y Acad Sci* 2006;1068:367-401.

124. Rossouw JE, Anderson GL, Prentice RL, LaCroix AZ, Kooperberg C, Stefanick ML et al. Risks and benefits of estrogen plus progestin in healthy postmenopausal women: principal results From the Women's Health Initiative randomized controlled trial. *JAMA* 2002;288:321-33.
125. National Osteoporosis Foundation. *Clinician's Guide to Prevention and Treatment of Osteoporosis*. National Osteoporosis Foundation 2010.
126. Baron R, Hesse E. Update on bone anabolics in osteoporosis treatment: rationale, current status, and perspectives. *J Clin Endocrinol Metab* 2012;97:311-25.
127. Neer RM, Arnaud CD, Zanchetta JR, Prince R, Gaich GA, Reginster JY et al. Effect of parathyroid hormone (1-34) on fractures and bone mineral density in postmenopausal women with osteoporosis. *N Engl J Med* 2001;344:1434-41.
128. Pageau SC. Denosumab. *MABs* 2009;1:210-5.
129. Pierroz DD, Bonnet N, Baldock PA, Ominsky MS, Stolina M, Kostenuik PJ et al. Are osteoclasts needed for the bone anabolic response to parathyroid hormone? A study of intermittent parathyroid hormone with denosumab or alendronate in knock-in mice expressing humanized RANKL. *J Biol Chem* 2010;285:28164-73.
130. Cummings SR, San MJ, McClung MR, Siris ES, Eastell R, Reid IR et al. Denosumab for prevention of fractures in postmenopausal women with osteoporosis. *N Engl J Med* 2009;361:756-65.
131. Baron R, Ferrari S, Russell RG. Denosumab and bisphosphonates: different mechanisms of action and effects. *Bone* 2011;48:677-92.
132. Costa AG, Bilezikian JP. Sclerostin: therapeutic horizons based upon its actions. *Curr Osteoporos Rep* 2012;10:64-72.
133. Li X, Ominsky MS, Warmington KS, Morony S, Gong J, Cao J et al. Sclerostin antibody treatment increases bone formation, bone mass, and bone strength in a rat model of postmenopausal osteoporosis. *J Bone Miner Res* 2009;24:578-88.
134. Eddleston A, Marenzana M, Moore AR, Stephens P, Muzylak M, Marshall D et al. A short treatment with an antibody to sclerostin can inhibit bone loss in an ongoing model of colitis. *J Bone Miner Res* 2009;24:1662-71.
135. Ominsky MS, Vlasseros F, Jolette J, Smith SY, Stouch B, Doellgast G et al. Two doses of sclerostin antibody in cynomolgus monkeys increases bone formation, bone mineral density, and bone strength. *J Bone Miner Res* 2010;25:948-59.
136. Li X, Warmington KS, Niu QT, Asuncion FJ, Barrero M, Grisanti M et al. Inhibition of sclerostin by monoclonal antibody increases bone formation, bone mass, and bone strength in aged male rats. *J Bone Miner Res* 2010;25:2647-56.
137. Marenzana M, Greenslade K, Eddleston A, Okoye R, Marshall D, Moore A et al. Sclerostin antibody treatment enhances bone strength but does not prevent growth retardation in young mice treated with dexamethasone. *Arthritis Rheum* 2011;63:2385-95.
138. Padhi D, Jang G, Stouch B, Fang L, Posvar E. Single-dose, placebo-controlled, randomized study of AMG 785, a sclerostin monoclonal antibody. *J Bone Miner Res* 2011;26:19-26.
139. Amgen and UCB Announce Positive Phase 2 Results of AMG 785/CDP7851 in Patients With Postmenopausal Osteoporosis (PMO). http://www.amgen.com/media/media_pr_detail.jsp?releaseID=1553039 . 21-4-2011.

140. Cole RP, Palushock S, Haboubi A. Osteoporosis management: physicians' recommendations and womens' compliance following osteoporosis testing. *Women Health* 1999;29:101-15.
141. McCombs JS, Thiebaud P, McLaughlin-Miley C, Shi J. Compliance with drug therapies for the treatment and prevention of osteoporosis. *Maturitas* 2004;48:271-87.
142. Lau E, Papaioannou A, Dolovich L, Adachi J, Sawka AM, Burns S et al. Patients' adherence to osteoporosis therapy: exploring the perceptions of postmenopausal women. *Can Fam Physician* 2008;54:394-402.
143. Huas D, Debiais F, Blotman F, Cortet B, Mercier F, Rousseaux C et al. Compliance and treatment satisfaction of post menopausal women treated for osteoporosis. Compliance with osteoporosis treatment. *BMC Womens Health* 2010;10:26.
144. Dias N, Stein CA. Antisense oligonucleotides: basic concepts and mechanisms. *Mol Cancer Ther* 2002;1:347-55.
145. Larrouy B, Blonski C, Boiziau C, Stuer M, Moreau S, Shire D et al. RNase H-mediated inhibition of translation by antisense oligodeoxyribonucleotides: use of backbone modification to improve specificity. *Gene* 1992;121:189-94.
146. Helene C, Toulme JJ. Specific regulation of gene expression by antisense, sense and antigene nucleic acids. *Biochim Biophys Acta* 1990;1049:99-125.
147. Vickers TA, Koo S, Bennett CF, Crooke ST, Dean NM, Baker BF. Efficient reduction of target RNAs by small interfering RNA and RNase H-dependent antisense agents. A comparative analysis. *J Biol Chem* 2003;278:7108-18.
148. Kole R, Krainer AR, Altman S. RNA therapeutics: beyond RNA interference and antisense oligonucleotides. *Nat Rev Drug Discov* 2012;11:125-40.
149. Monia BP, Lesnik EA, Gonzalez C, Lima WF, McGee D, Guinosso CJ et al. Evaluation of 2'-modified oligonucleotides containing 2'-deoxy gaps as antisense inhibitors of gene expression. *J Biol Chem* 1993;268:14514-22.
150. Giles RV, Spiller DG, Grzybowski J, Clark RE, Nicklin P, Tidd DM. Selecting optimal oligonucleotide composition for maximal antisense effect following streptolysin O-mediated delivery into human leukaemia cells. *Nucleic Acids Res* 1998;26:1567-75.
151. Stein CA. The experimental use of antisense oligonucleotides: a guide for the perplexed. *J Clin Invest* 2001;108:641-4.
152. Detrick B, Nagineni CN, Grillone LR, Anderson KP, Henry SP, Hooks JJ. Inhibition of human cytomegalovirus replication in a human retinal epithelial cell model by antisense oligonucleotides. *Invest Ophthalmol Vis Sci* 2001;42:163-9.
153. McGowan MP, Tardif JC, Ceska R, Burgess LJ, Soran H, Gouni-Berthold I et al. Randomized, placebo-controlled trial of mipomersen in patients with severe hypercholesterolemia receiving maximally tolerated lipid-lowering therapy. *PLoS One* 2012;7:e49006.
154. OncoGeneX. Custirsen (OGX-011). <http://www.oncogenex.com/physicians/custirsen-ogx-011> . 2012. 25-3-2013.
155. Dominski Z, Kole R. Restoration of correct splicing in thalassemic pre-mRNA by antisense oligonucleotides. *Proc Natl Acad Sci U S A* 1993;90:8673-7.

156. Sierakowska H, Sambade MJ, Agrawal S, Kole R. Repair of thalassemic human beta-globin mRNA in mammalian cells by antisense oligonucleotides. *Proc Natl Acad Sci U S A* 1996;93:12840-4.
157. Friedman KJ, Kole J, Cohn JA, Knowles MR, Silverman LM, Kole R. Correction of aberrant splicing of the cystic fibrosis transmembrane conductance regulator (CFTR) gene by antisense oligonucleotides. *J Biol Chem* 1999;274:36193-9.
158. Gilbert W. Why genes in pieces? *Nature* 1978;271:501.
159. Grabowski PJ, Black DL. Alternative RNA splicing in the nervous system. *Prog Neurobiol* 2001;65:289-308.
160. Black DL. Mechanisms of alternative pre-messenger RNA splicing. *Annu Rev Biochem* 2003;72:291-336.
161. Aartsma-Rus A, van Ommen GJ. Antisense-mediated exon skipping: a versatile tool with therapeutic and research applications. *RNA* 2007;13:1609-24.
162. Chan JH, Lim S, Wong WS. Antisense oligonucleotides: from design to therapeutic application. *Clin Exp Pharmacol Physiol* 2006;33:533-40.
163. Wickstrom E. Oligodeoxynucleotide stability in subcellular extracts and culture media. *J Biochem Biophys Methods* 1986;13:97-102.
164. Kurreck J. Antisense technologies. Improvement through novel chemical modifications. *Eur J Biochem* 2003;270:1628-44.
165. Summerton J, Weller D. Morpholino antisense oligomers: design, preparation, and properties. *Antisense Nucleic Acid Drug Dev* 1997;7:187-95.
166. Amantana A, Iversen PL. Pharmacokinetics and biodistribution of phosphorodiamidate morpholino antisense oligomers. *Curr Opin Pharmacol* 2005;5:550-5.
167. Furdon PJ, Dominski Z, Kole R. RNase H cleavage of RNA hybridized to oligonucleotides containing methylphosphonate, phosphorothioate and phosphodiester bonds. *Nucleic Acids Res* 1989;17:9193-204.
168. Emery AE. The muscular dystrophies. *Lancet* 2002;359:687-95.
169. Hoffman EP, Brown RH, Jr., Kunkel LM. Dystrophin: the protein product of the Duchenne muscular dystrophy locus. *Cell* 1987;51:919-28.
170. Koenig M, Monaco AP, Kunkel LM. The complete sequence of dystrophin predicts a rod-shaped cytoskeletal protein. *Cell* 1988;53:219-28.
171. Monaco AP. Dystrophin, the protein product of the Duchenne/Becker muscular dystrophy gene. *Trends Biochem Sci* 1989;14:412-5.
172. van Deutekom JC, Bremmer-Bout M, Janson AA, Ginjaar IB, Baas F, den Dunnen JT et al. Antisense-induced exon skipping restores dystrophin expression in DMD patient derived muscle cells. *Hum Mol Genet* 2001;10:1547-54.
173. Aartsma-Rus A, Janson AA, Kaman WE, Bremmer-Bout M, den Dunnen JT, Baas F et al. Therapeutic antisense-induced exon skipping in cultured muscle cells from six different DMD patients. *Hum Mol Genet* 2003;12:907-14.
174. Aartsma-Rus A, Janson AA, Kaman WE, Bremmer-Bout M, van Ommen GJ, den Dunnen JT et al. Antisense-induced multiexon skipping for Duchenne muscular dystrophy makes more sense. *Am J Hum Genet* 2004;74:83-92.

175. Suroño A, Van KT, Takeshima Y, Wada H, Yagi M, Takagi M et al. Chimeric RNA/ethylene-bridged nucleic acids promote dystrophin expression in myocytes of duchenne muscular dystrophy by inducing skipping of the nonsense mutation-encoding exon. *Hum Gene Ther* 2004;15:749-57.
176. van Deutekom JC, Janson AA, Ginjaar IB, Frankhuizen WS, Aartsma-Rus A, Bremmer-Bout M et al. Local dystrophin restoration with antisense oligonucleotide PRO051. *N Engl J Med* 2007;357:2677-86.
177. Goemans NM, Tulinius M, van den Akker JT, Burm BE, Ekhardt PF, Heuvelmans N et al. Systemic administration of PRO051 in Duchenne's muscular dystrophy. *N Engl J Med* 2011;364:1513-22.
178. Fairclough RJ, Bareja A, Davies KE. Progress in therapy for Duchenne muscular dystrophy. *Exp Physiol* 2011;96:1101-13.
179. Kinali M, Arechavala-Gomez V, Feng L, Cirak S, Hunt D, Adkin C et al. Local restoration of dystrophin expression with the morpholino oligomer AVI-4658 in Duchenne muscular dystrophy: a single-blind, placebo-controlled, dose-escalation, proof-of-concept study. *Lancet Neurol* 2009;8:918-28.
180. Cirak S, Arechavala-Gomez V, Guglieri M, Feng L, Torelli S, Anthony K et al. Exon skipping and dystrophin restoration in patients with Duchenne muscular dystrophy after systemic phosphorodiamidate morpholino oligomer treatment: an open-label, phase 2, dose-escalation study. *Lancet* 2011;378:595-605.
181. Kalbfuss B, Mabon SA, Misteli T. Correction of alternative splicing of tau in frontotemporal dementia and parkinsonism linked to chromosome 17. *J Biol Chem* 2001;276:42986-93.
182. Williams T, Kole R. Analysis of prostate-specific membrane antigen splice variants in LNCap cells. *Oligonucleotides* 2006;16:186-95.
183. Williams JH, Schray RC, Patterson CA, Ayitey SO, Tallent MK, Lutz GJ. Oligonucleotide-mediated survival of motor neuron protein expression in CNS improves phenotype in a mouse model of spinal muscular atrophy. *J Neurosci* 2009;29:7633-8.
184. Graziewicz MA, Tarrant TK, Buckley B, Roberts J, Fulton L, Hansen H et al. An endogenous TNF-alpha antagonist induced by splice-switching oligonucleotides reduces inflammation in hepatitis and arthritis mouse models. *Mol Ther* 2008;16:1316-22.
185. Yilmaz-Elis S, Aartsma-Rus A, Vroon A, van Deutekom J, de Kimpe S, 't Hoen PA et al. Antisense oligonucleotide mediated exon skipping as a potential strategy for the treatment of a variety of inflammatory diseases such as rheumatoid arthritis. *Ann Rheum Dis* 2012;71 Suppl 2:i75-i77.
186. Aartsma-Rus A, Houllberghs H, van Deutekom JC, van Ommen GJ, 't Hoen PA. Exonic sequences provide better targets for antisense oligonucleotides than splice site sequences in the modulation of Duchenne muscular dystrophy splicing. *Oligonucleotides* 2010;20:69-77.
187. Cartegni L, Chew SL, Krainer AR. Listening to silence and understanding nonsense: exonic mutations that affect splicing. *Nat Rev Genet* 2002;3:285-98.
188. Stojdl DF, Bell JC. SR protein kinases: the splice of life. *Biochem Cell Biol* 1999;77:293-8.
189. Aartsma-Rus A, van Vliet L, Hirschi M, Janson AA, Heemskerck H, de Winter CL et al. Guidelines for antisense oligonucleotide design and insight into splice-modulating mechanisms. *Mol Ther* 2009;17:548-53.
190. Aartsma-Rus A. Overview on AON design. *Methods Mol Biol* 2012;867:117-29.

191. Harding PL, Fall AM, Honeyman K, Fletcher S, Wilton SD. The influence of antisense oligonucleotide length on dystrophin exon skipping. *Mol Ther* 2007;15:157-66.
192. Wee KB, Pramono ZA, Wang JL, MacDorman KF, Lai PS, Yee WC. Dynamics of co-transcriptional pre-mRNA folding influences the induction of dystrophin exon skipping by antisense oligonucleotides. *PLoS One* 2008;3:e1844.
193. Zuker M. Mfold web server for nucleic acid folding and hybridization prediction. *Nucleic Acids Res* 2003;31:3406-15.

A vertical strip on the left side of the page contains a grayscale microscopic image of bone tissue. The image shows a complex, porous structure with various layers and textures, characteristic of bone microarchitecture. The text 'Chapter 2' is overlaid on this image.

Chapter 2

Sclerostin: current knowledge and future perspectives

M.J.C. Moester
S.E. Papapoulos
C.W.G.M. Löwik
R.L. van Bezooijen

Adapted from:
Calcif Tissue Int. 2010 Aug;87(2):99-107

Abstract

In recent years study of rare human bone disorders led to the identification of important signaling pathways that regulate bone formation. Such diseases include the bone sclerosing dysplasias sclerosteosis and Van Buchem disease, which are due to deficiency of sclerostin, a protein secreted by osteocytes that inhibits bone formation by osteoblasts. The restricted expression pattern of sclerostin in the skeleton and the exclusive bone phenotype of good quality of patients with sclerosteosis and Van Buchem disease provide the basis for the design of therapeutics that stimulate bone formation. We review here current knowledge of the regulation of the expression and formation of sclerostin, its mechanism of action and its potential as a bone building treatment for patients with osteoporosis.

Introduction

Osteoporosis is characterized by low bone mass and microarchitectural deterioration of bone tissue with a consequent increase in bone fragility and susceptibility to fractures [1]. The balance between bone resorption and bone formation determines the mass and structural integrity of the skeleton and is disturbed in osteoporosis. Current therapies of osteoporosis, with the exception of parathyroid hormone (PTH), decrease the risk of osteoporotic fractures by reducing bone resorption and preserving its architecture but cannot stimulate bone formation. Elucidating the mechanisms regulating bone formation may lead to the development of therapeutics able to rebuild bone mass and architecture.

In recent years, study of rare human bone disorders and of genetically manipulated animal models has led to the identification of signaling pathways that regulate bone formation which provide potential targets for the development of novel therapeutics. Fundamental for this progress have been studies of two rare bone sclerosing dysplasias, sclerosteosis and Van Buchem disease, that led to the identification of sclerostin, an important negative regulator of bone formation.

Sclerosteosis and Van Buchem disease

Sclerosteosis (OMIM 269500) and Van Buchem disease (OMIM 239100) are two rare sclerosing bone disorders, first described in the 1950's as distinct clinical entities, with closely related phenotypes [2]. Sclerosteosis has been mainly diagnosed among Afrikaners of Dutch descent in South Africa, while most patients diagnosed with Van Buchem disease come from a small fishing village in The Netherlands. A few individuals and families with sclerosteosis or Van Buchem disease have been reported in other parts of the world, including Spain, Brazil, USA, Germany, Japan, Switzerland, and Senegal [3].

The skeletal manifestations of sclerosteosis and Van Buchem disease are the result of endosteal hyperostosis and are characterized by progressive generalized osteosclerosis [3-8]. The manifestations are most pronounced in mandible and skull, with characteristic enlargement of the jaw and facial bones leading to facial distortion, increased intracranial pressure and entrapment of cranial nerves, often associated with facial palsy, hearing loss and/or loss of smell (Figure 1). Patients with



Figure 1. Chronological portraits of a patient with sclerosteosis from the age of 3 years onwards. She was born with syndactyly at both hands and developed facial palsy, deafness, facial distortion, and maxillary overgrowth during childhood. By the age of 30, she had developed proptosis and elevated intracranial pressure due to overgrowth of the calvarium. Craniectomy was performed, but she died nevertheless because of elevated intracranial pressure at the age of 54 years (description of this case was previously published by Epstein *et al.* [14]).

sclerosteosis have a more severe phenotype compared to patients with Van Buchem disease and usually have syndactyly. In a limited number of bone biopsies of affected individuals there is evidence of increased bone formation including predominance of cuboidal active osteoblasts, increased double tetracycline label spacing and increased osteoid that mineralizes normally, while no consistent alteration of osteoclast numbers or activity has been reported [9-13]. Information about markers of bone turnover in such patients is also limited. Beighton's group reported elevated serum alkaline phosphatase (AP) activity in the majority of patients with sclerosteosis [14, 15] while Wergedal *et al.* [16] found significantly higher levels of bone formation (AP, procollagen type 1 amino-terminal propeptide [P1NP], osteocalcin) and resorption (urinary amino-terminal type I collagen telopeptide [NTX]) markers in six patients with Van Buchem disease compared to carriers of the disease.

The genetic defect that leads to sclerosteosis was identified in a newly cloned gene called *SOST*, which is located on chromosome 17q12-21 and encodes for the protein

sclerostin. Five mutations have so far been identified in patients with sclerosteosis, of which three introduce a premature termination codon and the others interfere with splicing of the gene [17-20]. No mutations within this gene could be found in patients with Van Buchem disease, but instead a 52kb deletion 35kb downstream of the *SOST* gene was identified [21, 22]. The deleted region was later found to contain regulatory elements for *SOST* transcription explaining its ability to induce a phenotype closely resembling that of patients with sclerosteosis [23]. The different defects of the *SOST* gene cannot readily explain the differences in clinical phenotypes between the two diseases. However, serum sclerostin was severely decreased in patients with Van Buchem disease compared to controls, but could not be detected in patients with sclerosteosis [13, 24]. This difference may give rise to differences in disease severity. A gene-dose effect is also indicated by the fact that serum sclerostin concentrations in carriers of both diseases were significantly higher than in affected individuals, but lower than in controls. With regard to the digit malformations present only in sclerosteosis it may be that the genomic region deleted in Van Buchem disease does not contain regulatory elements required for sclerostin expression during digit formation. This could be the reason for the absence of syndactyly (or other digit malformations) in these patients as opposed to patients with sclerosteosis.

SOST/sclerostin expression

SOST mRNA is, especially during embryogenesis, expressed in many tissues, whereas sclerostin protein expression has only been reported postnatally in terminally differentiated cells embedded within a mineralized matrix, i.e. osteocytes, mineralized hypertrophic chondrocytes and cementocytes [11, 12, 25, 26]. *SOST* mRNA expression in unmineralized tissues has been detected during mouse embryogenesis in the otic vesicle and peridigital or interdigital regions of the limb buds, of which the latter may be implicated in the pathogenesis of syndactyly in patients with sclerosteosis [27]. In humans, *SOST* mRNA is expressed in heart, aorta, liver and at high levels in the kidney [17, 18, 28, 29], but no sclerostin protein has been detected in these organs. Accordingly, patients with sclerosteosis or Van Buchem disease do not have renal or cardiovascular abnormalities [3].

In adult murine and human bone, sclerostin expression is restricted to osteocytes with diffuse staining representing dendrites in osteocytic canaliculi [11, 25, 26,

30]. Osteoclasts, osteoblasts and bone lining cells do not express sclerostin. Due to the difficulties with isolating and culturing osteocytes from mammalian bone, *in vitro* studies of *SOST*/sclerostin expression are technically difficult. Osteogenic cell cultures that form mineralized bone nodules are one of the few available methods for generating osteocyte-like cells *in vitro* [31]. In mouse primary osteogenic bone marrow and mouse mesenchymal KS483 cell cultures, *SOST* mRNA expression is induced at low levels after onset of bone nodule mineralization [11, 32]. Similar to the induction of *SOST* mRNA *in vitro*, newly embedded osteocytes within unmineralized osteoid in humans *in vivo* do not express sclerostin, but become positive for the protein at, or shortly after primary mineralization [26]. When mineralization of osteoid is inhibited by administration of the bisphosphonate etidronate in rats, osteocytes within the unmineralized matrix remain immature and do not express sclerostin [33]. However, *SOST* mRNA is expressed by some osteoblast-like osteosarcoma cell lines [34].

As expected, sclerostin is not expressed by osteocytes in bone biopsies of patients with sclerosteosis [11]. In addition, no sclerostin expression was found in bone biopsies from patients with Van Buchem disease, supporting the function of the genomic region deleted in these patients in the regulation of sclerostin expression in bone [12].

Sclerostin mechanism of action

In patients with sclerosteosis, the combination of high bone mass due to increased bone formation with premature termination codons in the *SOST* gene suggested an inhibitory effect of the gene product sclerostin on bone formation. This is supported by the observation that addition of exogenous sclerostin to osteogenic cultures inhibited proliferation and differentiation of mouse and human osteoblastic cells [11, 25, 35]. In addition, sclerostin was shown to decrease the lifespan of osteoblasts by stimulating their apoptosis [35]. *In vivo*, overexpression of sclerostin using either the osteocalcin promoter or BAC recombination induced osteopenia in mice [23, 25]. Bone formation in these animals was decreased, while bone resorption was unaffected. Furthermore, analysis of *Sost* knockout mice showed significant increases in radiodensity, bone mineral density (BMD), cortical and trabecular bone volume, bone formation rate, and bone strength [36]. Together these data support a negative

effect of sclerostin on bone formation.

Two processes are responsible for construction and reconstruction of the skeleton throughout life, bone remodeling and modeling. Bone remodeling enables constant renewal of the skeleton. In this process, bone resorption by osteoclasts and formation by osteoblasts are tightly coupled within a basic multicellular unit (BMU) and bone resorption always precedes bone formation. Sclerostin expression by newly embedded osteocytes at the onset of mineralization of osteoid may serve as a negative feedback signal on osteoblasts to prevent overfilling of the BMU (Figure 2a)

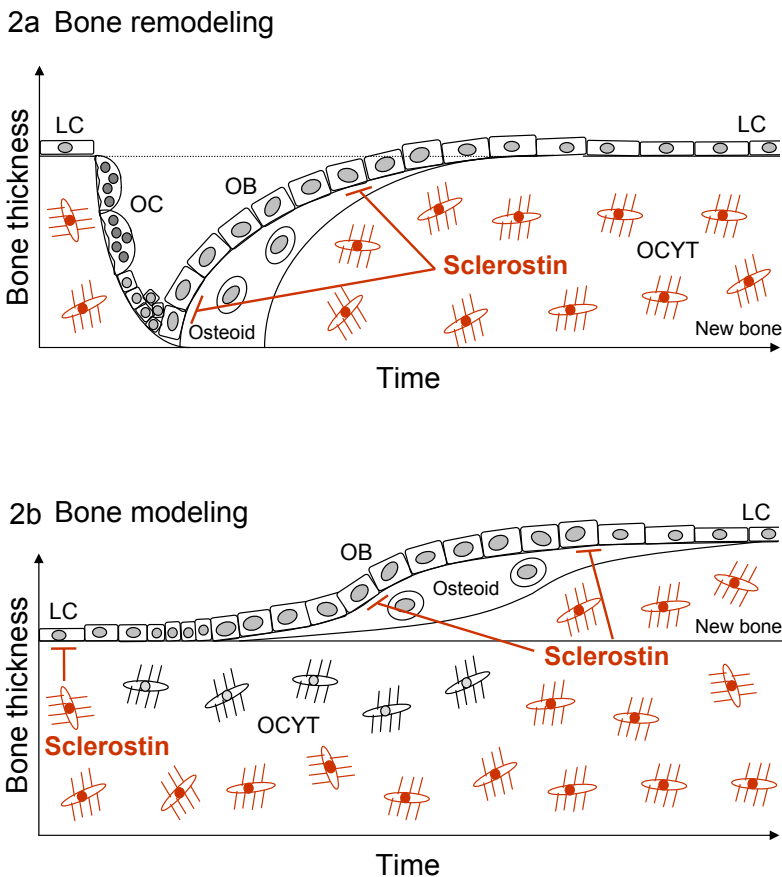


Figure 2. Schematic model of the mechanism of action of sclerostin in bone remodeling and modeling. In remodeling (A), sclerostin produced and secreted by newly embedded osteocytes may be transported to the bone surface where it inhibits osteoblastic bone formation and prevents overfilling of the basic multicellular unit (BMU). In modeling (B), sclerostin may serve two actions. First, it may keep bone lining cells in a state of quiescence and prevent, thereby, initiation of de novo bone formation. In addition, sclerostin produced and secreted by newly embedded osteocytes may inhibit osteoblastic bone formation similar as in a BMU (reproduced from van Bezooijen *et al.* [8]).

[11, 26]. Data on the effect of sclerostin on osteoclastic bone resorption in humans are scarce and inconsistent, reporting unaffected, low or increased bone resorption in patients with sclerosteosis and Van Buchem disease [9, 10, 16]. In addition, during bone modeling sclerostin may keep bone lining cells in a quiescent state [26] and may thereby prevent activation of osteoblasts and bone formation without previous bone resorption (Figure 2b) [8]. Sclerostin expression by osteocytes embedded in newly formed bone by modeling may serve a similar negative feedback mechanism on bone formation as in a BMU.

On the basis of its amino acid sequence, which indicates a cystine knot structure, sclerostin was classified as a member of the DAN (Differential screening-selected gene aberrant in neuroblastoma) family of glycoproteins [6, 17, 18, 37]. This family consists of a group of secreted proteins that share the ability to antagonize bone morphogenetic protein (BMP) activity. The currently available data, however, suggest that sclerostin is not a classical BMP antagonist [11]. Some DAN family members have also been reported to antagonize canonical Wnt signaling, among which Wise is the most closely related to sclerostin [38]. Wnts are secreted glycoproteins that bind to seven transmembrane-spanning receptors of the Frizzled family. Stimulation of these receptors causes the intracellular signaling molecule β -catenin to accumulate and translocate into the nucleus, where it initiates transcription of target genes via complex formation with TCF/Lef1 transcription factors. Conversely, in the absence of Wnt, β -catenin forms a complex with the tumor suppressor proteins APC and Axin, and the kinases glycogen synthase kinase 3 (GSK3) and casein kinase I (CK1), which facilitates phosphorylation and proteosomal degradation of β -catenin [39].

The identification of gain-of-function mutations in the first β -propeller of the low-density lipoprotein receptor-related protein LRP5, an essential membrane bound co-factor in canonical Wnt signaling, in patients with high bone mass (HBM)-phenotype [40, 41] and loss-of-function mutations in LRP5 in patients with the osteoporosis pseudoglioma syndrome (OPPG) [42] demonstrated the importance of LRP5-mediated canonical Wnt signaling in regulating bone formation. Sclerostin has been shown to bind LRP5 and its closely related co-receptor LRP6 and, thereby, inhibit the canonical Wnt signaling via LRP5/6 (Figure 3) [43-45]. However, although sclerostin binds LRP5/6 to antagonize Wnt signaling, sclerostin and Wnts do not appear to compete for binding of this co-receptor [43], and may antagonize different

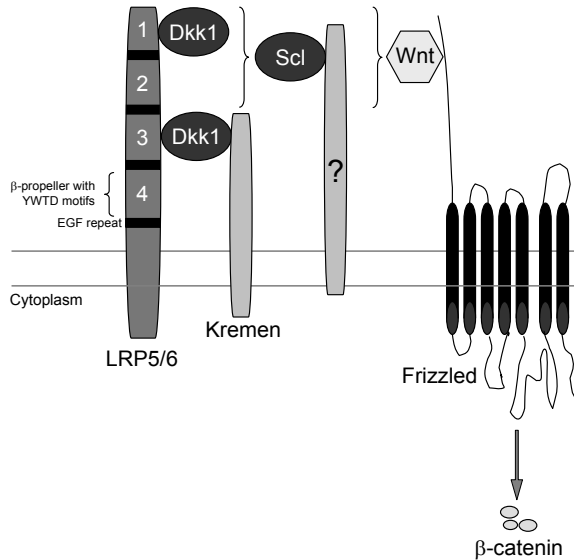


Figure 3. Schematic model of antagonized canonical Wnt signaling. Canonical Wnt signaling involves the formation of complexes of Wnts with Frizzled receptors and LRP5/6 co-receptors, resulting in the accumulation of β -catenin in the cytoplasm and translocation into the nucleus. The antagonist Dkk1 inhibits canonical Wnt signaling by the formation of complexes with LRP5/6 and Kremen, resulting in the removal of LRP5/6 from the membrane. Dkk1 binds to the first and third β -propeller of LRP5/6. The antagonist sclerostin inhibits canonical Wnt signaling by binding to probably the first β -propeller of LRP5/6. Whether sclerostin requires a co-factor like Kremen for Dkk1 to exert its antagonistic effect remains to be established (reproduced from van Bezooijen *et al.* [8]).

Wnts depending on the conformation of LRP5 or 6 [46]. It may be that sclerostin exerts its effect through binding to a co-receptor and inducing internalization of LRP5/6 as has been shown for Dkk1, another Wnt antagonist. Characterization of the structure of sclerostin showed that sclerostin indeed consists out of a cystine knot and three loops [47, 48]. One of these loops is high in positively charged residues, showing a possible site of interaction with the predicted binding site on the first of 6 β -propellers of LRP5, which is negatively charged. The binding site of a neutralizing antibody to sclerostin was mapped to this loop, suggesting a functional role of this region in the inhibition of Wnt signaling. In addition, the loop contains a highly conserved sequence with an NXI motif (in the sequence PNAIG). This motif was also found in the closely related protein WISE, in DKK proteins, and in the interaction between laminin with nidogen, another six-bladed β -propeller containing protein. Mutation of the amino acids in this motif destroyed the ability of sclerostin and Dkk1 to inhibit Wnt signaling [46, 49]. A potential binding site for heparin was

also found within sclerostin, which may mediate localization of sclerostin at the cell surface of target cells and possibly facilitate inhibition of Wnt signaling.

The precise mechanism by which sclerostin secreted by osteocytes inhibits Wnt-mediated bone formation is still unclear. It may be transported to the bone surface via the canaliculi or it may induce another signal in osteocytes that is transported to osteoblasts to inhibit bone formation. In support of the latter, Wnt signaling has been found in osteocytes [50, 51]. Another mechanism was proposed by Krause *et al.* [52]. They found that, even though sclerostin is not a classical BMP antagonist, it could inhibit BMP7-induced responses when both proteins were expressed in the same cell. Sclerostin then bound to BMP7, leading to intracellular retention and proteasomal degradation. The effect of sclerostin may therefore be different in osteocytes that produce the protein, and osteoblasts or sclerostin-negative osteocytes.

Several ELISA methods have become available for the measurement of sclerostin in serum or plasma samples, showing that sclerostin also circulates in the bloodstream. Over the past few years many reports have been published on sclerostin serum concentrations in humans, showing variations in healthy adults [53, 54] and associations between sclerostin and a variety of diseases and conditions. Increased sclerostin concentrations have been found in hypercortisolism [55], type 2 diabetes mellitus (T2DM) [56], atherosclerosis in T2DM [57], immobilization [58], fracture healing [59], thalassemia-associated osteoporosis [60], and high bone turnover as in Paget's disease [61], while sclerostin was decreased in hyperparathyroidism [62], idiopathic osteoporosis in men [63] and ankylosing spondylitis [64, 65]. However, not much is known about the importance of sclerostin in the serum; whether it has a function in circulation, whether serum concentrations reflect changes in the bone, and the temporal resolution of changes in serum concentrations. It is important to elucidate these mechanisms before sclerostin measurements can be routinely used as diagnostic tools in the clinic.

Recently, the role of bone expressed LRP5 in the regulation of bone formation was questioned, since targeted deletion of LRP5 in osteoblasts using the collagen type 1 promoter failed to induce osteopenia and targeted knock-in of LRP5 with a HBM mutation (G171V) using the same promoter did not increase bone mass in mice [66]. It was shown that LRP5-mediated signaling in the duodenum inhibited the expression of Tph1, the rate-limiting enzyme for serotonin production outside the

brain, and, thereby, decreased serum levels of serotonin. Conversely, LRP5 knockout mice that have low bone mass had high serum serotonin levels. In addition, reduction of these elevated serotonin levels by administration of parachlorophenylalanine or a low tryptophan diet normalized bone formation parameters and bone mass. Cui *et al.* [67] could not replicate the results presented by Yadav *et al.* and found no relation between serotonin and bone mass. This discrepancy may be explained by differences in the mouse models that were used. At this point a definitive answer has not been found, and further research may prove if both models can be integrated.

Regulation of *SOST*/sclerostin expression

Due to their location and morphology, osteocytes have been long implicated in mechanosensing and initiation of the bone anabolic response to mechanical load [68, 69]. In support of this, specific ablation of osteocytes in mice resulted in fragile bone and these mice did not respond with bone loss to unloading [70]. Wnt signaling may play an important role in the anabolic response to deformation and loading, since increased Wnt signaling has been found after loading of osteoblastic cells *in vitro* and of tibiae *in vivo* [50, 71, 72]. Wnt signaling and the co-receptor LRP5 were found to be essential for the increase in bone mass after loading [73, 74]. Since sclerostin is produced by osteocytes in bone and inhibits bone formation by antagonizing canonical Wnt signaling, it may play a role in regulating Wnt-signaling in response to mechanical loading. Consistent with this hypothesis, loading decreased *SOST* mRNA and sclerostin levels, while unloading increased *Sost* mRNA expression *in vivo* (Figure 4) [72, 75, 76]. Interestingly, reduction of sclerostin staining intensity was most pronounced in areas with the highest strain, indicating a response to local loading conditions. Furthermore, *Sost* knock-out mice do not exhibit bone loss after unloading [72], and constitutive over-expression of *Sost* severely reduced bone formation after loading [74].

Several systemic and local factors have been suggested as possible regulators of *SOST*/sclerostin expression by osteocytes and the *SOST* promoter region includes Runx2, E-box and C/EBP binding motives [77]. Recombinant human PTH and active fragments of this protein are used in the treatment of osteoporosis [78]. In contrast to the bone resorption stimulating effect of continuous elevation of endogenous PTH as is seen in patients with hyperparathyroidism, intermittent increases of PTH provided

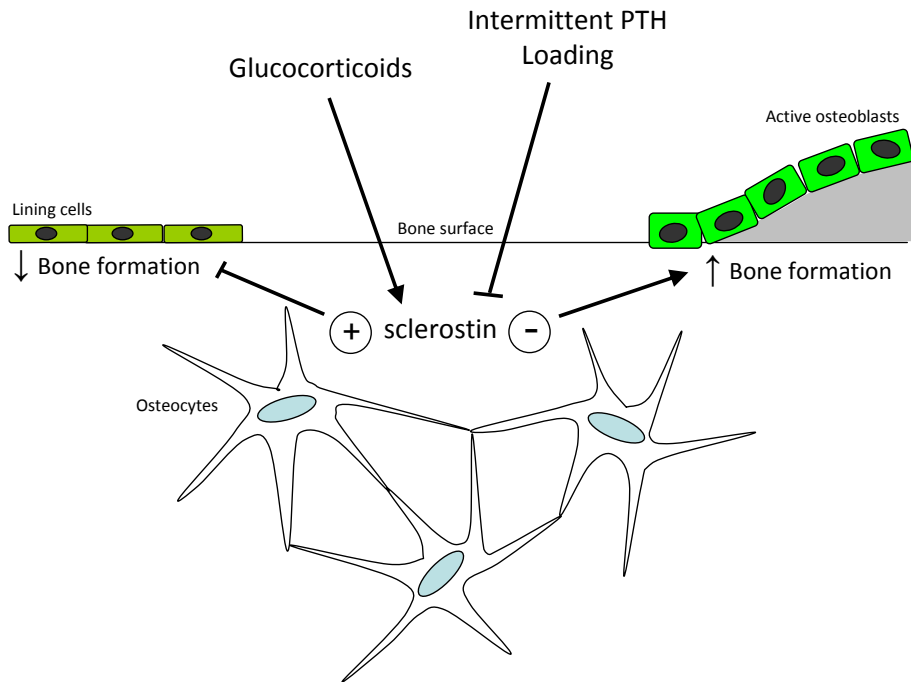


Figure 4. Schematic model for the regulation of the control of bone formation by sclerostin. Sclerostin may exert its inhibitory effect on bone formation by preventing the activation of lining cells as well as the inactivation of active osteoblasts. Glucocorticoids stimulate sclerostin expression and, thereby, inhibit bone formation, whereas intermittent PTH and loading inhibit sclerostin expression in osteocytes and, thereby, stimulate bone formation.

by daily injections are associated with distinct anabolic effects. The mechanisms by which PTH mediates this bone anabolic effect are not completely understood. Part of it may be mediated via sclerostin, as PTH has been shown to inhibit its expression both *in vitro* and *in vivo* (Figure 4). *In vitro*, PTH decreased *SOST* transcription by osteoblastic and osteocytic cells within 4 hours. This was not affected by the protein synthesis inhibitor cyclohexamide, but decreased by the cAMP inducer forskolin [30, 34]. These observations suggest a direct and cAMP dependent regulatory effect of PTH on the expression of *SOST*. Within the 52kb genomic region deleted in Van Buchem disease, a MEF2 response element (ECR5) has been identified that is essential for the PTH-induced downregulation of *SOST* expression [79, 80]. *In vivo*, PTH administration resulted in a decrease in *SOST* mRNA and sclerostin expression in mice and rats [23, 30, 79, 81]. In addition, a constitutively active PTH receptor 1 (caPTHr1) exclusively expressed in osteocytes resulted in increased remodeling with decreased osteoblast apoptosis and suppression of *SOST* expression [82]. This

effect was blunted in mice lacking LRP5, suggesting that the effect of caPTHr1 was mediated by increased Wnt signaling due to suppression of *SOST*. The importance of *SOST* regulation by PTH is further supported by the observations that the anabolic effect of PTH is blunted in *Sost* deficient mice as well as in mice overexpressing *Sost* using a constitutive active promoter [83].

Two other systemic factors have also been shown to affect *SOST*/sclerostin expression. 1,25-Dihydroxyvitamin D3 alone or in combination with retinoic acid increased *SOST* expression in human osteoblastic cells *in vitro* [32, 77]. The specific effect of glucocorticoids on *SOST* expression depends on the experimental conditions. *In vitro*, dexamethason suppressed *SOST* expression in osteoblastic cells [32], while *in vivo* treatment of mice with prednisolone increased *Sost* expression in tibiae, suggesting that suppression of Wnt signaling by the upregulation of sclerostin may account for the glucocorticoid-induced suppression in bone formation (Figure 4) [84].

BMP2, 4, and 6 are local growth factors shown to stimulate *SOST* expression in osteoblastic cells *in vitro* [27, 32], probably by an indirect mechanism [85]. Decreased BMP signaling due to osteoblast specific knockout of *Bmpr1a* decreased *Sost* mRNA and sclerostin protein expression in embryonic mice calvariae and was associated with increased bone mass [86]. In these mice, however, both bone formation and resorption were inhibited. The authors proposed that the decrease in bone formation was independent of sclerostin expression and a direct result of decreased BMP signaling. The decrease in bone resorption, however, may be an effect of increased Wnt signaling due to the decrease in sclerostin expression. This in turn may be due to upregulation of osteoprotegerin in mature osteoblasts by Wnts and, thereby, inhibition of RANKL-induced osteoclastogenesis [87].

Despite the rapid progress in our understanding of the regulation of the production and function of sclerostin, there are still important questions that need to be addressed in future research. These include the identification of factors that regulate sclerostin/*SOST* expression and determine its highly restricted expression pattern. Furthermore, the mechanism by which sclerostin binding to LRP5/6 interferes with canonical Wnt signaling as well as potential additional functions of sclerostin, besides antagonizing canonical Wnt signaling, should be further explored. While sclerostin measurements in serum revealed some interesting associations

with disease, the precise function and relevance of circulating sclerostin need to be elucidated. More detailed and structured analysis of bone metabolism in patients with sclerosteosis and Van Buchem disease, sclerostin expression in pathological conditions, and a genotype-phenotype characterization of *SOST* are required to better understand its function and regulation in humans.

Therapeutic potential

The identification of sclerostin deficiency as the cause of sclerosteosis and Van Buchem disease and the progress in our understanding of the action of sclerostin on bone formation has opened a new area in bone therapeutics. The restricted expression pattern of sclerostin and the exclusive bone phenotype of good quality of patients with sclerosteosis and Van Buchem disease provide the basis for the design of therapeutics that specifically stimulate bone formation, an action relevant to the treatment of osteoporosis. As sclerostin is a secreted protein, one approach to achieve this is to develop antibodies capable of inhibiting the biological activity of sclerostin, mimicking, thus, its absence in sclerosteosis. Such antibodies have already been shown to increase BMD, bone volume and bone strength in ovariectomized rats [88] and primates [89] and to reverse bone loss in a model of colitis [90] and are currently in Phase III clinical trials (AMG 785, NCT01575834 and NCT01631214 on www.clinicaltrials.gov). Placebo-controlled studies and a recent phase II study comparing sclerostin antibody to alendronate and teriperatide demonstrated a markedly increased BMD at spine, hip and femoral neck that was significantly higher than in patients that were treated with other drugs [91, 92]. Bone formation markers were rapidly increased and bone resorption markers were decreased. While the increase in bone formation markers was transitory, the changes in bone resorption was sustained over the 12-month study period and resulted in a large anabolic window which has not been observed in other osteoporosis therapies.

Other approaches to inhibit sclerostin production or activity are also feasible. However, given the availability of efficacious treatments, any novel treatment for osteoporosis should not only be effective but also devoid of adverse effects. The absence of any extraskeletal complications of patients with sclerosteosis and Van Buchem disease are reassuring. Furthermore, the finding of consistently higher BMD values in carriers of sclerosteosis with no skeletal complications [6] suggests

that the sclerostin inhibition can be titrated and can lead to the desired outcome without any side effects, but safety margins need to be determined. However, there have been concerns that stimulation of bone formation by increasing Wnt signaling may lead to unwanted skeletal effects [93, 94]. The Wnt inhibitor factor 1 (WIF1), for example, has been identified as a candidate tumor suppressor gene in human osteosarcoma, suggesting that the susceptibility to osteosarcoma may be increased in patients receiving novel anabolic treatments targeting Wnt antagonists [95]. This is another issue that needs to be further investigated.

Study of the molecular defects of rare bone disorders such as sclerosteosis and Van Buchem disease can, thus, lead to the development of new bone forming agents allowing to tailor pharmacotherapy to the needs of the individual patient with osteoporosis. In addition, they may help in the management of the small group of patients with sclerosteosis or Van Buchem disease, for whom the only currently available treatment is the technically difficult and often risky removal of excess bone tissue from the skull.

Acknowledgments

The authors like to thank Dr. H. Hamersma for providing clinical information and pictures of the patient with sclerosteosis presented in figure 1. This work was supported by grants from the European Commission (HEALTH-F2-2008-201099, TALOS) and NL Agency/IOP Genomics (IGE07001A). All authors have no competing interests to disclose.

References

1. National Osteoporosis Foundation. Facts on Osteoporosis. <http://www.nof.org/osteoporosis/diseasefacts.htm> . 2008.
2. van Buchem FS, Hadders HN, Ubbens R. An uncommon familial systemic disease of the skeleton: hyperostosis corticalis generalisata familiaris. *Acta radiol* 1955;44:109-20.
3. Hamersma H, Gardner J, Beighton P. The natural history of sclerosteosis. *Clin Genet* 2003;63:192-7.
4. Beighton P, Barnard A, Hamersma H, van der Wouden A. The syndromic status of sclerosteosis and Van Buchem disease. *Clin Genet* 1984;25:175-81.
5. Beighton P. Sclerosteosis. *J Med Genet* 1988;25:200-3.
6. Gardner JC, van Bezooijen RL, Mervis B, Hamdy NA, Löwik CW, Hamersma H *et al*. Bone mineral density in sclerosteosis; affected individuals and gene carriers. *J Clin Endocrinol Metab* 2005;90:6392-5.
7. van Bezooijen RL, ten Dijke P, Papapoulos SE, Löwik CW. *SOST*/sclerostin, an osteocyte-derived negative regulator of bone formation. *Cytokine Growth Factor Rev* 2005;16:319-27.
8. van Bezooijen RL, Papapoulos SE, Hamdy NAT, Löwik CWGM. *SOST*/sclerostin; an osteocyte-derived inhibitor of bone formation that antagonizes canonical Wnt signaling. In: Raisz LG, Martin TJ, Bilezikian JP, editors. *Principles of bone biology*. New York: Academic Press; 2008; p. 139-52.
9. Hill SC, Stein SA, Dwyer A, Altman J, Dorwart R, Doppman J. Cranial CT findings in sclerosteosis. *AJNR Am J Neuroradiol* 1986;7:505-11.
10. Stein SA, Witkop C, Hill SC, Fallon MD, Viernstein L, Gucer G *et al*. Sclerosteosis: neurogenetic and pathophysiologic analysis of an American kinship. *Neurology* 1983;33:267-77.
11. van Bezooijen RL, Roelen BA, Visser A, van der Wee-Pals, de Wilt E, Karperien M *et al*. Sclerostin is an osteocyte-expressed negative regulator of bone formation, but not a classical BMP antagonist. *J Exp Med* 2004;199:805-14.
12. van Bezooijen RL, Bronckers AL, Gortzak RA, Hogendoorn PC, van der Wee-Pals L, Balemans W *et al*. Sclerostin in mineralized matrices and Van Buchem disease. *J Dent Res* 2009;88:569-74.
13. van Lierop AH, Hamdy NA, Hamersma H, van Bezooijen RL, Power J, Loveridge N *et al*. Patients with sclerosteosis and disease carriers: human models of the effect of sclerostin on bone turnover. *J Bone Miner Res* 2011;26:2804-11.
14. Epstein S, Hamersma H, Beighton P. Endocrine function in sclerosteosis. *S Afr Med J* 1979;55:1105-10.
15. Beighton P, Durr L, Hamersma H. The clinical features of sclerosteosis. A review of the manifestations in twenty-five affected individuals. *Ann Intern Med* 1976;84:393-7.
16. Wergedal JE, Veskovc K, Hellan M, Nyght C, Balemans W, Libanati C *et al*. Patients with Van Buchem disease, an osteosclerotic genetic disease, have elevated bone formation markers, higher bone density, and greater derived polar moment of inertia than normal. *J Clin Endocrinol Metab* 2003;88:5778-83.
17. Balemans W, Ebeling M, Patel N, van Hul E, Olson P, Dioszegi M *et al*. Increased bone density in sclerosteosis is due to the deficiency of a novel secreted protein (*SOST*). *Hum Mol Genet* 2001;10:537-43.

18. Brunkow ME, Gardner JC, Van Ness J, Paeper BW, Kovacevich BR, Proll S *et al.* Bone dysplasia sclerosteosis results from loss of the *SOST* gene product, a novel cystine knot-containing protein. *Am J Hum Genet* 2001;68:577-89.
19. Balemans W, Cleiren E, Siebers U, Horst J, van Hul W. A generalized skeletal hyperostosis in two siblings caused by a novel mutation in the *SOST* gene. *Bone* 2005;36:943-7.
20. Kim CA, Honjo R, Bertola D, Albano L, Oliveira L, Jales S *et al.* A known *SOST* gene mutation causes sclerosteosis in a familial and an isolated case from Brazilian origin. *Genet Test* 2008;12:475-9.
21. Balemans W, Patel N, Ebeling M, Van Hul E, Wuyts W, Lacza C *et al.* Identification of a 52 kb deletion downstream of the *SOST* gene in patients with Van Buchem disease. *J Med Genet* 2002;39:91-7.
22. Staehling-Hampton K, Proll S, Paeper BW, Zhao L, Charmley P, Brown A *et al.* A 52-kb deletion in the *SOST*-*MEOX1* intergenic region on 17q12-q21 is associated with Van Buchem disease in the Dutch population. *Am J Med Genet* 2002;110:144-52.
23. Loots GG, Kneissel M, Keller H, Baptist M, Chang J, Collette NM *et al.* Genomic deletion of a long-range bone enhancer misregulates sclerostin in Van Buchem disease. *Genome Res* 2005;15:928-35.
24. van Lierop AH, Hamdy NA, van Egmond ME, Bakker E, Dijkers FG, Papapoulos SE. Van Buchem disease: Clinical, biochemical, and densitometric features of patients and disease carriers. *Journal of bone and mineral research* 2013;28:848-54.
25. Winkler DG, Sutherland MK, Geoghegan JC, Yu C, Hayes T, Skonier JE *et al.* Osteocyte control of bone formation via sclerostin, a novel BMP antagonist. *EMBO J* 2003;22:6267-76.
26. Poole KE, van Bezooijen RL, Loveridge N, Hamersma H, Papapoulos SE, Löwik CW *et al.* Sclerostin is a delayed secreted product of osteocytes that inhibits bone formation. *FASEB J* 2005;19:1842-4.
27. Ohshima Y, Nifuji A, Maeda Y, Amagasa T, Noda M. Spatiotemporal association and bone morphogenetic protein regulation of sclerostin and osterix expression during embryonic osteogenesis. *Endocrinology* 2004;145:4685-92.
28. Balemans W, Van Hul W. Extracellular regulation of BMP signaling in vertebrates: a cocktail of modulators. *Dev Biol* 2002;250:231-50.
29. Kusu N, Laurikkala J, Imanishi M, Usui H, Konishi M, Miyake A *et al.* Sclerostin is a novel secreted osteoclast-derived bone morphogenetic protein antagonist with unique ligand specificity. *J Biol Chem* 2003;278:24113-7.
30. Bellido T, Ali AA, Gubrij I, Plotkin LI, Fu Q, O'Brien CA *et al.* Chronic elevation of parathyroid hormone in mice reduces expression of sclerostin by osteocytes: a novel mechanism for hormonal control of osteoblastogenesis. *Endocrinology* 2005;146:4577-83.
31. Pockwinse SM, Wilming LG, Conlon DM, Stein GS, Lian JB. Expression of cell growth and bone specific genes at single cell resolution during development of bone tissue-like organization in primary osteoblast cultures. *J Cell Biochem* 1992;49:310-23.
32. Sutherland MK, Geoghegan JC, Yu C, Winkler DG, Latham JA. Unique regulation of *SOST*, the sclerosteosis gene, by BMPs and steroid hormones in human osteoblasts. *Bone* 2004;35:448-54.
33. Irie K, Ejiri S, Sakakura Y, Shibui T, Yajima T. Matrix mineralization as a trigger for osteocyte maturation. *J Histochem Cytochem* 2008;56:561-7.

34. Keller H, Kneissel M. *SOST* is a target gene for PTH in bone. *Bone* 2005;37:148-58.
35. Sutherland MK, Geoghegan JC, Yu C, Turcott E, Skonier JE, Winkler DG *et al.* Sclerostin promotes the apoptosis of human osteoblastic cells: a novel regulation of bone formation. *Bone* 2004;35:828-35.
36. Li X, Ominsky MS, Niu QT, Sun N, Daugherty B, D'Agostin D *et al.* Targeted deletion of the sclerostin gene in mice results in increased bone formation and bone strength. *J Bone Miner Res* 2008;23:860-9.
37. Aysian-Kretchmer O, Hsueh AJ. Comparative genomic analysis of the eight-membered ring cystine knot-containing bone morphogenetic protein antagonists. *Mol Endocrinol* 2004;18:1-12.
38. Ellies DL, Viviano B, McCarthy J, Rey JP, Itasaki N, Saunders S *et al.* Bone density ligand, Sclerostin, directly interacts with LRP5 but not LRP5G171V to modulate Wnt activity. *J Bone Miner Res* 2006;21:1738-49.
39. Clevers H. Wnt/beta-catenin signaling in development and disease. *Cell* 2006;127:469-80.
40. Boyden LM, Mao J, Belsky J, Mitzner L, Farhi A, Mitnick MA *et al.* High bone density due to a mutation in LDL-receptor-related protein 5. *N Engl J Med* 2002;346:1513-21.
41. Little RD, Carulli JP, Del Mastro RG, Dupuis J, Osborne M, Folz C *et al.* A mutation in the LDL receptor-related protein 5 gene results in the autosomal dominant high-bone-mass trait. *Am J Hum Genet* 2002;70:11-9.
42. Gong Y, Slee RB, Fukai N, Rawadi G, Roman-Roman S, Reginato AM *et al.* LDL receptor-related protein 5 (LRP5) affects bone accrual and eye development. *Cell* 2001;107:513-23.
43. Li X, Zhang Y, Kang H, Liu W, Liu P, Zhang J *et al.* Sclerostin binds to LRP5/6 and antagonizes canonical Wnt signaling. *J Biol Chem* 2005;280:19883-7.
44. Semenov M, Tamai K, He X. *SOST* is a ligand for LRP5/LRP6 and a Wnt signaling inhibitor. *J Biol Chem* 2005;280:26770-5.
45. van Bezooijen RL, Svensson JP, Eefting D, Visser A, van der Horst G, Karperien M *et al.* Wnt but not BMP signaling is involved in the inhibitory action of sclerostin on BMP-stimulated bone formation. *J Bone Miner Res* 2007;22:19-28.
46. Holdsworth G, Slocombe P, Doyle C, Sweeney B, Veverka V, Le Riche K *et al.* Characterization of the interaction of sclerostin with the low density lipoprotein receptor-related protein (LRP) family of Wnt co-receptors. *J Biol Chem* 2012;287:26464-77.
47. Veverka V, Henry AJ, Slocombe PM, Ventom A, Mulloy B, Muskett FW *et al.* Characterization of the structural features and interactions of sclerostin: molecular insight into a key regulator of Wnt-mediated bone formation. *J Biol Chem* 2009;284:10890-900.
48. Weidauer SE, Schmieder P, Beerbaum M, Schmitz W, Oschkinat H, Mueller TD. NMR structure of the Wnt modulator protein Sclerostin. *Biochem Biophys Res Commun* 2009;380:160-5.
49. Bourhis E, Wang W, Tam C, Hwang J, Zhang Y, Spittler D *et al.* Wnt antagonists bind through a short peptide to the first beta-propeller domain of LRP5/6. *Structure* 2011;19:1433-42.
50. Hens JR, Wilson KM, Dann P, Chen X, Horowitz MC, Wysolmerski JJ. TOPGAL mice show that the canonical Wnt signaling pathway is active during bone development and growth and is activated by mechanical loading *in vitro*. *J Bone Miner Res* 2005;20:1103-13.
51. Bonewald LF, Johnson ML. Osteocytes, mechanosensing and Wnt signaling. *Bone* 2008;42:606-15.

52. Krause C, Korchynskiy O, de Rooij K, Weidauer SE, de Gorter DJ, van Bezooijen RL *et al.* Distinct modes of inhibition by sclerostin on bone morphogenetic protein and Wnt signaling pathways. *J Biol Chem* 2010;285:41614-26.
53. Amrein K, Amrein S, Drexler C, Dimai HP, Dobnig H, Pfeifer K *et al.* Sclerostin and its association with physical activity, age, gender, body composition, and bone mineral content in healthy adults. *J Clin Endocrinol Metab* 2012;97:148-54.
54. Modder UI, Hoey KA, Amin S, McCready LK, Achenbach SJ, Riggs BL *et al.* Relation of age, gender, and bone mass to circulating sclerostin levels in women and men. *J Bone Miner Res* 2011;26:373-9.
55. Belaya ZE, Rozhinskaya LY, Melnichenko GA, Solodovnikov AG, Dragunova NV, Iljin AV *et al.* Serum extracellular secreted antagonists of the canonical Wnt/beta-catenin signaling pathway in patients with Cushing's syndrome. *Osteoporos Int* 2013.
56. Garcia-Martin A, Rozas-Moreno P, Reyes-Garcia R, Morales-Santana S, Garcia-Fontana B, Garcia-Salcedo JA *et al.* Circulating levels of sclerostin are increased in patients with type 2 diabetes mellitus. *J Clin Endocrinol Metab* 2012;97:234-41.
57. Morales-Santana S, Garcia-Fontana B, Garcia-Martin A, Rozas-Moreno P, Garcia-Salcedo JA, Reyes-Garcia R *et al.* Atherosclerotic Disease in Type 2 Diabetes Is Associated With an Increase of Sclerostin Levels. *Diabetes Care* 2013.
58. Gaudio A, Pennisi P, Bratengeier C, Torrisi V, Lindner B, Mangiafico RA *et al.* Increased sclerostin serum levels associated with bone formation and resorption markers in patients with immobilization-induced bone loss. *J Clin Endocrinol Metab* 2010;95:2248-53.
59. Sarahrudi K, Thomas A, Albrecht C, Aharinejad S. Strongly enhanced levels of sclerostin during human fracture healing. *J Orthop Res* 2012;30:1549-55.
60. Voskaridou E, Christoulas D, Plata E, Bratengeier C, Anastasilakis AD, Komninaka V *et al.* High circulating sclerostin is present in patients with thalassemia-associated osteoporosis and correlates with bone mineral density. *Horm Metab Res* 2012;44:909-13.
61. Yavropoulou MP, van Lierop AH, Hamdy NA, Rizzoli R, Papapoulos SE. Serum sclerostin levels in Paget's disease and prostate cancer with bone metastases with a wide range of bone turnover. *Bone* 2012;51:153-7.
62. van Lierop AH, Witteveen JE, Hamdy NA, Papapoulos SE. Patients with primary hyperparathyroidism have lower circulating sclerostin levels than euparathyroid controls. *Eur J Endocrinol* 2010;163:833-7.
63. Lapauw BM, Vandewalle S, Taes Y, Goemaere S, Zmierzczak HG, Collette J *et al.* Serum Sclerostin Levels In Men With Idiopathic Osteoporosis. *Eur J Endocrinol* 2013.
64. Appel H, Ruiz-Heiland G, Listing J, Zwerina J, Herrmann M, Mueller R *et al.* Altered skeletal expression of sclerostin and its link to radiographic progression in ankylosing spondylitis. *Arthritis Rheum* 2009;60:3257-62.
65. Saad CG, Ribeiro AC, Moraes JC, Takayama L, Goncalves CR, Rodrigues MB *et al.* Low sclerostin levels: a predictive marker of persistent inflammation in ankylosing spondylitis during anti-tumor necrosis factor therapy? *Arthritis Res Ther* 2012;14:R216.
66. Yadav VK, Ryu JH, Suda N, Tanaka KF, Gingrich JA, Schutz G *et al.* Lrp5 controls bone formation by inhibiting serotonin synthesis in the duodenum. *Cell* 2008;135:825-37.
67. Cui Y, Niziolek PJ, MacDonald BT, Zylstra CR, Alenina N, Robinson DR *et al.* Lrp5 functions in bone to regulate bone mass. *Nat Med* 2011;17:684-91.

68. Knothe Tate ML, Adamson JR, Tami AE, Bauer TW. The osteocyte. *Int J Biochem Cell Biol* 2004;36:1-8.
69. Han Y, Cowin SC, Schaffler MB, Weinbaum S. Mechanotransduction and strain amplification in osteocyte cell processes. *Proc Natl Acad Sci U S A* 2004;101:16689-94.
70. Tatsumi S, Ishii K, Amizuka N, Li M, Kobayashi T, Kohno K *et al*. Targeted ablation of osteocytes induces osteoporosis with defective mechanotransduction. *Cell Metab* 2007;5:464-75.
71. Robinson JA, Chatterjee-Kishore M, Yaworsky PJ, Cullen DM, Zhao W, Li C *et al*. Wnt/beta-catenin signaling is a normal physiological response to mechanical loading in bone. *J Biol Chem* 2006;281:31720-8.
72. Lin C, Jiang X, Dai Z, Guo X, Weng T, Wang J *et al*. Sclerostin mediates bone response to mechanical unloading through antagonizing Wnt/beta-catenin signaling. *J Bone Miner Res* 2009;24:1651-61.
73. Sawakami K, Robling AG, Ai M, Pitner ND, Liu D, Warden SJ *et al*. The Wnt co-receptor LRP5 is essential for skeletal mechanotransduction but not for the anabolic bone response to parathyroid hormone treatment. *J Biol Chem* 2006;281:23698-711.
74. Tu X, Rhee Y, Condon KW, Bivi N, Allen MR, Dwyer D *et al*. *Sost* downregulation and local Wnt signaling are required for the osteogenic response to mechanical loading. *Bone* 2012;50:209-17.
75. Robling AG, Niziolek PJ, Baldrige LA, Condon KW, Allen MR, Alam I *et al*. Mechanical stimulation of bone *in vivo* reduces osteocyte expression of *Sost/sclerostin*. *J Biol Chem* 2008;283:5866-75.
76. Moustafa A, Sugiyama T, Saxon LK, Zaman G, Sunters A, Armstrong VJ *et al*. The mouse fibula as a suitable bone for the study of functional adaptation to mechanical loading. *Bone* 2009;44:930-5.
77. Sevetson B, Taylor S, Pan Y. *Cbfa1/RUNX2* directs specific expression of the sclerosteosis gene (*SOST*). *J Biol Chem* 2004;279:13849-58.
78. Pleiner-Duxneuner J, Zwettler E, Paschalis E, Roschger P, Nell-Duxneuner V, Klaushofer K. Treatment of osteoporosis with parathyroid hormone and teriparatide. *Calcif Tissue Int* 2009;84:159-70.
79. Leupin O, Kramer I, Collette NM, Loots GG, Natt F, Kneissel M *et al*. Control of the *SOST* bone enhancer by PTH using MEF2 transcription factors. *J Bone Miner Res* 2007;22:1957-67.
80. Collette NM, Genetos DC, Economides AN, Xie L, Shahnazari M, Yao W *et al*. Targeted deletion of *Sost* distal enhancer increases bone formation and bone mass. *Proc Natl Acad Sci U S A* 2012;109:14092-7.
81. Silvestrini G, Ballanti P, Leopizzi M, Sebastiani M, Berni S, Di VM *et al*. Effects of intermittent parathyroid hormone (PTH) administration on *SOST* mRNA and protein in rat bone. *J Mol Histol* 2007;38:261-9.
82. O'Brien CA, Plotkin LI, Galli C, Goellner JJ, Gortazar AR, Allen MR *et al*. Control of bone mass and remodeling by PTH receptor signaling in osteocytes. *PLoS One* 2008;3:e2942.
83. Kramer I, Loots GG, Studer A, Keller H, Kneissel M. Parathyroid hormone (PTH)-induced bone gain is blunted in *SOST* overexpressing and deficient mice. *J Bone Miner Res* 2010;25:178-89.
84. Yao W, Cheng Z, Pham A, Busse C, Zimmermann EA, Ritchie RO *et al*. Glucocorticoid-induced bone loss in mice can be reversed by the actions of parathyroid hormone and risedronate on different pathways for bone formation and mineralization. *Arthritis Rheum* 2008;58:3485-97.

85. Yu L, van der Valk M, Cao J, Han CY, Juan T, Bass MB *et al.* Sclerostin expression is induced by BMPs in human Saos-2 osteosarcoma cells but not via direct effects on the sclerostin gene promoter or ECR5 element. *Bone* 2011;49:1131-40.
86. Kamiya N, Ye L, Kobayashi T, Lucas DJ, Mochida Y, Yamauchi M *et al.* Disruption of BMP signaling in osteoblasts through type IA receptor (BMPRIA) increases bone mass. *J Bone Miner Res* 2008;23:2007-17.
87. Goldring SR, Goldring MB. Eating bone or adding it: the Wnt pathway decides. *Nat Med* 2007;13:133-4.
88. Li X, Ominsky MS, Warmington KS, Morony S, Gong J, Cao J *et al.* Sclerostin antibody treatment increases bone formation, bone mass, and bone strength in a rat model of postmenopausal osteoporosis. *J Bone Miner Res* 2009;24:578-88.
89. Ominsky M, Stouch B, Doellgast G, Gong J, Cao J, Gao Y *et al.* Administration of Sclerostin Monoclonal Antibodies to Female Cynomolgus Monkeys Results in Increased Bone Formation, Bone Mineral Density and Bone Strength. *Proc Am Soc Bone Miner Res* . 2006.
90. Eddleston A, Marenzana M, Moore AR, Stephens P, Muzylak M, Marshall D *et al.* A Short Treatment with an Antibody to Sclerostin can Inhibit Bone Loss in an Ongoing Model of Colitis. *J Bone Miner Res* 2009.
91. Padhi D, Jang G, Stouch B, Fang L, Posvar E. Single-dose, placebo-controlled, randomized study of AMG 785, a sclerostin monoclonal antibody. *J Bone Miner Res* 2011;26:19-26.
92. McClung MR, Grauer A, Boonen S, Bolognese MA, Brown JP, Diez-Perez A *et al.* Romosozumab in postmenopausal women with low bone mineral density. *N Engl J Med* 2014;370:412-20.
93. Whyte MP, Reinus WH, Mumm S. High-bone-mass disease and LRP5. *N Engl J Med* 2004;350:2096-9.
94. Rickels MR, Zhang X, Mumm S, Whyte MP. Oropharyngeal skeletal disease accompanying high bone mass and novel LRP5 mutation. *J Bone Miner Res* 2005;20:878-85.
95. Kansara M, Tsang M, Kodjabachian L, Sims NA, Trivett MK, Ehrich M *et al.* Wnt inhibitory factor 1 is epigenetically silenced in human osteosarcoma, and targeted disruption accelerates osteosarcomagenesis in mice. *J Clin Invest* 2009;119:837-51.

A vertical strip on the left side of the page contains a grayscale microscopic image of bone tissue, showing various cellular structures and mineralized matrix.

Chapter 3

Serum dickkopf 1 levels in sclerostin deficiency

A.H. van Lierop
M.J.C. Moester
N.A.T. Hamdy
S.E. Papapoulos

Abstract

Context: Sclerostin and DKK1 are antagonists of the canonical Wnt signaling pathway, both binding to the same LRP5/6 receptor on osteoblasts, thereby inhibiting bone formation. It is not known whether there is an interaction between sclerostin and DKK1.

Objective: We examined whether a lack of sclerostin is compensated by increased DKK1 levels.

Design, setting and patients: We measured DKK1 levels in serum samples of patients and carriers of sclerosteosis (19 patients, 24 carriers) and Van Buchem disease (VBD) (13 patients, 22 carriers), and 25 healthy controls. Sclerosteosis and VBD are caused by deficient sclerostin synthesis and are characterised by increased bone formation and hyperostotic phenotypes.

Main outcome measures: DKK1 levels were compared between patients and carriers, and between patients and healthy controls. We also examined associations between levels of DKK1 and bone turnover markers P1NP and CTX.

Results: We found that DKK1 levels were significantly higher in patients with both sclerosteosis [4.28ng/ml (95%CI: 3.46-5.11ng/ml)] and VBD [5.28 ng/ml (95%CI: 3.84-6.71ng/ml)] compared to levels in carriers of the two diseases [sclerosteosis: 2.03ng/ml (95%CI: 1.78-2.29ng/ml) $p < 0.001$, VBD: 3.47ng/ml (95%CI: 2.97-3.97ng/ml) $p = 0.017$] and to levels in healthy controls [2.77ng/ml (95%CI: 2.45-3.08ng/ml), $p = 0.004$ and $p < 0.001$ respectively]. Serum DKK1 levels were positively associated with levels of P1NP and CTX in both disorders.

Conclusions: These results suggest that increased DKK1 levels observed in patients with sclerosteosis and VBD represent an adaptive response to the increased bone formation characterizing these diseases, although these increased levels do not compensate for the lack of sclerostin on bone formation.

Introduction

Sclerosteosis and Van Buchem disease (VBD) are two rare bone sclerosing dysplasias with closely related phenotypes, characterized by progressive bone overgrowth and very high bone mass [1]. Sclerosteosis is caused by loss-of-function mutations in the *SOST* gene, while patients with VBD lack a regulatory element for the *SOST* gene caused by a 52 kb deletion of genomic DNA 35 kb downstream of the *SOST* gene [1]. In both disorders, these genetic defects lead to impaired synthesis of sclerostin.

Sclerostin is a protein, predominantly synthesized in the skeleton by osteocytes, which decreases bone formation by inhibiting the terminal differentiation of osteoblasts and by promoting their apoptosis. Sclerostin binds to the low density lipoprotein receptor-related protein (LRP) 5/6 receptors and antagonizes the canonical Wnt-signaling pathway in osteoblasts [2]. The binding of sclerostin to LRP5/6 is facilitated by LRP4, a negative regulator of LRP5/6 signaling that augments the inhibitory activity of sclerostin on the Wnt signaling pathway [3]. Dickkopf 1 (DKK1) is a structurally unrelated Wnt antagonist, which similar to sclerostin, blocks the signaling cascade by binding to LRP5/6, a process facilitated by its co-receptor Kremen [4, 5], and inhibits bone formation by acting at different stages of osteoblast development [6]. A direct interaction between sclerostin and DKK1 has not been identified but it has been reported that sclerostin and DKK1 act through a common mechanism involving binding to the first β -propeller of LRP6 with a conserved amino acid motif present in both proteins, suggesting an interaction between them [7].

Because both sclerostin and DKK1 bind to the same receptors and both proteins inhibit bone formation, we hypothesized that the lack of sclerostin in sclerosteosis and VBD might affect the production of DKK1. In the present study we tested this hypothesis by measuring serum DKK1 levels in patients with sclerosteosis and VBD and in respective heterozygous carriers of these diseases.

Subjects and methods

Subjects

Previously collected serum samples from 19 patients with sclerosteosis and 24 carriers of the disease, and from 13 patients with Van Buchem disease (VBD) and 22 carriers of the disease were available for analysis. Detailed clinical characteristics of the subjects have been previously reported [8, 9]. In brief, patients and disease carriers of sclerosteosis were all Afrikaners from South Africa. Patients with sclerosteosis had the characteristic clinical manifestations of the disease, including syndactyly, facial distortion, facial palsy, hearing loss and increased intracranial pressure. None of the disease carriers had any symptoms or complications associated with sclerosteosis. The diagnosis was genetically confirmed in all subjects by the presence of homozygous or heterozygous mutations within the first exon of the *SOST* gene (C69T) in patients and carriers respectively. All patients and disease carriers of VBD were Dutch. Patients with VBD had clinical characteristics and complications similar, but of a milder degree than those of patients with sclerosteosis. In all patients and carriers with VBD the diagnosis was confirmed by presence of homozygous or heterozygous 52kb deletions downstream of the *SOST* gene in patients and carriers respectively.

Informed consent was obtained from all subjects and the study was approved by the Medical Ethical Committee of Leiden University Medical Center.

Serum biochemistry

Serum samples were measured for sclerostin using the MSD® 96-well MULTI-ARRAY® Human Sclerostin Assay (Meso-Scale Discoveries, Gaithersburg, USA), as previously described [8]. Serum was also measured for calcium adjusted for albumin, phosphate and creatinine using semi automated techniques. Serum procollagen type 1 amino-terminal propeptide (PINP) and carboxy-terminal cross-linking telopeptide (CTX) levels were determined by the E-170 system (Roche, Basel, Switzerland), 25-hydroxyvitamin D (25OHD) by the LIAISON 25-OH-Vitamin D TOTAL assay (DiaSorine S.A./N.V., Brussels, Belgium) and 1,25-dihydroxyvitamin D (1,25-DHD) concentrations by the LIAISON 1,25-(OH)₂ Vitamin D TOTAL assay (DiaSorine S.A./N.V., Brussels, Belgium). Serum DKK1 was measured by

the Quantikine® Human DKK-1 Immunoassay R&D systems (R&D systems Inc., Minneapolis, USA). In our hands the inter-assay and intra-assay precision were 5.8% and 10.4%, respectively. In 25 healthy men and women aged 20 to 63 years, with normal renal function and serum calcium concentrations, and serum P1NP concentration below 65 ng/ml, the mean serum DKK1 level was 2.77 ng/ml (95%CI: 2.45-3.08 ng/ml) range 1.40 to 4.83 ng/ml. These serum DKK1 values are very similar to those reported by the manufacturer of the assay (mean 2.5 ng/ml range 1.4 to 5.2 ng/ml) and by other investigators [10] with this assay (mean 2.4 ng/ml range 1.0 to 3.0 ng/ml). Fibroblast Growth Factor 23 (FGF23) levels were measured using the Kainos Intact Human FGF23 Elisa (Kainos Laboratories Inc., Tokyo, Japan). Intra-assay and inter-assay precisions were 9% and 11%, respectively. In 30 healthy controls with normal renal function, normal calcium and phosphate metabolism and normal serum P1NP levels, mean serum FGF23 was 28.7 pg/ml (95% CI:25.9-31.5 pg/ml).

Statistical analysis

Differences between patients and carriers of sclerosteosis and VBD were assessed using the Student's t-test. Pearson correlation test was used to assess the relationships between DKK1, biochemical markers of bone turnover and age. The SPSS 17.0 program (SPSS Inc., Chicago, USA) was used for the statistical analysis.

Results

Characteristics and biochemical measurements of all studied subjects are summarized in Table 1. Subjects were aged between 5 and 82 years. Patients with sclerosteosis were significantly younger than carriers of the disease, although there was no difference in mean age between patients with VBD and carriers.

All studied subjects had normal biochemical indices of mineral metabolism, and normal renal function. As previously reported, serum sclerostin levels were undetectable in patients with sclerosteosis and were very low in patients with VBD. Sclerostin levels were higher in the respective carriers of the two diseases, although still significantly lower than levels measured in healthy subjects [8, 9]. Serum 1,25-DHD concentrations were higher in patients with sclerosteosis compared to carriers of the disease. Serum FGF23 levels were within the normal reference range and not different between patients and carriers of both diseases.

Table 1. Group characteristics and biochemical parameters

	Sclerosteosis		Van Buchem disease		Reference Range
	Patients (n=19)	Carriers (n=24)	Patients (n=13)	Carriers (n=22)	
Age	28.3 ± 15.0	41.1 ± 14.5 *	40.5 ± 21.1	38.0 ± 17.3	
Creatinine (µmol/l)	62.2 ± 20.4	55.2 ± 12.4	77.5 ± 38.5	72.2 ± 12.0	< 120
Calcium (mmol/l)	2.33 ± 0.07	2.28 ± 0.11	2.25 ± 0.43	2.20 ± 0.19	2.15 - 2.55
Phosphate (mmol/l)	1.37 ± 0.32	1.20 ± 0.32	1.12 ± 0.34	1.11 ± 0.22	0.90 - 1.50
PTH (pmol/l)	5.39 ± 3.20	5.03 ± 2.75	8.09 ± 5.52	6.2 ± 4.17	1.5 - 8.0
1,25-DHD (pmol/l)	147.8 ± 55.2	92.0 ± 48.6 *	115.0 ± 56.6	117.1 ± 36.7	50 - 155
PINP (ng/ml)	353.8 ± 426.0	94.1 ± 122.5 *	293.1 ± 525.4	53.9 ± 24.4 *	< 65
CTX (pg/ml)	397.9 ± 393.8	133.5 ± 98.0 *	855.4 ± 1147.2	244.5 ± 136.3 *	< 600
Sclerostin (pg/ml)	0.0 ± 0.0	15.9 ± 4.7 *	8.1 ± 6.2	27.2 ± 8.5 *	14 - 66 \$
FGF23 (pg/ml)	29.4 ± 16.4	33.1 ± 9.1	24.8 ± 7.7	29.4 ± 9.9	13.3 - 44.1 \$\$

Values reported as mean ± standard deviation

* patients vs carriers p<0.05

\$ defined by mean levels ± 2 SD of 77 healthy controls

\$\$ defined by mean levels ± 2 SD of 30 healthy controls

PTH=parathyroid hormone

FGF23= fibroblast growth factor

1,25-DHD= 1,25 Dihydroxyvitamine D

Serum DKK1 levels ranged between 1.19 ng/ml and 10.02 ng/ml and children with sclerosteosis or VBD had the highest measured values. Patients with sclerosteosis had significantly higher DKK1 levels than carriers of the disease [4.28 ng/ml (95%CI: 3.46-5.11 ng/ml) vs 2.03 ng/ml (95%CI: 1.78-2.29 ng/ml), $p<0.001$]. Similarly, patients with VBD had significantly higher serum DKK1 levels [5.28 ng/ml (95%CI: 3.84-6.71 ng/ml)] than carriers of the disease [3.47 ng/ml (95%CI: 2.97-3.97 ng/ml), $p=0.017$] (Figure 1). These differences between patients with sclerostin deficiency and carriers remained significant after removal of the higher values of the children included in the analysis from the calculations [patients 3.90 ng/ml (95%CI: 3.32-4.48 ng/ml), carriers 2.7 ng/ml (95%CI: 2.39-3.07 ng/ml), $p<0.001$]. Compared to controls [2.77 ng/ml (95%CI: 2.45-3.08 ng/ml)], patients had significantly higher serum DKK1 values [sclerosteosis $p=0.004$, VBD $p<0.001$].

In patients and carriers of both diseases serum DKK1 levels were negatively correlated with age (sclerosteosis: $r=-0.64$, $p<0.001$; VBD: $r=-0.33$, $p=0.050$). DKK1 levels were positively correlated with serum PINP levels (sclerosteosis: $r=0.78$, $p<0.001$; VBD: $r=0.69$, $p<0.001$) and serum CTX levels (sclerosteosis: $r=0.74$, $p<0.001$; VBD: $r=0.64$, $p<0.001$). These relationships remained significant after adjustment for age.

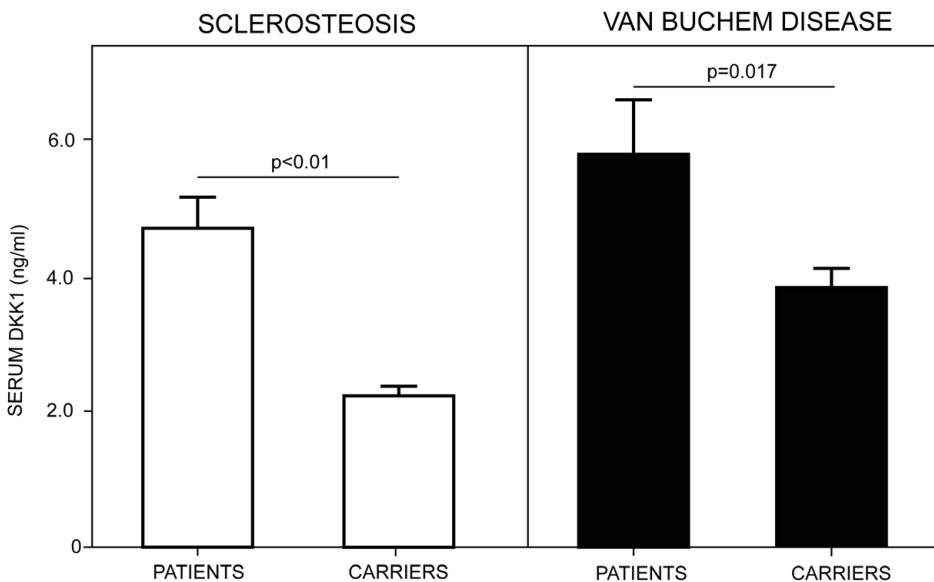


Figure 1. Mean serum DKK1 levels in patients and carriers of sclerosteosis (A) and VBD (B). Bars represent SEM.

Discussion

Our study shows that sclerostin deficiency, as occurs in patients with sclerosteosis or Van Buchem disease, is associated with higher circulating DKK1 levels compared to those of heterozygous carriers of either disease and of healthy subjects. Serum DKK1 concentrations have not been previously reported in sclerostin deficiency, but increased DKK1 expression has been observed in *Sost* knock-out mice (Dr. M. Kneissel, unpublished observations). These findings suggest an interaction between sclerostin and DKK1, two of the known inhibitors of the Wnt-signaling pathway in osteoblasts.

Previously reported measurements of both serum sclerostin and DKK1 in humans have provided variable results not allowing any conclusion to be drawn about a potential functional relationship between the two proteins. For example, serum DKK1 levels were found to be normal in patients with the high bone mass phenotype and high serum sclerostin levels, [11] as was also the case in women with osteoporosis treated with a bisphosphonate [12]. In patients with multiple myeloma and osteolytic bone disease, the levels of both inhibitors were found to be increased [13], whereas DKK1 levels were found to be increased in women with osteoporosis treated with teriparatide, which is associated with a decrease in serum sclerostin levels [14], also consistent with recent findings in patients with primary hyperparathyroidism [15]. Conversely, treatment with denosumab was associated with decreases in serum DKK1 and increases in serum sclerostin levels [16].

The increased serum DKK1 levels in patients with sclerostin deficiency we found in the present study may be related to the higher rate of bone formation and turnover observed in these patients, as illustrated by the positive correlation between DKK1 and the bone turnover markers P1NP, and CTX. Alternatively or in addition to this potential explanation, the higher serum DKK1 levels found in sclerostin deficiency may be an adaptive response to the lack of sclerostin, in an attempt to protect the skeleton from unrestrained bone formation. This notion is supported by the finding of the highest DKK1 values in children in whom the effect of sclerostin deficiency is most pronounced [8, 9]. Previous studies have shown no association between DKK1 values and age in either healthy adults [17-19] or children (Dr. P. Dimitri, personal communication). In sclerosteosis and VBD, bone overgrowth is progressive mainly during childhood, and both diseases stabilize during adulthood, as shown by a decline in serum levels of PINP with age [8, 9]. The finding of the

highest DKK1 levels in children is, therefore, in keeping with the natural course of the two sclerosing disorders and with the potential compensatory role of DKK1 for the underlying sclerostin deficiency. The hyperostotic phenotypes of sclerosteosis and VBD indicate, however, that the increased DKK1 synthesis is not able to fully compensate for the lack of sclerostin in these patients. Whereas both Wnt antagonists act by binding to the same LRP5/6 receptor, they have different mechanisms of action and expression pattern (sclerostin is expressed in bone by osteocytes while DKK1 by osteoblasts and osteocytes and outside bone) and they act on osteoblasts at different developmental stages. This might explain therefore why the functions of these two proteins are not fully compensatory, although sclerostin and DKK1 are both antagonists of the Wnt signaling pathway in osteoblasts.

Despite the profound changes in bone metabolism observed in patients with sclerostin deficiency, mineral metabolism is not generally affected in these patients. A recent study in *Sost* knock-out mice reported increased serum concentrations of 1,25-DHD and decreased levels of FGF-23 in these mice, suggesting that sclerostin deficiency may also affect mineral metabolism [20]. In contrast to patients with VBD, in whom there was no difference in 1,25-DHD levels between patients and carriers, we found higher serum 1,25-DHD concentrations in patients with sclerosteosis compared to carriers of the disease. Serum 1,25-DHD concentrations bore, however, no relationship to serum FGF-23 levels, which were within the normal range in all subjects whether patient or carrier, with no difference between patients and carriers of both diseases or healthy controls. Our results in humans do not, therefore, support the findings from the animal study.

In conclusion, we hypothesize that the higher levels of DKK1 we found in patients with sclerosteosis and Van Buchem disease and their carriers are a compensatory response to the prevalent sclerostin deficiency found in both diseases. This response is however insufficient to protect against the excessive bone formation characteristic of these disorders.

Acknowledgements

We are grateful to Dr. M. Kneissel and Dr. P. Dimitri for providing us their unpublished observations in mice and children, respectively. This work was supported by, and carried out within the FP7 program TALOS, funded by the EC (Grant Number: TALOS:Health-F2-2008-201099).

References

1. Moester MJC, Papapoulos SE, Löwik CWGM, Bezooijen RL. Sclerostin: Current Knowledge and Future Perspectives. *Calcif Tissue Int* 2010;87:99-107.
2. Li X, Zhang Y, Kang H, Liu W, Liu P, Zhang J *et al*. Sclerostin binds to LRP5/6 and antagonizes canonical Wnt signaling. *J Biol Chem* 2005;280:19883-7.
3. Leupin O, Piters E, Halleux C, Hu S, Kramer I, Morvan F *et al*. Bone overgrowth-associated mutations in the LRP4 gene impair sclerostin facilitator function. *J Biol Chem* 2011;286:19489-500.
4. Bafico A, Liu G, Yaniv A, Gazit A, Aaronson SA. Novel mechanism of Wnt signalling inhibition mediated by Dickkopf-1 interaction with LRP6/Arrow. *Nat Cell Biol* 2001;3:683-6.
5. Mao B, Wu W, Davidson G, Marhold J, Li M, Mechler BM *et al*. Kremen proteins are Dickkopf receptors that regulate Wnt/beta-catenin signalling. *Nature* 2002;417:664-7.
6. Tian E, Zhan F, Walker R, Rasmussen E, Ma Y, Barlogie B *et al*. The role of the Wnt-signaling antagonist DKK1 in the development of osteolytic lesions in multiple myeloma. *N Engl J Med* 2003;349:2483-94.
7. Bourhis E, Wang W, Tam C, Hwang J, Zhang Y, Spittler D *et al*. Wnt antagonists bind through a short peptide to the first beta-propeller domain of LRP5/6. *Structure* 2011;19:1433-42.
8. van Lierop AH, Hamdy NA, Hamersma H, van Bezooijen RL, Power J, Loveridge N *et al*. Patients with sclerosteosis and disease carriers: human models of the effect of sclerostin on bone turnover. *J Bone Miner Res* 2011;26:2804-11.
9. van Lierop AH, Hamdy NA, van Egmond ME, Bakker E, Dijkers FG, Papapoulos SE. Van Buchem disease: Clinical, biochemical, and densitometric features of patients and disease carriers. *Journal of bone and mineral research* 2013;28:848-54.
10. Daoussis D, Liossis SN, Solomou EE, Tsanaktsi A, Bounia K, Karampetsou M *et al*. Evidence that Dkk-1 is dysfunctional in ankylosing spondylitis. *Arthritis Rheum* 2010;62:150-8.
11. Frost M, Andersen T, Gossiel F, Hansen S, Bollerslev J, Van Hul W *et al*. Levels of serotonin, sclerostin, bone turnover markers as well as bone density and microarchitecture in patients with high-bone-mass phenotype due to a mutation in Lrp5. *J Bone Miner Res* 2011;26:1721-8.
12. Gatti D, Viapiana O, Adami S, Idolazzi L, Fracassi E, Rossini M. Bisphosphonate treatment of postmenopausal osteoporosis is associated with a dose dependent increase in serum sclerostin. *Bone* 2012;50:739-42.
13. Terpos E, Christoulas D, Katodritou E, Bratengeier C, Gkatzamanidou M, Michalis E *et al*. Elevated circulating sclerostin correlates with advanced disease features and abnormal bone remodeling in symptomatic myeloma: reduction post-bortezomib monotherapy. *Int J Cancer* 2012;131:1466-71.
14. Anastasilakis AD, Polyzos SA, Avramidis A, Toulis KA, Papatheodorou A, Terpos E. The effect of teriparatide on serum Dickkopf-1 levels in postmenopausal women with established osteoporosis. *Clin Endocrinol (Oxf)* 2010;72:752-7.
15. Viapiana O, Fracassi E, Troplini S, Idolazzi L, Rossini M, Adami S *et al*. Sclerostin and DKK1 in primary hyperparathyroidism. *Calcif Tissue Int* 2013;92:324-9.
16. Gatti D, Viapiana O, Fracassi E, Idolazzi L, Dartizio C, Povino MR *et al*. Sclerostin and DKK1 in postmenopausal osteoporosis treated with denosumab. *J Bone Miner Res* 2012;27:2259-63.

17. Voorzanger-Rousselot N, Journe F, Doriath V, Body JJ, Garnero P. Assessment of circulating Dickkopf-1 with a new two-site immunoassay in healthy subjects and women with breast cancer and bone metastases. *Calcif Tissue Int* 2009;84:348-54.
18. Marshall MJ, Evans SF, Sharp CA, Powell DE, McCarthy HS, Davie MW. Increased circulating Dickkopf-1 in Paget's disease of bone. *Clin Biochem* 2009;42:965-9.
19. Butler JS, Murray DW, Hurson CJ, O'Brien J, Doran PP, O'Byrne JM. The role of Dkk1 in bone mass regulation: correlating serum Dkk1 expression with bone mineral density. *J Orthop Res* 2011;29:414-8.
20. Ryan ZC, Ketha H, McNulty MS, McGee-Lawrence M, Craig TA, Grande JP *et al.* Sclerostin alters serum vitamin D metabolite and fibroblast growth factor 23 concentrations and the urinary excretion of calcium. *Proc Natl Acad Sci U S A* 2013;110:6199-204.



Chapter 4

First missense mutation in the SOST gene causing sclerosteosis by loss of sclerostin function

E. Piters, C. Culha,
M. Moester, R. van Bezooijen,
D. Adriaensen, T. Mueller,
S. Weidauer, K. Jennes,
F. de Freitas, C. Löwik,
J.P. Timmermans, W. Van Hul,
S. Papapoulos

Hum Mutat. 2010 Jul;31(7):E1526-43

Abstract

Sclerosteosis is a rare bone dysplasia characterized by greatly increased bone mass, especially of the long bones and the skull. Patients are tall, show facial asymmetry and often have syndactyly. Clinical complications are due to entrapment of cranial nerves. The disease is thought to be due to loss-of-function mutations in the *SOST* gene. The *SOST* gene product, sclerostin, is secreted by osteocytes and transported to the bone surface where it inhibits osteoblastic bone formation by antagonizing Wnt signaling. In a small Turkish family with sclerosteosis, we identified a missense mutation (c.499T>C; p.Cys167Arg) in exon 2 of the *SOST* gene. This type of mutation has not been previously reported and using different functional approaches, we show that it has a devastating effect on the biological function of sclerostin. The affected cysteine is the last cysteine residue of the cystine-knot motif and loss of this residue leads to retention of the mutant protein in the ER, possibly as a consequence of impaired folding. Together with a significant reduced ability to bind to LRP5 and inhibit Wnt signaling, the p.Cys167Arg mutation leads to a complete loss of function of sclerostin and thus to the characteristic sclerosteosis phenotype.

Introduction

Bone mineral density (BMD) in humans is a quantitative trait determined to a great extent by genetic factors [1, 2]. The involvement of genes has been clearly demonstrated in patients with sclerosing bone dysplasias, a heterogeneous group of 40 different monogenetic diseases associated with increased BMD. One subgroup comprises the craniotubular hyperostoses, mainly characterized by increased cortical thickness of the long bones and the skull [3, 4]. Sclerosteosis (SCL; MIM# 269500) and Van Buchem disease (VBD; MIM# 239100) are two closely related, rare craniotubular hyperostoses with an autosomal recessive mode of inheritance.

Patients with SCL show progressive bone overgrowth and thickening, especially of the skull, the mandible and the tubular bones. Patients are tall and have facial distortion due to enlargement of the mandible and forehead. Entrapment of cranial nerves often results in facial nerve palsy, hearing loss, and loss of smell. Calvarial overgrowth leads to elevated intracranial pressure causing headache and occasionally sudden death. The majority of patients with SCL have some degree of hand malformations, mainly syndactyly. These features are not present in patients with VBD and together with tall stature, may allow the clinical differentiation of the two conditions [5-8]. Sclerosteosis has a high prevalence in the Afrikaner population in South-Africa. In addition, it has been reported in isolated individuals or families from Spain, Brazil, the USA, Germany, Japan and Senegal [9-16]. Apart from an isolated family in Scotland, patients with VBD are Dutch, originating from an isolated community in The Netherlands [17]. Because the Afrikaner population is of Dutch origin, it was assumed that SCL and VBD were caused by the same genetic defect. The mapping of SCL to locus 17q12-21, the region that was also shown to contain the gene responsible for VBD, further supported this hypothesis [18, 19]. However, genetic analysis revealed that the two conditions have a different genetic defect. Through positional cloning, Balemans *et al.* identified two homozygous nonsense mutations (c.372G>A (p.Trp124X); c.376C>T (p.Arg126X)) in a Brazilian and an American SCL family, respectively, and a splice site mutation (c.220+3A>T) in a Senegalese patient with SCL in the previously unknown *SOST* gene (MIM# 605740) [20]. Simultaneously, Brunkow *et al.* identified a homozygous nonsense mutation (c.70C>T (p.Gln24X)) in affected individuals from South Africa. The nonsense mutations lead to premature termination of the protein, while the c.220+3A>T

mutation was shown to alter splicing of the *SOST* gene [21]. In 2005, another splice-site mutation (c.220+1G>C) in the *SOST* gene was reported in two affected siblings of German origin, putatively disease-causing in the same way as the c.220+3A>T mutation [22]. In the Dutch patients diagnosed with VBD no *SOST* mutation was present, but a 52kb deletion downstream of the *SOST* gene was identified. This deleted region harbours an enhancer element that drives the expression of the *SOST* gene explaining the similarities between the two conditions [23, 24]. All of the reported mutations in *SOST* as well as the deletion found in patients with VBD, result in the absence of expression of the *SOST* gene product sclerostin by osteocytes [25, 26].

In patients with SCL and VBD, the increase in BMD is due to increased bone formation [14, 26-28]. In addition, mouse models with deletion or overexpression of the *SOST* gene as well as *in vitro* studies of osteoblast proliferation and differentiation, matrix mineralization and apoptosis demonstrated that sclerostin has an inhibitory action on bone formation [26, 29-32]. Although the precise molecular mechanism of action of sclerostin still needs to be elucidated, it has been shown that it antagonizes Wingless-Int (Wnt) signaling and binds directly to the first two β -propellers of low density lipoprotein receptor related protein (LRP) 5, but does not compete with the binding of Wnt proteins to LRP5/6 receptors [31, 33, 34]. LRP5 is required for the transduction of Wnt signals and the first β -propeller domain of LRP5 is known to harbour mutations causing a High Bone Mass (HBM) phenotype [35-37]. This condition is also classified among the craniotubular hyperostoses and has an autosomal dominant mode of inheritance. For all these LRP5 mutants, binding to sclerostin was found to be impaired [38-40]. Furthermore, just like in patients with VBD and SCL, the bone thickening is most obvious at the long bones and the mandible, favouring a shared pathogenesis with SCL and VBD [41].

In this paper, we describe the genetic analysis of a patient with SCL and her relatives resulting in the identification of the first missense mutation in the *SOST* gene. This mutation results in the exchange of a cysteine residue of the cysteine-knot motif of sclerostin for a non-cysteine amino acid, a defect that leads to a complete loss of function of sclerostin due to retention of the mutated protein in the ER.

Materials and methods

Mutation analysis

We analysed both exons of the *SOST* gene as well as exon 2, 3 and 4 of the *LRP5* gene that comprise the first β -propeller domain of the *LRP5* protein, in which all mutations causing craniotubular hyperostoses cluster. In a first step, amplification was performed by GoTaq DNA polymerase-mediated PCR (Promega Corporation, Madison, Wisconsin, USA). Primers used to generate fragments containing the exons and its exon-intron boundaries of the *SOST* gene were: forward primer (FW) 5'-AGAATTCTCTCCTCCACCC-3' and reverse primer (R) 5'-GTGCTACTGGAAGGTGGC-3' for exon 1 and FW 5'-CCCCTGCCCTGGGTTGC-3' and R 5'-CTTTCCACCAGCTCTAGAGC-3' for exon 2. For *LRP5*, exon 2 was amplified using FW 5'-AACTTCCTGACAACGCCTTAGG-3' and R 5'-TGCCATTGAGGTTGGCCACC-3', exon 3 using FW 5'-CGATGGGTGAGATTTTAGGG-3' and R 5'-TGACGCTGTTCCAAGTTCTG-3', and exon 4 with FW 5'-GGGTCAGCAGCAATGACTGTCCG-3' and R 5'-CCAGAGCATGGGCTTCTGCAGG-3'. Amplified fragments were verified by agarose gel electrophoresis and compared with the Generuler 100 bp Plus DNA Ladder (Fermentas International Inc, Ontario, Canada). Primers and unincorporated deoxyribonucleotide triphosphates (dNTPs) were removed using exonuclease I (New England Biolabs, Inc, Ipswich, Massachusetts, USA) and calf intestine alkaline phosphatase (CIAP, Roche Applied Science, Hoffmann-La Roche AG, Basel, Switzerland). Sequencing was carried out directly on purified fragments with the ABI 310 Genetic Analyser (Applied Biosystems, Foster City, California, USA), using ABI Prism BigDye Terminator Cycle Sequencing Ready Reaction Kit, version 1.1 (Applied Biosystems, Foster City, California, USA). The BigDye XTerminator Purification Kit was used as purification method for DNA sequencing to remove unincorporated BigDye terminators.

Expression constructs and *in vitro* mutagenesis

Alignment of the human sclerostin protein sequence (GenBank RefSeq NM_025237.2) and its homologue in mouse (GenBank RefSeq NM_024449.5) showed that c.493T>C (p.Cys165Arg) in mouse corresponds with c.499T>C (p.Cys167Arg) in human (nucleotide numbering refers to the cDNA RefSeq

using the A of the ATG translation initiation codon as nucleotide +1). Using the QuikChange Site-Directed Mutagenesis Kit (Stratagene, La Jolla, California), we introduced this mutation in a pcDNA3.1 plasmid that produces a secreted form of the WT mouse sclerostin with an HA tag at the amino terminus (WT mSost-HA). This construct contains the following elements (5' to 3'): NheI site, IgG kappa light chain signal peptide sequence (QTHILLWVLLLWVQGSTD), HA tag sequence (YPYDVPDYA), two linker peptide residues (GA), EcoRI site, mSost lacking endogenous signal peptide, termination codon, and XhoI site. Following primers were used for *in vitro* mutagenesis: FW 5'CCTCGTGCAAGCGCAAGCGCC- 3' and R 5'-GGTGAGGCGCTTGCGCTTGCA-3'. The complete insert sequence was verified for the presence of the mutation and for the absence of PCR introduced errors, using FW 5'ACCGAGTTGGTGTGCTCC- 3' and R 5'-GCACAGCAGCTGCACCC-3' as primers for direct sequencing on plasmid DNA. Although the mouse *Sost* gene has high similarity with the human *SOST* gene in the affected region, a human *SOST* construct was also used and the p.Cys167Arg mutation was introduced by site-directed mutagenesis at Genscript, Piscataway, USA.

The expression construct mouse Wnt1-V5 was kindly provided by Bart Williams (Van Andel Research Institute, USA) and *Mesdc2* by Bernadette Holdener (State University of New York, USA). Both untagged full-length human WT-LRP5 and truncated human WT-LRP5 lacking the transmembrane and cytoplasmic domains but with a c-myc epitope at the carboxy-terminus were obtained from Matthew Warman (Howard Hughes Medical Institute, Orthopaedic Research Laboratories, USA). Bert Vogelstein (The Johns Hopkins University School of Medicine, USA) provided the Topflash Wnt reporter construct (pGL3-OT) while the BAT-luc Wnt reporter construct was provided by Stefano Piccolo (University of Padua School of Medicine, Italy). The Renilla luciferase constructs pRL-TK and pRL-SV40 were purchased from Promega Corporation.

Red fluorescent protein (RFP) fusion proteins for WT and MT mouse *Sost* were generated using the above described WT and MT mSost-HA as a template. PCR amplification was performed to disrupt the termination codon and the complete region of interest was subcloned into a pTurboFP635-N vector (Evrogen JSC, Moscow, Russia) to obtain WT and MT mSost-RFP, respectively. A vector encoding a termination codon in the mSost gene served as a negative control (ter-mSost-RFP).

Immunoblotting

The human embryonic kidney (HEK) cell line 293T obtained from Danny Huylebroeck (University of Leuven, Leuven, Belgium), was grown in DMEM (Gibco- Invitrogen Ltd, Paisley, UK) supplemented with FBS (10% v/v). Twenty-four hours prior to transfection, HEK293T cells were plated at 4×10^5 cells/well in 6-well plates (Greiner Bio-One, Kremsmünster, Austria). Cells were transiently transfected with either WT or MT *mSost*-HA or empty pcDNA3.1 vector (500 ng/well) using FuGENE 6 (Roche Applied Science), according to the manufacturer's instructions. Twenty-four hours after transfection, the culture medium was changed to 1 ml serum-free DMEM and 48 h after transfection, conditioned medium (CM) was collected and cells were lysed with 500 μ l radioimmune precipitation (RIPA) buffer per well (50 mM Tris-HCl pH 8.0; 150 mM NaCl; 1% NP-40; 0.5% Na-deoxycholate; 0.1% SDS; complete protease inhibitor cocktail tablet (Roche Applied Science); benzonase endonuclease (Merck, Darmstadt, Germany)). Total protein in cell lysates was quantified using a bicinchoninic acid (BCA) assay (Pierce, Illinois, USA) with the purpose of loading equal protein amounts on SDS-PAGE. CM and cell lysates were diluted in 5x SDS-PAGE loading buffer and subjected to reducing SDS-PAGE. After transfer to a PVDF membrane, sclerostin-HA was detected using a rabbit polyclonal HA antibody (1:2000; BD Biosciences, San Diego, CA). Equal protein loading for lysate fractions was verified with a mouse β -actin antibody (1:5000; Sigma-Aldrich, St. Louis, MO). Secondary incubation was performed using a goat anti-rabbit IgG-HRP (1:10000; Biorad) and a sheep anti-mouse IgG-HRP (1:5000; Amersham Biosciences), respectively, for 2 h at room temperature. Chemiluminescence detection was carried out using the Enhanced Chemiluminescence (ECL) Western Blotting Substrate (Pierce) according to the manufacturer's instructions.

Electrochemiluminescence assay by Meso-Scale Discovery

HEK293T cells and Saos-2 human sarcoma cells (ATCC) were grown in DMEM supplemented with FBS (10% v/v). Twenty-four hours prior to transfection, HEK293T and Saos-2 cells were plated at 1.3×10^5 and 4.5×10^4 cells/well in 24-well plates (Greiner Bio-One), respectively. Cells were transfected with WT and MT constructs of both mouse and human *Sost/SOST* or a control plasmid (empty pcDNA3.1). After 24h, medium was replaced and after further incubation for 24 h, CM was collected

and cells were lysed with 250 μ l Meso-Scale Discovery (MSD, Gaithersburg, MD, USA) lysis buffer per well (20 mM Tris-HCl pH 7.5; 150 mM NaCl; 1 mM EDTA; 1 mM EGTA; 1% Triton X-100; complete protease inhibitor cocktail tablet (Roche Applied Science); 10 mM NaF) or total RNA was isolated for RT-PCR analysis. Sclerostin levels in CM and cell lysates were determined using the 96-well MULTI-ARRAY[®] human sclerostin assay (MSD) according to the manufacturer's instructions and corrected for *SOST* mRNA expression as determined by RT-PCR analysis.

Co-localisation studies using confocal live cell imaging

HEK293T and Saos-2 cells were grown in DMEM supplemented with FBS (10% v/v). Twenty-four hours prior to transfection, cells were plated at low-density (0.5×10^5 cells/well) in 24-well plates (Greiner Bio-One). Both cell types were transfected with WT or MT *mSost*-RFP plasmid DNA, or with the *ter-mSost*-RFP as an empty control (200 ng). FuGENE 6 (Roche Applied Science) was used for transfection; FuGENE 6 reagent: DNA ratio was slightly higher for Saos-2 cells (4:1) than for HEK293T cells (6:1). Twenty-four hours after transfection, medium was removed and cells were rinsed with 1x Hanks balanced salt solution (HBSS) (Gibco Invitrogen Ltd). In addition, staining with a green fluorescent tracer for live-cell ER labeling (ER-Tracker[™] Green (glibenclamide BODIPY[®] FL); Molecular Probes Invitrogen Ltd) was performed. Cells were incubated for 20 min at 37°C after adding 1 μ M ER-Tracker[™] Green staining solution. Subsequently, the staining solution was replaced by probe-free medium and cells were imaged using an inverted microscope (Zeiss Axiovert 200; Carl Zeiss, Jena, Germany) attached to a microlensenhanced dual spinning disk confocal system (UltraVIEW ERS, PerkinElmer, Seer Green, UK), equipped with a three-line (488, 568 and 647 nm) argon–krypton laser. Red fluorescent fusion proteins (excitation maximum (ex max): 553 nm; emission maximum (em max): 574 nm) were excited by the 568 nm line while the green ER stain (ex max: 504 nm; em max: 511 nm) was excited by the 488 nm line. Fluorescence was recorded using 527/55 nm and 615/70 nm band pass filters, respectively. Multicolor high-resolution time-lapse images (4 images/s) of the living cells were captured over a time period of 5 min. Data were analyzed by Volocity 5 software (Improvision, PerkinElmer).

Wnt activity reporter assays

Saos-2 cells were grown in DMEM supplemented with FBS (10% v/v). Twenty-four hours prior to transfection, cells were plated at 1.25×10^5 cells/well in 24-well plates and at 6.75×10^3 cells/well in 96-well plates (Greiner Bio-One) for stimulation with Wnt1-V5 and recombinant Wnt3A (rec Wnt3A), respectively. Cells were transfected using FuGENE 6 or FuGENE HD (Roche Applied Science), respectively, according to the manufacturer's instructions. For stimulation with Wnt1-V5 (100 ng/well), cells were co-transfected with *Mesdc2* (20 ng/well), pGL3-OT reporter (100 ng/well) and untagged full length WT-LRP5 (20 ng/well) in the presence or absence of WT or MT *mSost*-HA (40 ng/well). For stimulation with rec Wnt3A, cells were transfected with untagged full length WTLRP5 (40 ng/well) and BAT-luc (20 ng/well) and stimulated with 30 ng/ml rec Wnt3A, 24h after the transfection. When necessary, empty pcDNA3.1 vector was added to make the total DNA amount equal for all transfection experiments. The Renilla luciferase constructs pRL-TK and pRL-SV40 were co-transfected to correct for transfection efficiency of Wnt1-V5 and rec Wnt3A, respectively. Forty-eight hours after transfection, cells were lysed using 100 μ l passive lysis buffer (Promega Corporation). Firefly and Renilla luciferase activity were measured using the dual-luciferase reporter assay system (Promega Corporation) according to manufacturer's instructions.

Co-immunoprecipitation

Conditioned media and cell lysates containing WT or MT-sclerostin-HA were obtained as described above. In case of LRP5, HEK293T cells were co-transfected with truncated human WT-LRP5-myc (1 μ g) and, in equal amounts, *Mesdc2*. Proper expression of LRP5-myc protein in CM was evaluated by immunoblotting with c-myc antibodies (clone 9E10; Sigma-Aldrich; dilution 1:5000). Rabbit polyclonal HA antibody was used to verify the presence of WT and MT sclerostin-HA in CM or total cell lysates. Equal protein loading for lysate fractions was verified using β -actin antibodies. Based on these results, sclerostin-containing CM or total cell lysates were diluted more in the co-immunoprecipitation (co-IP) reactions than LRP5-containing CM. Co-IP between sclerostin and LRP5 was carried out by mixing CM containing truncated WT-LRP5-myc with CM containing WT-sclerostin-HA or cell lysates containing MT-sclerostin-HA, respectively. For the co-

IP reactions, EZ-view™ Red Anti-HA affinity gel (Sigma-Aldrich) was pre-blocked for 1h with 3% BSA (Sigma-Aldrich) in 1x TBS buffer (pH7.8) at 4°C using a rotation shaker. Hundred µl of CM containing WT-sclerostin-HA or cell lysates containing MTsclerostin-HA was mixed with equivalent amounts of secreted LRP5 (total CM volume of 250 µl), together with 45 µl of pre-blocked EZ-view™ Red Anti-HA affinity gel. The final volume was adjusted to 1 ml with 1x TBS, and incubated for 4h at 4°C using a rotation shaker. To remove unbound proteins, the affinity gel was washed at 4°C in wash buffer (50 mM Tris-HCl pH7.5; 150 mM NaCl; 0.1% Triton-X100) for 5 min, and then pelleted. Protein complexes were eluted by resuspending the pellets in 1x PBS buffer containing 100 µg/ml HA-peptide (Sigma- Aldrich). After 15 min incubation at room temperature, supernatants were collected and stored for SDS-PAGE. To serve as a positive control for binding to the affinity column, IP was also performed by adding a comparable volume of CM containing WT-sclerostin-HA, or cell lysates containing MT-sclerostin-HA to the preblocked EZ- view™ Red Anti-HA affinity gel. In the same way, a comparable volume of CM containing truncated WT-LRP5myc not expressing the HA-tag, was used as a negative control for IP on an anti-HA affinity gel. Following transfer to PVDF, LRP5-myc and sclerostin-HA were incubated with anti-c-myc and anti-HA, respectively. Subsequently, LRP5-myc and β-actin proteins were incubated with secondary anti-mouse IgG-HRP for 2h at room temperature; sclerostin-HA with a secondary goat anti-rabbit IgG-HRP. Chemiluminescence detection was carried as described above.

Statistical analysis

Data are expressed as mean values \pm SD. Comparisons between two or more measurements for a single experiment were performed using a Student's t-test and one-way ANOVA, respectively. For a set of experiments, general linear model (GLM) was used. Values of $p < 0.05$ were considered significant. In case of post hoc multiple comparisons, Bonferroni was used. All statistical tests were provided by the SPSS 15.0 software package (SPSS Inc.).

Modeling of MT sclerostin

Modeling of the effect of the mutation was based on the NMR structure of mouse sclerostin (PDB entry 2KD3). The coordinates comprising the residues Asn59 to

Arg167 of mouse sclerostin (corresponding to residues Asn61 to Arg169 of human sclerostin) were used for the analysis. After adapting the numbering to human sclerostin residue Cys167 was replaced by arginine using the protein modeling tools of the software package Quanta2006 (Accelrys Inc, San Diego). Due to the previous amino acid Cys167 being involved in a disulfide bond with residue Cys109 and the resulting steric clash with the large side chain of the Arg167 introduced, the side chain was manually reoriented such that the side chain of Arg167 pointed towards the solvent requiring changes in the backbone conformation of the lower part of the flexible loop (starting from residue Gly110). The structure was subsequently refined by energy minimization runs; only geometrical energy terms without any electrostatic contribution were employed. Analysis of the resulting structure of MT sclerostin showed comparable statistics for backbone torsion angle distribution and van der Waals contacts. To test whether the replacement of Cys167 into Arg167 influences the flexibility of the loop, which has been proposed to contain the binding epitope of sclerostin for LRP5, molecular dynamics (MD) simulation runs were performed with or without NMR distance restraints derived for WT mouse sclerostin. All dynamics simulations were done using the software package Quanta2006 and the force field CHARMM22 without electrostatic energy terms (Accelrys Inc, San Diego), the non-bonded cut-off for van der Waals interactions was set to 10.5Å, the temperature of the bath was kept at 300K to allow for sufficient mobility of the atoms.

Results

Clinical description

A 28-year old Turkish woman from a consanguineous marriage was recognized with clinical features suggestive of SCL (Figure 1A) and HBM during investigation of a multinodular goitre. She suffered from recurrent facial nerve palsies at the ages of 9, 14 and 15 years, complained of severe headaches, and had bilateral mixed-type hearing loss and right visual loss. Her height was 190 cm, weight 76 kg and head circumference 66.5 cm. The skull and jaw were enlarged, and she had proptosis and high arched palate. No syndactyly or other hand malformations were observed. Skull radiographs showed thickening of the calvarium (Figure 1B-C), an enlarged mandible and a highly increased BMD (T-score: spine +10.6, femoral neck +9.6).

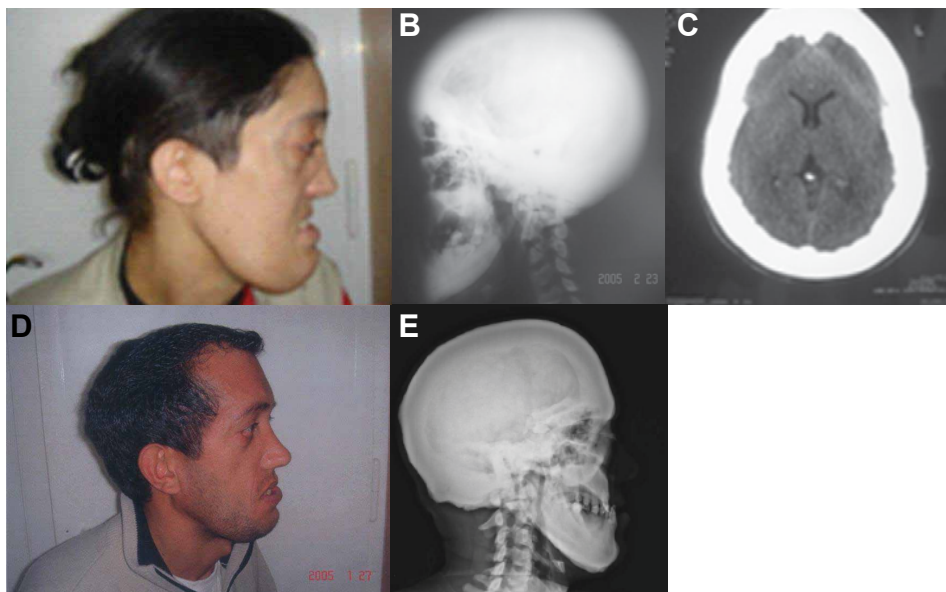


Figure 1. A) Lateral view of the female patient's face showing a marked mandibular prognathism. B) Plain radiograph of the skull (lateral view) showing uniform sclerosis of the calvaria, skull base and facial bones (particularly the mandible). C) Axial CT-scan of the brain showing marked thickening of the cranial vault. D) Lateral view of the face of the female's brother, who also shows a marked mandibular prognathism. E) Plain radiograph of the skull (lateral view) of the brother, showing uniform sclerosis of the skull and the mandible.

Endocrinological investigations revealed no abnormalities except for thyroid function compatible with subclinical hyperthyroidism. Her 35-year-old brother showed a similar phenotype with a rather uniform sclerosis of the skull, a thickened calvarium and an enlarged mandible, which can be noticed from the radiographs (Figure 1D-E). This patient also was of tall stature (190 cm), had a large head (head circumference: 66 cm) and a highly increased BMD (T-score: spine +9.8, femoral neck +7.3). Similar to his sister, he had no syndactyly or other hand malformations. Information on the presence of additional clinical symptoms was lacking. Other family members were phenotypically normal.

Mutation analysis

Because mutations in *LRP5* and *SOST* are known to be causal for craniotubular hyperostoses, we evidently included both genes in the mutation screening of the patient. Direct sequencing of the *LRP5* gene revealed no mutations in the coding region of the gene or in the exon-intron boundaries. Instead, we found a homozygous

c.499T>C (p.Cys167Arg) mutation in exon 2 of the *SOST* gene (nucleotide numbering refers to the cDNA RefSeq using the A of the ATG translation initiation codon as nucleotide +1) (data not shown). To investigate whether the mutation segregated with the disease, additional family members were recruited and sequenced. This resulted in the identification of the same homozygous missense mutation in an affected brother. Both unaffected parents and an unaffected sibling were found to be heterozygous carriers. Eighty unrelated healthy control individuals (160 chromosomes) from Turkish origin were checked for the presence of this mutation and all turned out to be negative.

Decreased intracellular and extracellular levels of MT sclerostin

Since sclerostin is a secreted protein, we initially tested the intra- and extracellular presence of the mutated protein by transient transfection of HEK293T cells with WT and MT mouse *Sost*-HA plasmids. Transfection with a negative control plasmid (empty pcDNA3.1) was also included. All transfection efficiencies were similar as measured by β -galactosidase activity (data not shown). By immunoblotting, both WT and MT sclerostin were detected in the cell lysates, indicating that the MT protein was formed and recognized by the HA antibody. Moreover, the increased presence of MT sclerostin in the cell lysate suggested an upregulation of expression of the functionally inactive MT sclerostin. In CM, only WT sclerostin was present (Supplementary Figure 1A).

To further investigate the effect of the mutation on intra- and extracellular levels of sclerostin, a quantitative electrochemiluminescence assay was used to measure the concentration of WT and MT mouse sclerostin in HEK293T cells (Supplementary Figure 1B-C) and Saos-2 cells (data not shown). In addition, human *SOST* plasmids with or without the mutation were tested in both cell lines. After correction for *SOST* mRNA, both the intra- and extracellular levels of mouse and human MT sclerostin were lower than those of WT sclerostin. The levels of human sclerostin were consistently higher than those of mouse sclerostin, which may be due to differences in expression efficiency of the plasmids and/or the sensitivity of the assay to mouse and human sclerostin.

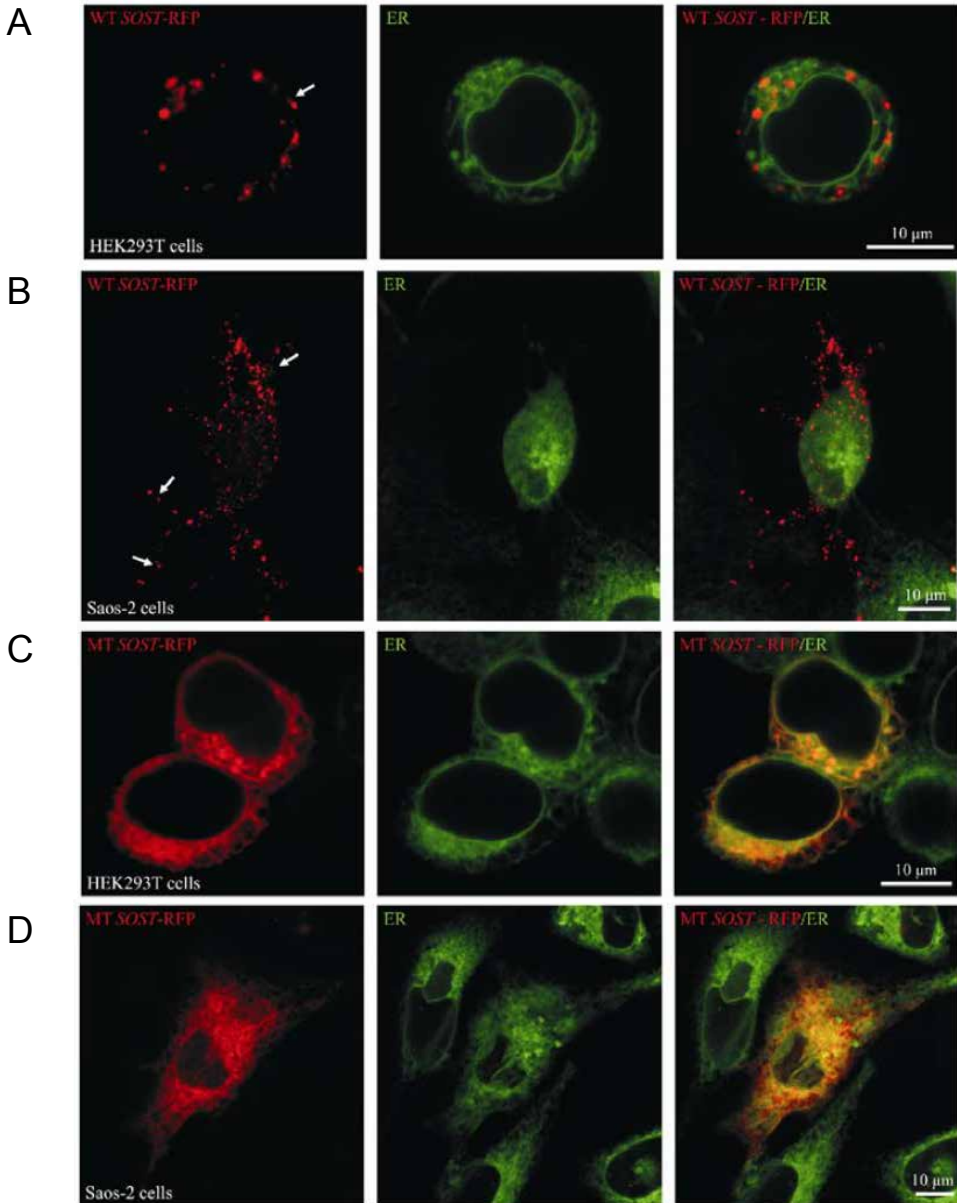


Figure 2. Retention of MT sclerostin in the ER. A-B. HEK293T (A) and Saos-2 cells (B) were transiently transfected with WT SOST-RFP plasmid to study the subcellular localization of WT mouse sclerostin (red channel). ER staining was performed using a green fluorescent ER tracker (green channel). Living cells were viewed using an UltraVIEW dual spinning disk confocal system. Arrows indicate the presence of WT sclerostin in variably sized granular cytoplasmic structures, preferentially in areas close to the cell membrane. The ER networks typically showed the highest density around the nucleus. Merging of the red and green channels clearly revealed that both labels are not co-localized. The latter was most obvious in the many cytoplasmic processes of Saos-2 cells. C-D. Similar to Figure 4 A-B, but now HEK293T (C) and Saos-2 cells (D) were transfected with MT SOST-RFP. The orange/yellow color in the merged channel images revealed a major co-localization of MT SOST protein with the ER tracker in both cell types. Scale bars are indicated.

Retention of MT sclerostin in the ER

As no previous intracellular localization studies had been reported for sclerostin, we hypothesized that, similar to other newly synthesized secreted proteins, it should be produced in the ER from where it is further targeted into the secretory pathway via the Golgi apparatus and cytoplasmic secretory granules. Mutations in proteins often lead to misfolding and subsequent retention in the ER [42]. To study the effect of the mutation on the subcellular localization of sclerostin in HEK293T and Saos-2 cells, we generated RFP fusion proteins for both WT and MT sclerostin, and the ER was visualized using a green fluorescent ER tracker. By confocal live-cell imaging, we found that the presence of WT sclerostin was concentrated in granular cytoplasmic structures, indicative of secretory granules (Figure 2A-B). The granular staining was most prominent in areas close to the cell membrane and hardly co-localized with the green fluorescent ER tracker, for which the staining was seen as a rather uniform network around the nucleus. The staining pattern of the MT sclerostin-RFP fusion protein was more diffuse and appeared to predominantly co-localize with the ER tracker (Figure 2C-D).

Decreased antagonistic activity of MT sclerostin

The effect of the mutation on the antagonistic capacity of sclerostin on Wnt signaling was tested in Saos-2 cells. Cells were transfected with a Wnt reporter construct and stimulated with either a Wnt1 expression plasmid or rec Wnt3a. Transfection of Wnt1 alone resulted in a 2-fold enhancement of Wnt signaling (Figure 3A). However, when the Wnt1 plasmid was co-transfected with an LRP5 expression plasmid, a 13-fold increase in Wnt signaling was observed. Wild type *mSost* plasmid significantly inhibited Wnt1-stimulated Wnt signaling to almost 50% of its original level ($p=0,007$), whereas the MT *mSost* plasmid could only induce a non-significant 20% reduction. Stimulation with rec Wnt3a resulted in an almost 20-fold increase in Wnt signaling (Figure 3B). Both mouse and human WT *Sost/SOST* plasmids significantly inhibited Wnt signaling, and the human *SOST* plasmid seemed to be more potent. Both MT *Sost/SOST* plasmids did not inhibit rec Wnt3a-induced signaling.

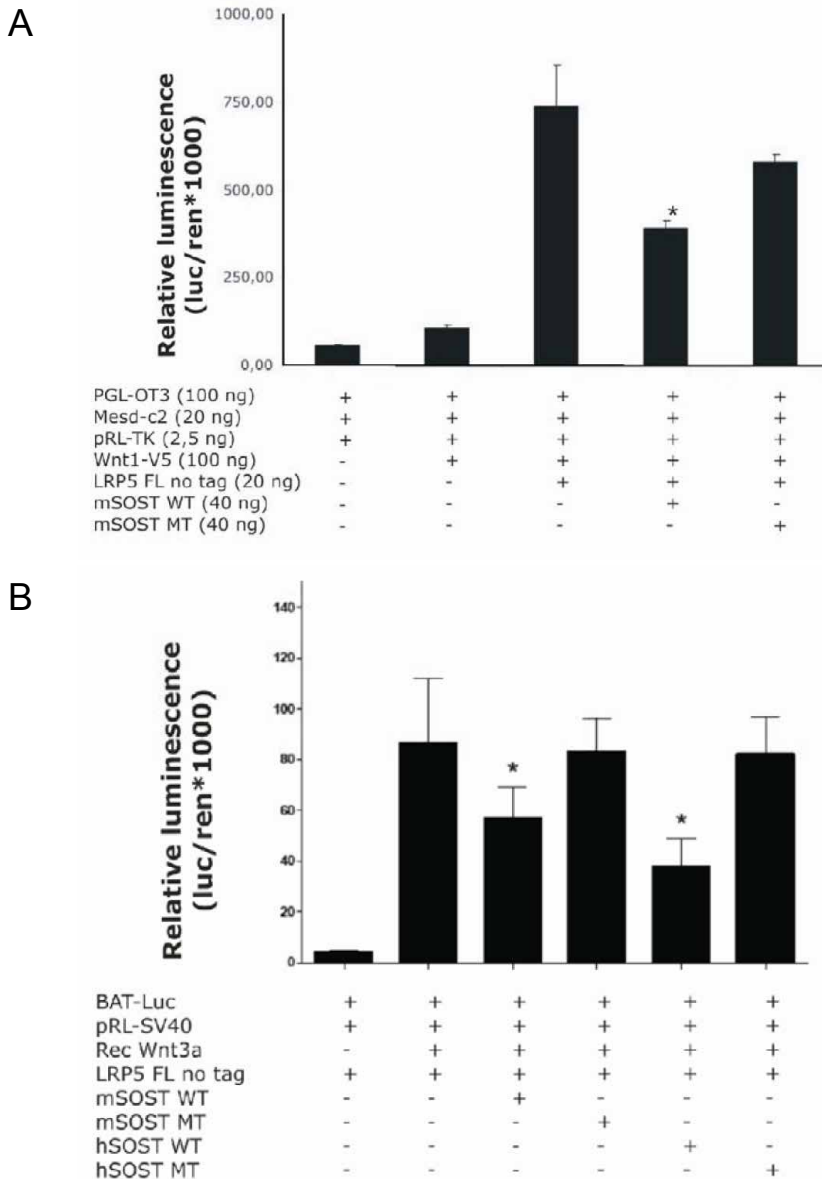


Figure 3. Decreased level of Wnt signal transduction both in the presence of human and mouse MT sclerostin. A) Saos-2 cells were transiently transfected with pGL3-OT, pRL-TK, Mesdc2, untagged full length WT-LRP5 in the presence or absence of Wnt1-V5. The antagonistic activity on Wnt signaling was evaluated by co-transfecting either WT or MT mSOST. Data were generated in three independent experiments, each performed in triplicate. Bars represent mean values \pm SD. * $p < 0.05$ cells transfected with WT mSOST compared to cells transfected without WT mSOST. B) Saos-2 cells were transfected with untagged full length WT-LRP5 and BAT-luc with or without mouse and human WT or MT SOST expression vectors and stimulated with rec Wnt3a 24h after transfection (n=8). Bars represent mean values \pm SD. * $p < 0.05$ cells transfected with mouse or human WT SOST compared to cells transfected without mouse or human WT SOST. All data were corrected for differences in transfection efficiency by co-transfection with constitutively active Renilla-luciferase expression plasmids.

Impaired binding of MT sclerostin to LRP5

Co-IP experiments were performed to evaluate the effect of the mutation on the ability of sclerostin to interact with LRP5. HEK293 cells were transfected with constructs either expressing truncated LRP5-myc (encoding only the extracellular part of the protein), WT-sclerostin-HA, or MT-sclerostin-HA. Figure 4A illustrates that truncated LRP5-myc and WT-sclerostin-HA were expressed in the CM, while MT-sclerostin-HA was found exclusively in the cell lysate (Figure 4A). Subsequently, CM of the truncated LRP5-myc transfected cells was mixed with either CM of WT-sclerostin-HA transfected cells or cell lysates of MT-sclerostin-HA transfected cells to determine binding between the extracellular part of LRP5 and WT- or MT-sclerostin. From the immune complexes, HA-tagged WT- and MT-sclerostin were precipitated using EZ-view™ Red Anti-HA affinity gel and immunoblotted with c-myc antibodies to demonstrate co-IP of truncated LRP5-myc with WT- or MT-sclerostin-HA. Truncated LRP5-myc was detected in precipitates that contained WT-sclerostin-HA, but not in precipitates that contained MT-sclerostin-HA, suggesting that the mutation in sclerostin resulted in a reduced affinity for LRP5 (Figure 4B). The immune complexes were also immunoblotted with anti-HA to demonstrate the presence of either WT- or MT-sclerostin-HA in all samples (Figure 4B).

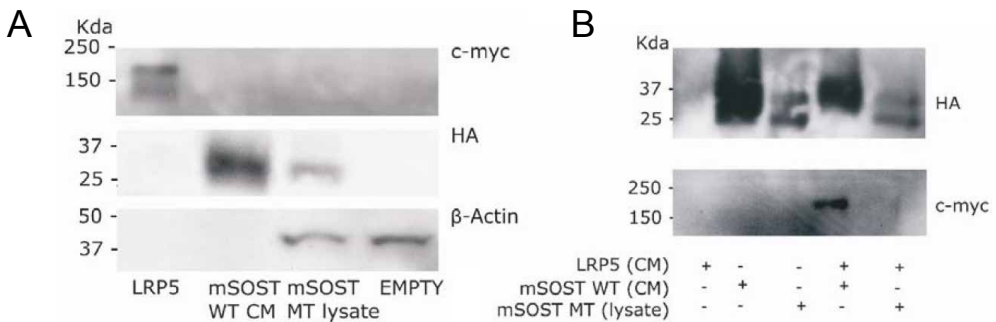


Figure 4. Impaired binding of MT sclerostin to LRP5. A) Total cell lysates and CM from HEK293T cells transfected with WT or MT SOST were analyzed for the expression of HA-tagged sclerostin by immunoblotting using HA antibodies. Expression of LRP5-myc protein in CM was evaluated by immunoblotting with cmyc antibodies. A negative control (empty pcDNA3.1) was included in both immunoblotting experiments. Equal protein loading was confirmed by immunoblotting of total cell lysates for β -actin. B) Mixtures of CM containing truncated WT-LRP5-myc and either CM containing WT-sclerostin-HA (lane 4) or cell lysates containing MT-sclerostin-HA (lane 5) were immunoprecipitated using EZ-view™ Red Anti-HA affinity gels. Cells that were transfected only with LRP5myc (lane 1) or WT and MT SOST-HA expression vectors (lane 2-3) were used as controls. Immunodetection of HA-immunoprecipitated protein was performed with both anti-HA and anti-myc. From lane 4 and 5 it is clear that WT but not MT sclerostin-HA was able to precipitate LRP5-myc.

Discussion

The clinical and radiological features of patients with SCL are thought to be due to complete absence of sclerostin resulting from loss-of-function mutations in the *SOST* gene. These include both nonsense mutations and splice site mutations [20-22]. In this study, we found for the first time a missense mutation in the *SOST* gene causing a cysteine to arginine amino acid substitution at position 167. The pathogenicity of this genetic variant was demonstrated by the cosegregation of the mutation with the disease in the, albeit small, Turkish family and the absence of the variant in 160 chromosomes of 80 control subjects of a matched ethnic background.

The nature of the mutation is strongly indicative for a pathogenic mutation, since the amino acid substitution results in the loss of a cysteine residue. Alignment of homologous cDNA and protein sequences using CLUSTALW (<http://www.ebi.ac.uk/Tools/clustalw2/index.html>) showed that the affected cysteine is highly conserved in multiple species (data not shown). Moreover, this cysteine is the last of six cysteines forming the characteristic cystine-knot motif (residues 80-167) [43]. Furthermore, the cysteine to arginine substitution implies a change from an uncharged polar amino acid into a basic amino acid. We tested the putative consequences of this substitution in several software programs, such as Polyphen and SIFT [44, 45]. These programs sort intolerant from tolerant amino acid substitutions, principally on the basis of sequence-homology. Polyphen also includes a search for structural parameters to predict whether an amino acid substitution in a protein has a possible phenotypic effect. According to both programs, the mutation is damaging with a high probability.

Cysteine residues are characterized by thiol-groups that can form disulfide bonds, covalent crosslinks between cysteine side chains that play an important role in the rate and efficiency of protein folding and most importantly in the stability of folded proteins. Some disulfide bonds have been shown to be indispensable for efficient secretion by promoting the production of more compact folded intermediates [46]. Removal of disulfides by site-directed mutagenesis has been demonstrated to be sufficient to cause misfolding, aggregation and impaired secretion of several proteins [47-53].

With regard to the p.Cys167Arg mutation in the *SOST* gene, we used NMR structure analysis of mouse sclerostin to predict the possible influence on the

sclerostin fold. Due to the architecture of the cystine-knot motif three peptide loops emanate from the cystine-knot, two of which run in the same direction (and form the so-called Finger 1 and 2), whereas the third emanates into the opposite direction. Finger 1 and 2 of the WT sclerostin are well defined forming two two-stranded anti-parallel β -sheets, whereas the third loop is highly flexible and disordered (Supplementary Figure 2A) [54, 55]. A zoom into the cystine-knot motif showed that it is rather loosely packed, with amino acid residues between the cysteine residues pointing towards the solvent, indicating that the cystine-knot of sclerostin exhibits partly elevated flexibility (Supplementary Figure 2B). Simulations *in silico* suggested that mutating cysteine 167 (equivalent to cysteine 142 of the mature protein) to arginine not only disrupts the outer disulfide bond present in the cystine-knot motif (Supplementary Figure 2C) but also requires conformational changes of the lower loop segment due to the increased spatial requirements of the larger arginine side chain. This will lead to global misfolding due to a decreased stability of the cystine-knot motif and the presence of an accessible reactive thiol-group at the protein surface as one cysteine residue remains unpaired. Even if a global misfolding does not occur, the large space requirements of the arginine side chain will lead to a further disorder of the loop segment, which has been proposed to be important for the activity of sclerostin by mapping the binding site of a neutralizing antibody to the tip of the loop segment [54]. Molecular dynamics simulation indeed showed a local unfolding of the remaining cysteine network, as the side chain of arginine introduced at position 167 (for mature sclerostin residue numbering is not accounting for the 25 residue signal peptide: Cys167 corresponds to Cys142) points towards the interior of the former cystine-knot requiring an opening of the ring in order to avoid steric clashes between the bulky side chain of the introduced arginine and surrounding residues like Cys109, Gly107 and Ser106. This rearrangement is complemented by conformational changes in the amino terminus, as the former packing has to be relieved to create enough space for Arg167. In addition, loss of the disulfide bond between Cys109 and Cys167 (now Arg167) enhances conformational variability in the loop segment since the few hydrophobic interactions between the antiparallel peptide segments of the loop are further weakened.

This *in silico* modeling suggests that loss of this crucial cysteine may indeed result in impaired folding and hence be responsible for retention of the mutant

protein in the ER. This is normally followed by degradation through delivery to the 26S proteasome in the cytoplasm or by lysosomal degradation by autophagy. The latter mechanism is especially used for misfolded proteins that aggregate in the secretory pathway or in the cytosol [56, 57]. Using subcellular localization experiments, we were able to show that MT sclerostin indeed does not exit the ER, explaining the decreased extracellular levels of MT sclerostin compared to WT found by immunoblotting and electrochemiluminescence. In addition, in reporter assays MT sclerostin was found to have strongly decreased antagonistic activity on Wnt signaling. Using co-IP experiments, we demonstrated that also the binding affinity of MT sclerostin for LRP5, which is required for its antagonist activity, is decreased. *In vivo*, these effects resulted in a complete loss of function of sclerostin reflected by a phenotype that is highly similar to that of previously reported patients with SCL. In the same way, loss-of-function mutations derived from folding problems in a variety of proteins with different activities, lead to retention of mutated proteins in the ER and their consequent degradation. This mechanism lies at the basis of a large number of ER-derived diseases, reviewed by Aridor et al [58]. In addition to this loss-of-function, increased levels of ER stress, known as unfolded protein response (UPR) (i.e. induction of inflammatory responses or cellular apoptosis), due to inability of the ER to efficiently dispose of the mutant protein, can contribute substantially to disease pathogenesis [58, 59]. It has been reported that strongly secretory cells (and maybe also the osteocyte) are extremely susceptible to this UPR, which often results in a pathogenic outcome [59]. Since we did not perform experiments to further investigate this disease mechanism, our data can not exclude the possibility that this mechanism additionally contributes to the phenotype in this family.

In conclusion, the present work describes here the first missense mutation in the *SOST* gene encoding sclerostin in a patient with SCL. This missense mutation involves one of the cysteine residues of the cystine-knot motif of sclerostin. The mutation has a devastating effect on the biological function of sclerostin by reducing extracellular sclerostin levels as well as the binding capacity of sclerostin to LRP5 and, thereby, its antagonistic activity on canonical Wnt signaling. It is possible that ER stress and UPR, as a consequence of the inability of the ER to efficiently dispose of the mutant protein, also contribute to the disease phenotype.

Acknowledgments

This work was supported by the European Commission [HEALTH-F2-2008-201099, TALOS]; and by grants from the 'Fonds voor Wetenschappelijk Onderzoek' [FWO, G.0117.06], from the Special Research Funds (BOF TOP and NOI) of the University of Antwerp, all to W.V.H.. Additional support was provided by Senternovem/IOP Genomics (IGE07001A).

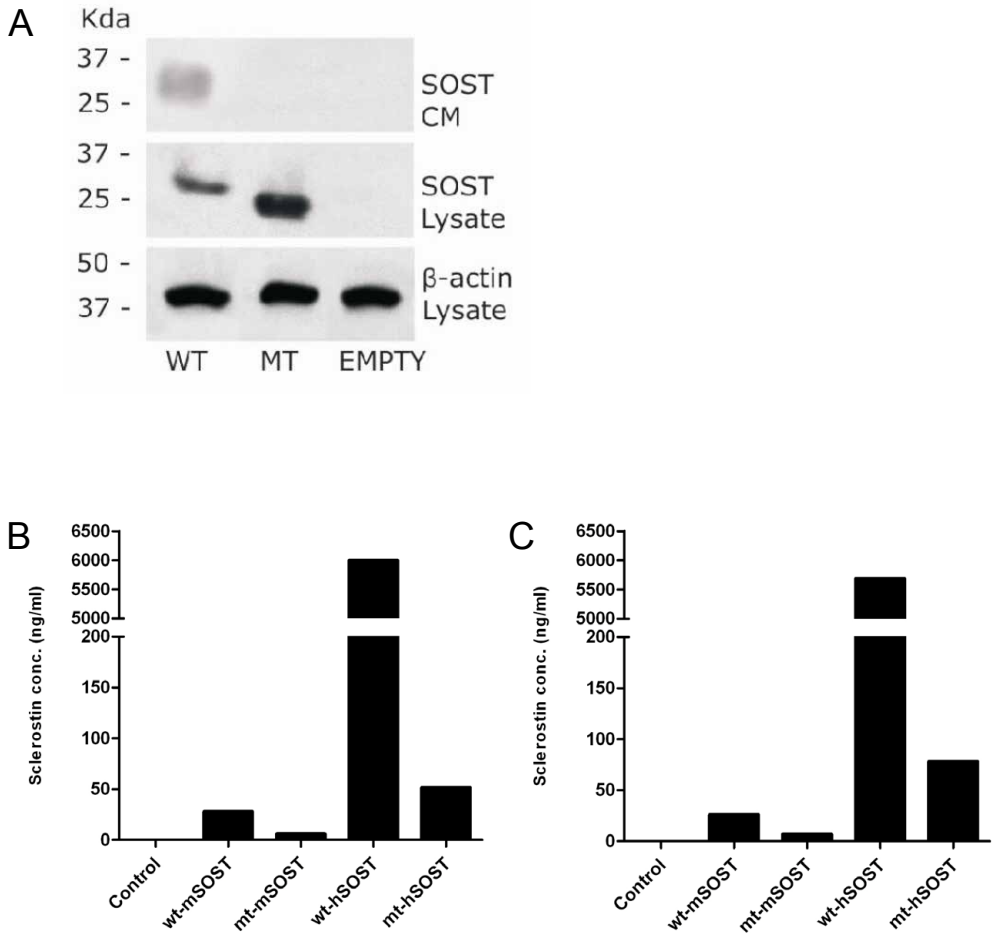
References

1. Gueguen R, Jouanny P, Guillemin F, Kuntz C, Pourel J, Siest G. Segregation analysis and variance components analysis of bone mineral density in healthy families. *J Bone Miner Res* 1995;10:2017-22.
2. Krall EA, Dawson-Hughes B. Heritable and life-style determinants of bone mineral density. *J Bone Miner Res* 1993;8:1-9.
3. Balemans W, Van Wesenbeeck L, Van Hul W. A clinical and molecular overview of the human osteopetroses. *Calcif Tissue Int* 2005;77:263-74.
4. Johnson ML, Harnish K, Nusse R, Van Hul W. LRP5 and Wnt signaling: a union made for bone. *J Bone Miner Res* 2004;19:1749-57.
5. Beighton P, Barnard A, Hamersma H, van der Wouden A. The syndromic status of sclerosteosis and Van Buchem disease. *Clin Genet* 1984;25:175-81.
6. Beighton P, Davidson J, Durr L, Hamersma H. Sclerosteosis - an autosomal recessive disorder. *Clin Genet* 1977;11:1-7.
7. Beighton P, Durr L, Hamersma H. The clinical features of sclerosteosis. A review of the manifestations in twenty-five affected individuals. *Ann Intern Med* 1976;84:393-7.
8. Hamersma H, Gardner J, Beighton P. The natural history of sclerosteosis. *Clin Genet* 2003;63:192-7.
9. Freire de Paes-Alves A, Cardoso L, Rabelo MM. Sclerosteosis: a marker for Dutch ancestry? *Rev Brasil Genet* 1982;4:825-34.
10. Bueno M, Oliván G, Jimenez A, Garagorri JM, Sarria A, Bueno AL *et al.* Sclerosteosis in a Spanish male: first report in a person of Mediterranean origin. *J Med Genet* 1994;31:976-7.
11. Kelley CH, Lawlah JW. Albers-Schonberg disease; a family survey. *Radiology* 1946;47:507-13.
12. Higinbotham NL, Alexander SF. Osteopetrosis: four cases in one family. *Am J Surgery* 1941;53:444-54.
13. Pietruschka G. [Further information on marble bones (Albers-Schonberg disease) with remarks on differential diagnosis]. *Klin Monbl Augenheilkd Augenarztl Fortbild* 1958;132:509-25.
14. Stein SA, Witkop C, Hill SC, Fallon MD, Viernstein L, Gucer G *et al.* Sclerosteosis: neurogenetic and pathophysiologic analysis of an American kinship. *Neurology* 1983;33:267-77.
15. Sugiura Y, Yasuhara T. Sclerosteosis. A case report. *J Bone Joint Surg Am* 1975;57:273-7.
16. Tacconi P, Ferrigno P, Cocco L, Cannas A, Tamburini G, Bergonzi P *et al.* Sclerosteosis: report of a case in a black African man. *Clin Genet* 1998;53:497-501.
17. Dixon JM, Cull RE, Gamble P. Two cases of Van Buchem's disease. *J Neurol Neurosurg Psychiatry* 1982;45:913-8.
18. Balemans W, van den Ende J, Freire de Paes-Alves A, Dijkers FG, Willems PJ, Vanhoenacker F *et al.* Localization of the gene for sclerosteosis to the Van Buchem disease-gene region on chromosome 17q12-q21. *Am J Hum Genet* 1999;64:1661-9.
19. Van Hul W, Balemans W, Van Hul E, Dijkers FG, Obee H, Stokroos RJ *et al.* Van Buchem disease (hyperostosis corticalis generalisata) maps to chromosome 17q12-q21. *Am J Hum Genet* 1998;62:391-9.

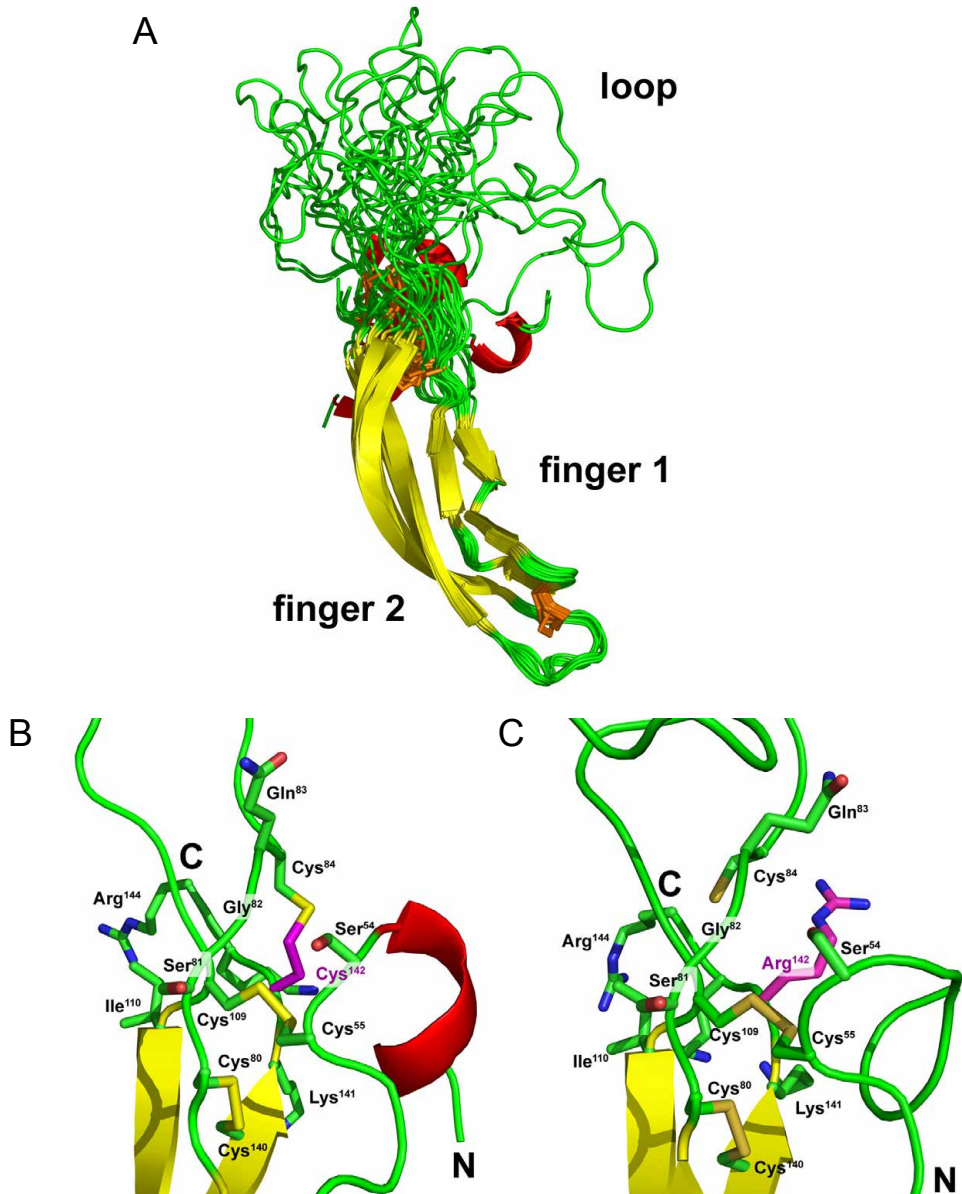
20. Balemans W, Ebeling M, Patel N, van Hul E, Olson P, Dioszegi M *et al.* Increased bone density in sclerosteosis is due to the deficiency of a novel secreted protein (SOST). *Hum Mol Genet* 2001;10:537-43.
21. Brunkow ME, Gardner JC, Van Ness J, Paeper BW, Kovacevich BR, Proll S *et al.* Bone dysplasia sclerosteosis results from loss of the *SOST* gene product, a novel cystine knot-containing protein. *Am J Hum Genet* 2001;68:577-89.
22. Balemans W, Cleiren E, Siebers U, Horst J, van Hul W. A generalized skeletal hyperostosis in two siblings caused by a novel mutation in the *SOST* gene. *Bone* 2005;36:943-7.
23. Balemans W, Patel N, Ebeling M, Van Hul E, Wuyts W, Lacza C *et al.* Identification of a 52 kb deletion downstream of the *SOST* gene in patients with Van Buchem disease. *J Med Genet* 2002;39:91-7.
24. Staehling-Hampton K, Proll S, Paeper BW, Zhao L, Charmley P, Brown A *et al.* A 52-kb deletion in the *SOST-MEOX1* intergenic region on 17q12-q21 is associated with Van Buchem disease in the Dutch population. *Am J Med Genet* 2002;110:144-52.
25. van Bezooijen RL, Bronckers AL, Gortzak RA, Hogendoorn PC, Wee-Pals L, Balemans W *et al.* Sclerostin in mineralized matrices and Van Buchem disease. *J Dent Res* 2009;88:569-74.
26. van Bezooijen RL, Roelen BA, Visser A, van der Wee-Pals, de Wilt E, Karperien M *et al.* Sclerostin is an osteocyte-expressed negative regulator of bone formation, but not a classical BMP antagonist. *J Exp Med* 2004;199:805-14.
27. Hill SC, Stein SA, Dwyer A, Altman J, Dorwart R, Doppman J. Cranial CT findings in sclerosteosis. *AJNR Am J Neuroradiol* 1986;7:505-11.
28. van Bezooijen RL, ten Dijke P, Papapoulos SE, Löwik CWGM. SOST/sclerostin, an osteocyte-derived negative regulator of bone formation. *Cytokine Growth Factor Rev* 2005;16:319-27.
29. Li X, Ominsky MS, Niu QT, Sun N, Daugherty B, D'Agostin D *et al.* Targeted deletion of the sclerostin gene in mice results in increased bone formation and bone strength. *J Bone Miner Res* 2008;23:860-9.
30. Sutherland MK, Geoghegan JC, Yu C, Turcott E, Skonier JE, Winkler DG *et al.* Sclerostin promotes the apoptosis of human osteoblastic cells: a novel regulation of bone formation. *Bone* 2004;35:828-35.
31. van Bezooijen RL, Svensson JP, Eefting D, Visser A, van der Horst G, Karperien M *et al.* Wnt but not BMP signaling is involved in the inhibitory action of sclerostin on BMP-stimulated bone formation. *J Bone Miner Res* 2007;22:19-28.
32. Winkler DG, Sutherland MK, Geoghegan JC, Yu C, Hayes T, Skonier JE *et al.* Osteocyte control of bone formation via sclerostin, a novel BMP antagonist. *EMBO J* 2003;22:6267-76.
33. Li X, Zhang Y, Kang H, Liu W, Liu P, Zhang J *et al.* Sclerostin binds to LRP5/6 and antagonizes canonical Wnt signaling. *J Biol Chem* 2005;280:19883-7.
34. Semenov M, Tamai K, He X. SOST is a ligand for LRP5/LRP6 and a Wnt signaling inhibitor. *J Biol Chem* 2005;280:26770-5.
35. Boyden LM, Mao J, Belsky J, Mitzner L, Farhi A, Mitnick MA *et al.* High bone density due to a mutation in LDL-receptor-related protein 5. *N Engl J Med* 2002;346:1513-21.
36. Little RD, Carulli JP, Del Mastro RG, Dupuis J, Osborne M, Folz C *et al.* A mutation in the LDL receptor-related protein 5 gene results in the autosomal dominant high-bone-mass trait. *Am J Hum Genet* 2002;70:11-9.

37. Van Wesenbeeck L, Cleiren E, Gram J, Beals RK, Benichou O, Scopelliti D *et al.* Six novel missense mutations in the LDL receptor-related protein 5 (LRP5) gene in different conditions with an increased bone density. *Am J Hum Genet* 2003;72:763-71.
38. Balemans W, Piters E, Cleiren E, Ai M, Van Wesenbeeck L, Warman ML *et al.* The binding between sclerostin and LRP5 is altered by DKK1 and by high-bone mass LRP5 mutations. *Calcif Tissue Int* 2008;82:445-53.
39. Ellies DL, Viviano B, McCarthy J, Rey JP, Itasaki N, Saunders S *et al.* Bone density ligand, Sclerostin, directly interacts with LRP5 but not LRP5G171V to modulate Wnt activity. *J Bone Miner Res* 2006;21:1738-49.
40. Semenov MV, He X. LRP5 mutations linked to high bone mass diseases cause reduced LRP5 binding and inhibition by SOST. *J Biol Chem* 2006;281:38276-84.
41. Piters E, Boudin E, Van Hul W. Wnt signaling: a win for bone. *Arch Biochem Biophys* 2008;473:112-6.
42. Ellgaard L, Helenius A. Quality control in the endoplasmic reticulum. *Nat Rev Mol Cell Biol* 2003;4:181-91.
43. Avsian-Kretchmer O, Hsueh AJ. Comparative genomic analysis of the eight-membered ring cysteine knot-containing bone morphogenetic protein antagonists. *Mol Endocrinol* 2004;18:1-12.
44. Ng PC, Henikoff S. SIFT: Predicting amino acid changes that affect protein function. *Nucleic Acids Res* 2003;31:3812-4.
45. Ramensky V, Bork P, Sunyaev S. Human non-synonymous SNPs: server and survey. *Nucleic Acids Res* 2002;30:3894-900.
46. Wittrup KD. Disulfide bond formation and eukaryotic secretory productivity. *Curr Opin Biotechnol* 1995;6:203-8.
47. Bedows E, Norton SE, Huth JR, Sukanuma N, Boime I, Ruddon RW. Misfolded human chorionic gonadotropin beta subunits are secreted from transfected Chinese hamster ovary cells. *J Biol Chem* 1994;269:10574-80.
48. Chen XZ, Shafer AW, Yun JS, Li YS, Wagner TE, Kopchick JJ. Conversion of bovine growth hormone cysteine residues to serine affects secretion by cultured cells and growth rates in transgenic mice. *Mol Endocrinol* 1992;6:598-606.
49. Omura F, Otsu M, Kikuchi M. Accelerated secretion of human lysozyme with a disulfide bond mutation. *Eur J Biochem* 1992;205:551-9.
50. Segal MS, Bye JM, Sambrook JF, Gething MJ. Disulfide bond formation during the folding of influenza virus hemagglutinin. *J Cell Biol* 1992;118:227-44.
51. Shani O, Pines O. The relationship between disulphide bond formation, processing and secretion of lipo-beta-lactamase in yeast. *Mol Microbiol* 1992;6:189-95.
52. Sukanuma N, Matzuk MM, Boime I. Elimination of disulfide bonds affects assembly and secretion of the human chorionic gonadotropin beta subunit. *J Biol Chem* 1989;264:19302-7.
53. Taniyama Y, Yamamoto Y, Nakao M, Kikuchi M, Ikehara M. Role of disulfide bonds in folding and secretion of human lysozyme in *Saccharomyces cerevisiae*. *Biochem Biophys Res Commun* 1988;152:962-7.

54. Veverka V, Henry AJ, Slocombe PM, Ventom A, Mulloy B, Muskett FW *et al.* Characterization of the structural features and interactions of sclerostin: molecular insight into a key regulator of Wnt-mediated bone formation. *J Biol Chem* 2009;284:10890-900.
55. Weidauer SE, Schmieder P, Beerbaum M, Schmitz W, Oschkinat H, Mueller TD. NMR structure of the Wnt modulator protein Sclerostin. *Biochem Biophys Res Commun* 2009;380:160-5.
56. Klionsky DJ. Autophagy: from phenomenology to molecular understanding in less than a decade. *Nat Rev Mol Cell Biol* 2007;8:931-7.
57. Nakatsukasa K, Brodsky JL. The recognition and retrotranslocation of misfolded proteins from the endoplasmic reticulum. *Traffic* 2008;9:861-70.
58. Aridor M. Visiting the ER: the endoplasmic reticulum as a target for therapeutics in traffic related diseases. *Adv Drug Deliv Rev* 2007;59:759-81.
59. Boot-Handford RP, Briggs MD. The unfolded protein response and its relevance to connective tissue diseases. *Cell Tissue Res* 2010;339:197-211.



Supplementary Figure 1. Decreased intra- and extracellular levels of MT sclerostin. A) Total cell lysates and CM from HEK293T cells transfected with WT or MT SOST or empty vector were analyzed for the expression of HA-tagged sclerostin by immunoblotting using an HA antibody. Equal protein loading was confirmed by immunoblotting of total cell lysates for β -actin. One representative experiment of three independent immunoblotting experiments is depicted. B) Quantitative expression analysis of sclerostin in cell lysates of HEK293T cells transfected with WT and MT constructs of both mouse and human SOST or an empty control vector using the MULTI-ARRAY[®] Human sclerostin assay (MSD). Sclerostin levels were corrected for SOST mRNA expression levels for each of the plasmids determined by RT-PCR analysis. C) Same in CM of transfected HEK293T cells.



Supplementary Figure 2. Effect of the mutating cysteine 167 to arginine on the NMR structure of sclerostin. A) Ribbon representation of the NMR structure ensemble of mouse sclerostin (residues Lys73 to Arg169 is shown, residue numbering includes the 25 residue signal peptide, PDB entry 2KD3). The secondary structure elements are indicated in yellow (β -strand), red (α -helix) and green (coil). The overlay of the 15 NMR structures of the ensemble shows that finger 1 and 2 are well defined, whereas the loop is highly flexible and disordered. B) Detail of the cystine-knot of sclerostin. The cystine-knot is rather loosely packed, with amino acid residues between the cysteine residues pointing towards the solvent, indicating that the cystine-knot of sclerostin is flexible in part. The cysteine residue, which is mutated in the patient, is colored in magenta, numbering is according to full-length sclerostin protein starting with residue 1. C) Same region displayed for MT mouse sclerostin variant. Mutating cysteine 167 to arginine disrupts the outer disulfide bond present in the cystine-knot motif.

A vertical strip on the left side of the page contains a grayscale micrograph of bone tissue, showing various cellular structures and mineralized matrix.

Chapter 5

Regulation of SOST mRNA expression through inhibition of GSK3 β independent of β -catenin

M.J.C. Moester
M.A.E. Schoeman
R.L. van Bezooijen
C.W.G.M. Löwik
K.E. de Rooij

In preparation

Abstract

Sclerostin is an important inhibitor of bone formation. When expression of this protein is reduced or completely absent, as in patients with Van Buchem disease and sclerosteosis, bone mass is dramatically increased. Sclerostin inhibits Wnt signalling and can also inhibit downstream effects of BMP such as alkaline phosphatase (ALP) activity and matrix mineralisation *in vitro*. The regulation of sclerostin or *SOST*, the gene encoding sclerostin, is not completely clear. Therefore, we investigated a possible feedback mechanism of Wnt signalling on the expression of *SOST*. Human osteosarcoma SaOS-2 cells were treated with different concentrations of Wnt3a or a specific GSK3 β inhibitor (GIN). Subsequent qRT-PCR analysis showed that *SOST* expression was dose-dependently decreased with increasing Wnt signalling. GSK3 β inhibition independent of Wnts and Frizzled receptors by GIN strongly stimulated Wnt reporter activity and inhibited *SOST* expression. Several Wnt signalling inhibitors, acting either on the binding of Wnt to its receptor, preventing the disruption of the Axin/APC/GSK3 β complex in the cytoplasm or preventing β -catenin binding to the TCF/LEF transcription complex in the nucleus, were examined in combination with Wnt3a stimulation or GSK3 β inhibition. None of these inhibitors could restore *SOST* expression after GSK3 β inhibition. We therefore conclude that GSK3 β influences *SOST* expression by a mechanism that is not dependent on Wnt/ β -catenin signalling.

Introduction

Sclerostin is an important regulator of bone formation. Mutations in the *SOST* gene or the surrounding regulatory regions lead to sclerostin deficiency and bone overgrowth in sclerosteosis and Van Buchem disease respectively [1-3]. Sclerostin is exclusively expressed in osteocytes in the mineralized matrix and is a marker for differentiation of osteoblasts into osteocytes [4]. It has been shown previously that sclerostin inhibits canonical Wnt signaling by binding to the LRP5/6 co-receptor and thereby preventing the interaction between WNTs and their receptor [4]. WNTs are a family of secreted proteins that regulate many developmental processes, for example body axis formation, chondrogenesis and limb development [5, 6] and has been proven important in bone formation [7]. In the absence of Wnt activation, β -catenin is phosphorylated by glycogen synthase kinase 3 β (GSK3 β) in a complex with axin and adenomatous polyposis coli (APC) and is subsequently degraded. When WNTs bind to the Frizzled receptor and LRP5/6 co-receptor, axin is recruited to the membrane and the destruction complex is disrupted. Consequently, the phosphorylating action of GSK3 β is prohibited and β -catenin accumulates in the cytoplasm, translocates into the nucleus and activates the transcription of the Wnt target genes by binding to the TCF/LEF transcription complex (Figure 1) [8, 9].

Sclerostin is one of several known Wnt signaling inhibitors (Figure 1). Dickkopf-1 (DKK1) and sclerostin inhibit canonical Wnt signaling in a similar manner by binding to the LRP5/6 co-receptor [10, 11]. Apart from endogenous inhibitors, many synthetic inhibitors have been developed to inhibit different aspects of the Wnt signaling pathway. One of these synthetic molecules is XAV939, a tankyrase inhibitor. Tankyrase marks axin for degradation, leading to disruption of the axin/APC/GSK3 β complex. Thus, inhibition of tankyrase leads to accumulation of axin, breakdown of β -catenin and inhibition of the Wnt pathway [12]. PNU74654 binds to β -catenin, preventing it from binding to the TCF/LEF transcription complex [13].

Even though knowledge on the role of sclerostin in bone biology is ever increasing, little is known about the regulation of its expression. Several factors have been shown to downregulate *SOST*, such as PTH [14-16] and mechanical loading [17, 18]. Bone Morphogenetic Proteins (BMPs) are known to stimulate *SOST* transcription, and this may in turn inhibit the canonical Wnt pathway [19, 20]. 1,25-Dihydroxyvitamin D3 alone or in combination with retinoic acid also

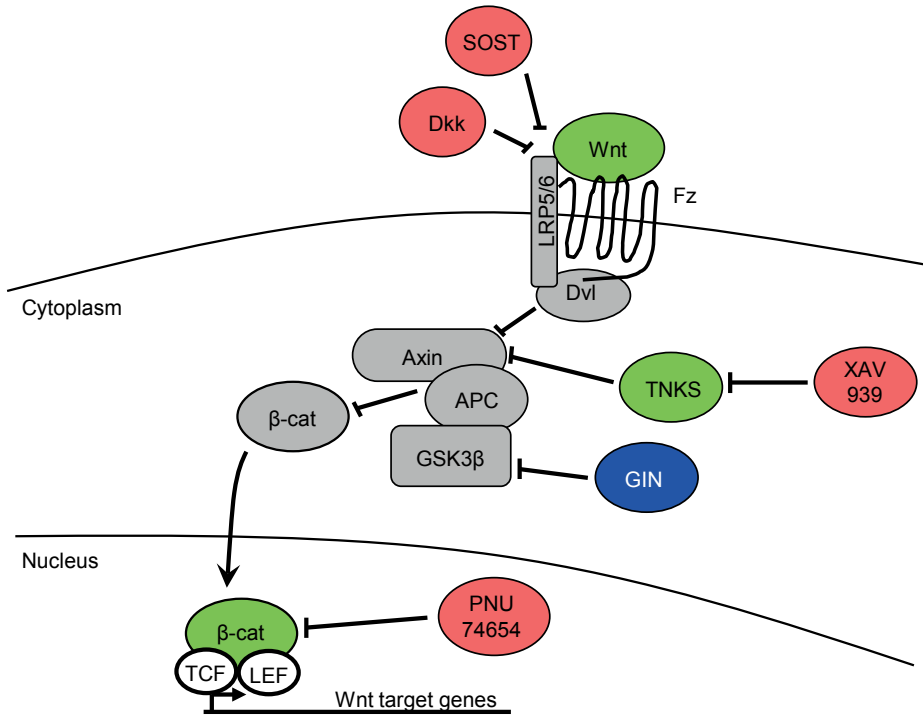


Figure 1. Wnt signaling pathway with the different Wnt signaling inhibitors described in this manuscript. Dickkopf 1 (DKK1) is an extracellular inhibitor that works in the same way as sclerostin by binding to the LRP5/6 co-receptor and preventing the interaction with WNTs and the Frizzled receptor. XAV939 is a tankyrase inhibitor. Tankyrase marks Axin for degradation, leading to disruption of the Axin/APC/GSK3 β complex. Inhibition of tankyrase therefore leads to accumulation of Axin, breakdown of β -catenin and inhibition of the canonical Wnt signaling pathway. PNU74654 binds to β -catenin itself and thereby prevents interaction with the transcription complex and transcription of the Wnt target genes.

increases SOST expression [19, 21]. In addition, several transcription factor binding motifs in the SOST promoter have been identified [21], and the ECR5 element has a clear function in regulation of SOST expression, as evidenced by patients with Van Buchem disease in whom this region is deleted [22]. In this study, we investigated a possible feedback mechanism of the Wnt signaling pathway on the expression of SOST.

Materials and Methods

Cells, materials and reagents

The human osteosarcoma cell line SaOS-2 (ATCC, Manassas, VA, USA) and rat osteosarcoma cell line UMR106 were cultured in cell culture flasks (Greiner Bio-One,

Kremsmünster, Austria) with 4,5 g/L Glutamax Dulbecco's Modified Eagle Medium (Gibco, Carlsbad, CA, USA) supplemented with 10% Fetal Calf Serum (FCS; Greiner Bio-One), 100 U/ml penicillin and 100 µg/ml streptomycin (Gibco). Recombinant BMP4, Wnt3a and DKK1 were purchased from R&D Systems (Minneapolis, MN, USA). The specific GSK3β inhibitor 3-imidazo[1,2-a]pyridin-3-yl-4-(1,2,3,4-tetrahydro-[1,4]diazepino-[6,7,1-hi]indol-7-yl)pyrrole-2,5-dione (further referred to as GIN) was kindly provided by Dr. Rawadi (Prostrakan, France) and previously described by Engler et al. and Miclea et al. [23, 24]. The Wnt signaling inhibitors XAV939 and PNU74654 were purchased at Sigma (St. Louis, MO, USA). The Wnt-responsive luciferase reporter BAT-luc [24, 25] and BMP responsive element luciferase reporter BRE-luc [26] have been described previously.

Luciferase experiments

SaOS-2 cells were seeded in 96-well plates (Greiner Bio-One) at a density of 22,500 cells/cm² and cultured overnight to 70-80% confluence. The cells were transfected with BAT-luc or BRE-luc reporter construct and a pGL4-CAG renilla luciferase construct using FuGene HD transfection reagent (Invitrogen, Carlsbad, CA, USA) according to the manufacturer's instructions. After 24 hours treatment with the indicated reagents, luciferase activity was determined using the Dual-Glo Luciferase assay system (Promega, Fitchburg, WI, USA) with a SpectraMax L luminometer (Molecular Devices, Sunnyvale, CA, USA). Relative luminescence was calculated as firefly luciferase/renilla luciferase and expressed as fold change versus control.

Quantitative RT-PCR and primers

Total RNA was isolated from SaOS-2 and UMR106 cells using TriPure Isolation Reagent (Roche, Penzberg, Germany) after 24 hours treatment with indicated reagents. cDNA was synthesized using M-MLV reverse transcriptase (Promega) according to the manufacturer's instructions. Real-time quantitative PCR was performed using the Quantitect SYBRgreen PCR kit (Qiagen, Venlo, the Netherlands) with an iQ5 PCR cycler (BioRad, Hercules, CA, USA). Primers (Eurogentec, Seraing, Belgium) (Table 1) were designed for SOST, and β2 microglobulin was used as an internal control. Measurements were performed in triplicate and analyzed using the 2^{-ΔΔCt} method [27].

Table 1. Primer sequences

Gene	Species	Forward	Reverse
<i>SOST</i>	Human	5'-tgctggtacacacagccttc-3'	5'-gtcacgtagcggggaagtg-3'
β 2-microglobulin	Human	5'-tgctgtctccatgttgatgtatct-3'	5'-tctctgtctcccacctctaagt-3'
<i>SOST</i>	Rat	5'-gagtaccagagcctcctca-3'	5'-agcacaccaactcggtgac-3'
β 2-microglobulin	Rat	5'-ccgtcgtgctgccattcagaaaact-3'	5'-tgaggtgggtggaactgagacacg-3'

Statistical analysis

Values represent means \pm SD. Differences were tested by One-way Analysis of Variance (ANOVA) followed by Tukey's post hoc test using Graphpad Prism 5 software (La Jolla, CA, USA). Results were considered significant at $p < 0.05$.

Results

To examine the effect of Wnt signaling on SOST expression, human SaOS-2 cells were incubated with different concentrations of Wnt3a and the GSK3 β inhibitor GIN. There was a dose-dependent increase of luciferase activity of the Wnt reporter BAT-luc after Wnt3a stimulation (Figure 2A). SOST expression decreased dose-dependently after stimulation with Wnt3a (Figure 2B). GIN was more potent than Wnt3a in inducing BAT-luc activation, showing an induction of more than 400 fold compared to the control (Figure 2C). Inhibition of GSK3 β with GIN resulted in a marked and dose-dependent decrease in SOST expression (Figure 2D). Interestingly, at a concentration of 3×10^{-9} M, GIN had no effect on BAT-luc activity, while SOST expression was decreased. The effect of GIN was also investigated in UMR106 cells (data not shown). A marked decrease (74%) in SOST expression was seen, indicating that the effect is not cell-specific.

Subsequently, we tested the hypothesis that the observed downregulation of SOST expression observed after stimulation of the Wnt signaling pathway was a direct effect of Wnt/ β -catenin signaling. Therefore three inhibitors of the Wnt signaling pathway were tested for their ability to counteract the effect of GIN on SOST expression. As expected, the extracellular inhibitor DKK1 could not inhibit Wnt signaling after stimulation with GIN (Figure 3A). While XAV939 and PNU74654 significantly inhibited BAT-luc reporter activity, neither of these inhibitors was able to restore SOST expression (Figure 3B).

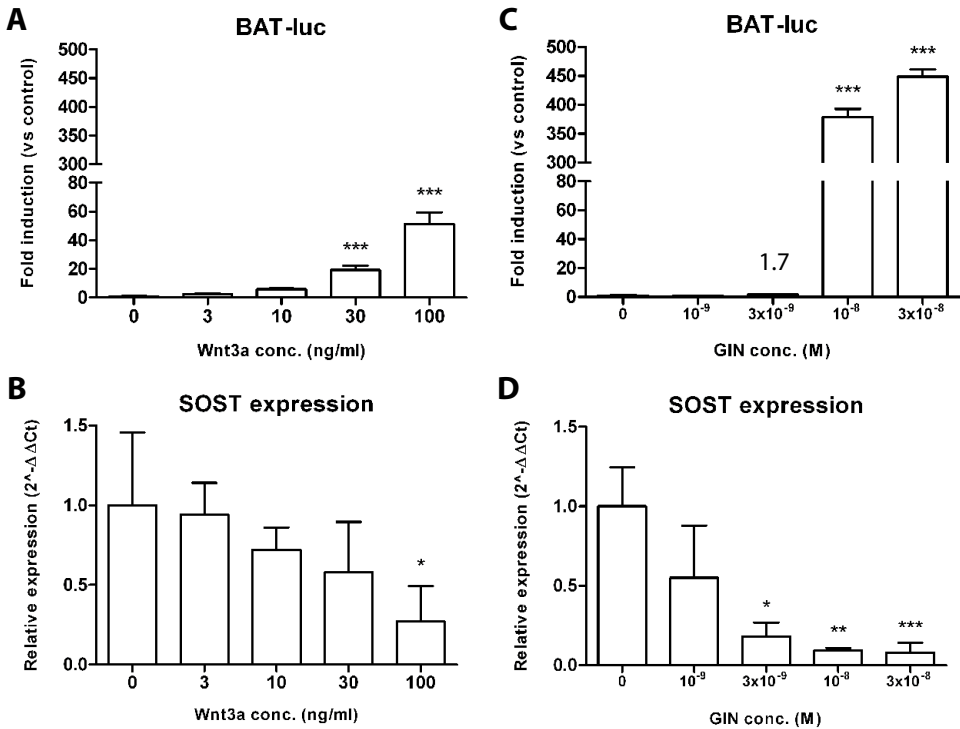


Figure 2. Wnt reporter BAT-luc activity and *SOST* expression after stimulation with WNT3a or GIN. SaOS-2 cells were transfected with the Wnt reporter construct BAT-luc and were stimulated with the indicated concentrations for 24 hours. Luciferase ($n = 6$) and *SOST* expression ($n = 3$) were measured. BAT-luc activity increased (A), while *SOST* expression decreased (B) dose-dependently with WNT3a stimulation in SaOS-2 cells. GIN was more potent in BAT-luc activation (C) and strongly decreased *SOST* expression in SaOS-2 cells in a dose-dependent manner (D). Compared to control: * $p < 0.05$, ** $p < 0.01$, *** $p < 0.001$.

Discussion

Wnt/ β -catenin or canonical Wnt signaling regulates many developmental processes, for example body axis formation, chondrogenesis and limb development [5, 6]. In bone, canonical Wnt signaling regulates the expression of several transcription factors that are essential to osteoblast differentiation such as Runx2 and Osterix [28, 29]. The signaling pathway is mediated by GSK3 β , a serine/threonine kinase that phosphorylates β -catenin to mark it for degradation. Inhibition of GSK3 β leads to accumulation of β -catenin, which is translocated to the nucleus and activates target gene transcription.

In the current study it was shown that inhibition of GSK3 β via the Wnt pathway with Wnt3a or direct inhibition with GIN resulted in decreased expression of the

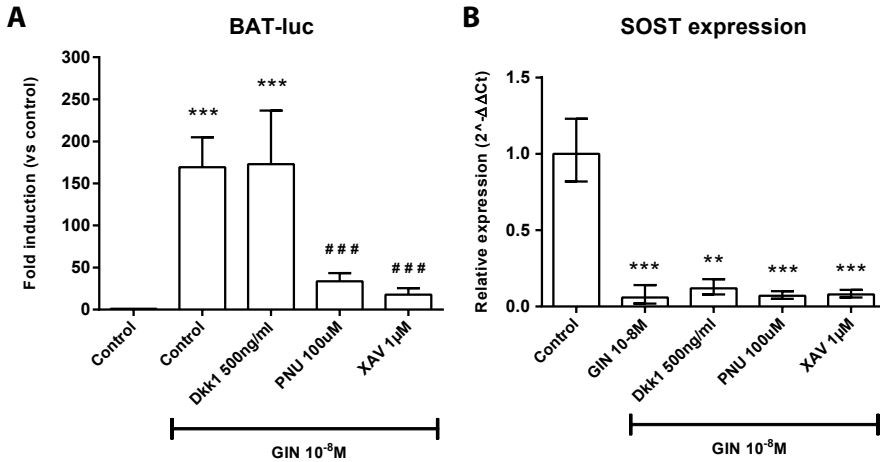


Figure 3. Wnt reporter BAT-luc activity and *SOST* expression after incubation with GIN and different Wnt signaling inhibitors. A) Wnt reporter BAT-luc activity in SaOS-2 cells after stimulation with GIN (n = 6). The extracellular inhibitor DKK1 could not inhibit GIN-induced BAT-luc activity. Both XAV939 and PNU74654 significantly inhibited BAT-luc activity. B) RNA from SaOS-2 cells was isolated after 24 hours incubation with GIN and inhibitors (n = 3). None of the inhibitors could restore *SOST* expression to control levels. Compared to control: ** p < 0.01, *** p < 0.001. Compared to GIN control: ### p < 0.001.

Wnt signaling inhibitor *SOST*. However, this did not appear to be a direct effect as *SOST* expression was decreased at a concentration of GIN where no increase in BAT-luc activity was seen. In addition, the β -catenin binding inhibitor PNU74654 was unable to restore *SOST* expression after treatment with GIN. Downregulation of *SOST* therefore appears to be mediated by GSK3 β , independent of β -catenin. However, even though GIN was thoroughly screened for selectivity against a panel of kinases [23], future experiments need to confirm the role of GSK3 β . Inhibition of GSK3 β using other synthetic inhibitors or an siRNA could for example exclude cross-reactivity or off-target effects of GIN. In addition, transfection of a construct containing a mutated GSK3 β that is insensitive to GIN would, in theory, abolish the effect of GIN on *SOST* expression.

Looking at the regulatory pathway involved in the downregulation of *SOST*, canonical Wnt signaling seems the most plausible option because of its clear connection to regulation of bone cells. However, as shown in this study, the effect on *SOST* was not dependent on β -catenin and therefore ruled out canonical Wnt signaling. GSK3 β is involved in other pathways like insulin and growth factor signaling [29], and has been suggested to influence Runx2 and Smad1 activity in bone [30, 31]. The transcription factor Runx2 is a good candidate for *SOST* regulation

considering the known binding site for Runx2 in the *SOST* promoter [21]. Kugimiya *et al.* [32] showed enhanced transcriptional activity of Runx2 in heterozygous GSK3 β -deficient mice, and a consequent increased bone formation. As sclerostin inhibits bone formation this may have been at least partly mediated by a decrease in sclerostin, but unfortunately expression of this protein was not measured in the GSK3 $\beta^{+/-}$ mice. *SOST* promoter studies by Yu *et al.* revealed an inhibitory effect of Runx2 on *SOST* expression [33]. Conversely, decreased *SOST* expression was found by Severson *et al.* when the Runx2 binding site was deleted from the *SOST* promoter, suggesting a stimulatory effect of Runx2 [21]. This difference is difficult to explain, especially since the studies by both Severson and Yu *et al.* were, like the current study, performed in SaOS-2 cells.

BMPs also play an important role in the regulation of bone cells. They induce osteoblast differentiation and are essential to bone development in embryos [7]. It has been shown previously that BMPs upregulate *SOST* expression [19, 20] via an indirect mechanism, not direct effects on the promoter or ECR5 element [33]. Interplay between GSK3 β and BMP signaling may therefore underlie the downregulation seen in the current study. Fuentealba *et al.* [34] described a mechanism in which MAPK and GSK3 β phosphorylations prime Smad1 for ubiquitination and degradation. With this mechanism GSK3 β controls the duration of Smad1 activation [35]. A similar mechanism may be true for Smad 6 and 7, which have been shown to inhibit *SOST* promoter activity [33].

Regulation of *SOST* by GSK3 β may have interesting clinical applications. Inhibition of GSK3 β would increase osteoblast differentiation through induction of the Wnt/ β -catenin pathway, while it reduces expression of the main Wnt inhibitor sclerostin. This could support fracture healing or increase bone formation in patients with osteoporosis using GSK3 β inhibitors already available. It is clear that further investigation is necessary as the results presented here may only apply to certain differentiation states or cell types. In addition, only *SOST* mRNA levels were measured in this study and these may not be accurately reflecting sclerostin protein production and therefore effects in the cell [33].

In conclusion, this study showed the existence of a new regulatory pathway for expression of *SOST*, which is mediated by GSK3 β but independent of β -catenin. Future research will need to identify the other elements in this pathway and the way it interacts with other pathways during bone metabolism.

References

1. van Buchem FS, Hadders HN, Ubbens R. An uncommon familial systemic disease of the skeleton: hyperostosis corticalis generalisata familiaris. *Acta radiol* 1955;44:109-20.
2. Hamersma H, Gardner J, Beighton P. The natural history of sclerosteosis. *Clin Genet* 2003;63:192-7.
3. Moester MJC, Papapoulos SE, Löwik CWGM, Bezooijen RL. Sclerostin: Current Knowledge and Future Perspectives. *Calcif Tissue Int* 2010;87:99-107.
4. van Bezooijen RL, Roelen BA, Visser A, van der Wee-Pals L, de Wilt E, Karperien M et al. Sclerostin is an osteocyte-expressed negative regulator of bone formation, but not a classical BMP antagonist. *J Exp Med* 2004;199:805-14.
5. Cadigan KM, Nusse R. Wnt signaling: a common theme in animal development. *Genes Dev* 1997;11:3286-305.
6. Yang Y. Wnts and wing: Wnt signaling in vertebrate limb development and musculoskeletal morphogenesis. *Birth Defects Res C Embryo Today* 2003;69:305-17.
7. Chen G, Deng C, Li YP. TGF-beta and BMP signaling in osteoblast differentiation and bone formation. *Int J Biol Sci* 2012;8:272-88.
8. Logan CY, Nusse R. The Wnt signaling pathway in development and disease. *Annu Rev Cell Dev Biol* 2004;20:781-810.
9. Nusse R, Varmus H. Three decades of Wnts: a personal perspective on how a scientific field developed. *EMBO J* 2012;31:2670-84.
10. Li X, Zhang Y, Kang H, Liu W, Liu P, Zhang J et al. Sclerostin binds to LRP5/6 and antagonizes canonical Wnt signaling. *J Biol Chem* 2005;280:19883-7.
11. Semenov MV, Tamai K, Brott BK, Kuhl M, Sokol S, He X. Head inducer Dickkopf-1 is a ligand for Wnt coreceptor LRP6. *Curr Biol* 2001;11:951-61.
12. Huang SM, Mishina YM, Liu S, Cheung A, Stegmeier F, Michaud GA et al. Tankyrase inhibition stabilizes axin and antagonizes Wnt signalling. *Nature* 2009;461:614-20.
13. Trosset JY, Dalvit C, Knapp S, Fasolini M, Veronesi M, Mantegani S et al. Inhibition of protein-protein interactions: the discovery of druglike beta-catenin inhibitors by combining virtual and biophysical screening. *Proteins* 2006;64:60-7.
14. Bellido T, Ali AA, Gubrij I, Plotkin LI, Fu Q, O'Brien CA et al. Chronic elevation of parathyroid hormone in mice reduces expression of sclerostin by osteocytes: a novel mechanism for hormonal control of osteoblastogenesis. *Endocrinology* 2005;146:4577-83.
15. Keller H, Kneissel M. SOST is a target gene for PTH in bone. *Bone* 2005;37:148-58.
16. Silvestrini G, Ballanti P, Leopizzi M, Sebastiani M, Berni S, Di VM et al. Effects of intermittent parathyroid hormone (PTH) administration on SOST mRNA and protein in rat bone. *J Mol Histol* 2007;38:261-9.
17. Robling AG, Niziolek PJ, Baldrige LA, Condon KW, Allen MR, Alam I et al. Mechanical stimulation of bone *in vivo* reduces osteocyte expression of *Sost/sclerostin*. *J Biol Chem* 2008;283:5866-75.

18. Lin C, Jiang X, Dai Z, Guo X, Weng T, Wang J *et al.* Sclerostin mediates bone response to mechanical unloading through antagonizing Wnt/beta-catenin signaling. *J Bone Miner Res* 2009;24:1651-61.
19. Sutherland MK, Geoghegan JC, Yu C, Winkler DG, Latham JA. Unique regulation of *SOST*, the sclerosteosis gene, by BMPs and steroid hormones in human osteoblasts. *Bone* 2004;35:448-54.
20. Kamiya N, Ye L, Kobayashi T, Mochida Y, Yamauchi M, Kronenberg HM *et al.* BMP signaling negatively regulates bone mass through sclerostin by inhibiting the canonical Wnt pathway. *Development* 2008;135:3801-11.
21. Severson B, Taylor S, Pan Y. *Cbfa1/RUNX2* directs specific expression of the sclerosteosis gene (*SOST*). *J Biol Chem* 2004;279:13849-58.
22. Balemans W, Patel N, Ebeling M, Van Hul E, Wuyts W, Lacza C *et al.* Identification of a 52 kb deletion downstream of the *SOST* gene in patients with Van Buchem disease. *J Med Genet* 2002;39:91-7.
23. Engler TA, Henry JR, Malhotra S, Cunningham B, Furness K, Brozinick J *et al.* Substituted 3-imidazo[1,2-a]pyridin-3-yl- 4-(1,2,3,4-tetrahydro-[1,4]diazepino-[6,7,1-hi]indol-7-yl)pyrrole-2,5-diones as highly selective and potent inhibitors of glycogen synthase kinase-3. *J Med Chem* 2004;47:3934-7.
24. Miclea RL, Siebelt M, Finos L, Goeman JJ, Löwik CW, Oostdijk W *et al.* Inhibition of Gsk3beta in cartilage induces osteoarthritic features through activation of the canonical Wnt signaling pathway. *Osteoarthritis Cartilage* 2011;19:1363-72.
25. Maretto S, Cordenonsi M, Dupont S, Braghetta P, Broccoli V, Hassan AB *et al.* Mapping Wnt/+1-catenin signaling during mouse development and in colorectal tumors. *Proceedings of the National Academy of Sciences* 2003;100:3299-304.
26. Korchynskiy O, ten Dijke P. Identification and Functional Characterization of Distinct Critically Important Bone Morphogenetic Protein-specific Response Elements in the *Id1* Promoter. *Journal of Biological Chemistry* 2002;277:4883-91.
27. Pfaffl MW. A new mathematical model for relative quantification in real-time RT-PCR. *Nucleic Acids Res* 2001;29:e45.
28. Bennett CN, Longo KA, Wright WS, Suva LJ, Lane TF, Hankenson KD *et al.* Regulation of osteoblastogenesis and bone mass by Wnt10b. *Proc Natl Acad Sci U S A* 2005;102:3324-9.
29. Yavropoulou MP, Yovos JG. The role of the Wnt signaling pathway in osteoblast commitment and differentiation. *Hormones (Athens)* 2007;6:279-94.
30. Gaur T, Lengner CJ, Hovhannisyan H, Bhat RA, Bodine PV, Komm BS *et al.* Canonical WNT signaling promotes osteogenesis by directly stimulating *Runx2* gene expression. *J Biol Chem* 2005;280:33132-40.
31. Song B, Estrada KD, Lyons KM. Smad signaling in skeletal development and regeneration. *Cytokine Growth Factor Rev* 2009;20:379-88.
32. Kugimiya F, Kawaguchi H, Ohba S, Kawamura N, Hirata M, Chikuda H *et al.* GSK-3beta controls osteogenesis through regulating *Runx2* activity. *PLoS One* 2007;2:e837.

33. Yu L, van der Valk M, Cao J, Han CY, Juan T, Bass MB *et al.* Sclerostin expression is induced by BMPs in human Saos-2 osteosarcoma cells but not via direct effects on the sclerostin gene promoter or ECR5 element. *Bone* 2011;49:1131-40.
34. Fuentelba LC, Eivers E, Ikeda A, Hurtado C, Kuroda H, Pera EM *et al.* Integrating patterning signals: Wnt/GSK3 regulates the duration of the BMP/Smad1 signal. *Cell* 2007;131:980-93.
35. Eivers E, Demagny H, De Robertis EM. Integration of BMP and Wnt signaling via vertebrate Smad1/5/8 and *Drosophila* Mad. *Cytokine Growth Factor Rev* 2009;20:357-65.

A vertical strip on the left side of the page contains a grayscale microscopic image of bone tissue, showing various cellular structures and mineralized matrix.

Chapter 6

Antisense oligonucleotide- mediated modulation of *SOST* and *Rank* expression

M.J.C. Moester
R.L. van Bezooijen
H. Sips
I.M. Mol
P.A.C. 't Hoen
A. Aartsma-Rus
E.L. Kaijzel
K.E. de Rooij
C.W.G.M. Löwik

Abstract

Osteoporosis is characterized by low bone mineral density and a loss of trabecular connectivity, leading to bone fragility and increased fracture risk. Sclerostin, the product of the *SOST* gene, is an important negative regulator of bone formation with a restricted expression pattern specifically in osteocytes. It is therefore regarded as a good target for new anabolic treatments for osteoporosis. Since sclerostin is a natural inhibitor of bone formation, inhibition of sclerostin function or downregulation of *SOST* expression will lead to increased bone formation as is seen in patients with sclerosteosis and Van Buchem disease. Another interesting target is the receptor activator of nuclear factor- κ B (RANK), which is the key activator for osteoclast differentiation. Blocking RANK or its ligand RANKL will therefore lead to a decrease in bone resorption.

Here we investigated antisense oligonucleotide-(AON) mediated exon skipping as a means of modulating expression of these targets and thereby influencing bone formation or resorption.

As *SOST* is a 2 exon gene, only qRT-PCR analysis could be used to assess efficacy of AONs. Several control AONs and AONs targeting *SOST* were examined and results showed widely varying *SOST* expression after transfection, and several AONs even increased expression of *SOST*. *SOST* expression was not decreased with any of the tested AONs compared to untransfected control cells. Exon skipping of *Rank* exon 6 was shown, with a maximum of 10.5% skip, and minimal skipping efficiency of exon 5 and 7. These levels were too low to be expected to have biological significance.

In conclusion, we have not been able to show substantial exon skipping activity in either of the targets. Skipping efficiency of *Rank* may be further optimized to reach biological significance.

Introduction

Osteoporosis is characterized by low bone mineral density and a loss of trabecular connectivity, leading to bone fragility and increased fracture risk [1]. Prevalence is highest among post-menopausal women, as the loss of estrogen production causes an imbalance in formation and resorption of the bone [2]. The socioeconomic burden of osteoporosis is growing in the ageing society due to the morbidity and mortality associated with fractures [3]. Most current therapies decrease the risk of fractures by reducing bone resorption, but cannot stimulate bone formation (with the exception of parathyroid hormone (PTH)) [4]. These therapies, therefore, are not able to rebuild the bone that is already lost. In addition, adherence of patients to current therapies such as bisphosphonates is poor and therapy is therefore not always effective [5, 6]. The discovery of regulatory pathways in bone metabolism has revealed new targets for the treatment of osteoporosis. For example, the Wnt/Low-density lipoprotein receptor-related protein 5 (LRP5) pathway is important in osteoblast differentiation and therefore has a great influence on bone formation, and the system containing Receptor Activator of Nuclear factor Kappa-B (RANK), RANK ligand (RANKL) and Osteoprotegerin (OPG) is the key regulator of osteoclast formation and bone resorption.

Targeting Wnt signaling

Wnt proteins belong to a family of secreted proteins that regulate many developmental processes, for example body axis formation, chondrogenesis and limb development [7, 8] and have an important role in the regulation of osteoblast differentiation [9]. When Wnts bind to the Frizzled receptor and its co-receptor LRP5/6, this triggers the disruption of the complex containing Axin, Adenomatous Polyposis Coli (APC) and Glycogen Synthase Kinase 3 beta (GSK3 β) that marks β -catenin for degradation. Consequently, β -catenin translocates to the nucleus and activates the transcription of the Wnt target genes [10, 11]. Sclerostin is an extracellular inhibitor of canonical Wnt signaling and inhibits this process by binding to LRP5/6. While it does not compete with WNTs for binding, sclerostin prevents the co-receptor's interaction with WNTs and the Frizzled receptor [12].

Sclerostin is exclusively expressed in osteocytes in the mineralized matrix and is a marker for differentiation of osteoblasts into osteocytes [13]. Mutations in the

SOST gene or its surrounding regulatory regions lead to sclerostin deficiency and the massive bone overgrowth seen in sclerosteosis and Van Buchem disease [14-19]. Due to its restricted expression pattern, sclerostin is considered a good target for the development of new therapies for osteoporosis [4, 20]. There is evidence that the beneficial effect of PTH, the only therapy currently in the clinic that is capable of increasing bone mass, is mediated at least in part by a decrease in sclerostin expression [21-23]. Patients with sclerosteosis or Van Buchem disease as well as *Sost* knockout mice have a very high bone mass with a normal structure and good quality [24-26]. In addition, heterozygous carriers of the inactivating *SOST* mutation have no skeletal complications while their bone mass is consistently higher than the mean of age-matched controls [25], sclerostin levels in serum are lower and bone formation is increased [18]. This effect is also seen in heterozygous *Sost* knockout mice compared to wild type littermates [27]. This suggests that inhibition of sclerostin production and/or activity can be titrated leading to increased bone mass without unwanted side effects. Neutralizing sclerostin antibodies for the treatment of osteoporosis have been developed and are currently in phase III clinical trials (AMG 785, NCT01575834 and NCT01631214 on www.clinicaltrials.gov).

Targeting the RANK/RANKL/OPG system

The RANK/RANKL/OPG system is one of the key regulators of bone resorption and plays a central role in bone metabolism [28]. In this system, the principal regulator of osteoclast differentiation is RANK, a membrane-bound cytokine of the tumor necrosis factor family. RANK is expressed on haematopoietic progenitor cells and the binding of RANK to its ligand (RANKL), which is expressed by osteoblasts, induces the NF- κ B pathway that leads to osteoclastogenesis and osteoclast survival [29, 30]. OPG is also produced by osteoblasts and acts as a soluble decoy receptor that competes with RANK for RANKL [31]. This interaction inhibits osteoclast differentiation and proliferation, and consequently decreases bone resorption. The ratio between RANKL and OPG determines the effect on osteoclasts. RANKL is not only essential for osteoclast differentiation and survival, it contributes to activation of mature osteoclast function as well [32].

The importance of the RANK/RANKL/OPG system was demonstrated by the effects of deletion and overexpression of these genes in animal and *in vitro* models [33].

For example, *Rank*^{-/-} and *Rankl*^{-/-} mice have shortened limbs and poorly remodeled structures blocking the marrow cavities and show a complete absence of osteoclasts [34, 35]. In contrast, *Opg*^{-/-} mice showed a progressive decrease in Bone mineral density (BMD) and excessive osteoclast activity [36, 37]. Further highlighting the importance of this system is the fact that mutations in *RANK* and *RANKL* were discovered in several bone-related diseases such as Paget's disease, autosomal recessive osteopetrosis and familial expansile osteolysis [33, 38-40]. Genome-wide association studies into the polymorphisms that have an effect on bone density or osteoporosis often find *RANK*, *RANKL* or *OPG* in strong associations [41, 42]. Moreover, decreased estrogen production as seen after menopause in females leads to an increase in RANKL production by osteoblasts [43, 44].

The RANK/RANKL/OPG system is therefore an interesting pathway to target in the search for new osteoporosis therapies. Recently, a human monoclonal antibody against RANKL (denosumab, Amgen) was approved for treatment of osteoporosis and bone destruction by bone metastases or rheumatoid arthritis [45]. Binding to RANKL, denosumab inhibits the formation, function and survival of osteoclasts and thereby inhibits bone resorption. Clinical trials revealed marked reduction of bone turnover markers and a BMD gain at all measured sites after 1 year of treatment. Few specific side-effects have been reported even though RANK and RANKL also have functions in the immune system and vascular system [46].

Exon skipping of *SOST* and *Rank*

A relatively new method of *in vivo* protein modification is antisense-mediated exon skipping. Antisense oligonucleotides (AONs) can interfere with the splicing process of the pre-mRNA and thereby induce skipping of an exon during splicing. Depending on the target, exon skipping can be used to restore aberrant splicing when this is disturbed by mutations, induce secretion of a membrane-bound protein by skipping of the membrane anchor, achieve alternative splicing or inactivation of a protein by removal of the active domain or disruption of the reading frame (reviewed in [47, 48]). Because exon skipping utilizes the natural splicing machinery in the cell and does not induce catalytic cleavage of the RNA, effects can be more subtly titrated than conventional knockdown with for example siRNA [49].

In this manuscript we investigated the use of exon skipping as a new method

for the treatment of osteoporosis and targeted both bone formation via inhibition of sclerostin, and bone resorption via inactivation of RANK. *SOST* is a gene that consists of only two exons. Exon skipping has, to our knowledge, not been attempted on two-exon genes or the final exon of a gene before. Nevertheless, mutations that interfere with splicing of this two-exon gene have been found in some patients with sclerosteosis [16, 50, 51]. This project was therefore a proof of principle for the efficacy of interfering with splicing using AONs on two-exon targets. The RANK gene encodes a transmembrane domain on exon 7 and is expressed as a membrane-bound protein. We aimed to skip exon 7 of RANK which would lead to the removal of the transmembrane domain and production of a soluble protein. This soluble RANK protein would not be able to transduce differentiation signals to osteoclast precursors and thereby inhibit osteoclast formation. In addition, solubilized RANK is a protein similar to OPG; it competes with other RANK molecules for RANKL and therefore potentially has a dual effect in inhibiting bone resorption.

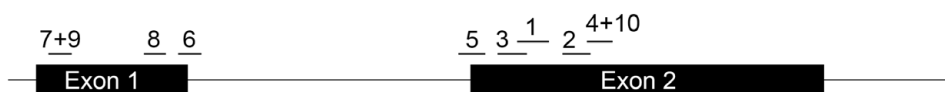
Materials and methods

Cells, materials and reagents

The human osteosarcoma cell line SaOS-2 and the murine monocytic cell line RAW264.7 (ATCC/LGC Standards, Wesel, Germany) were cultured in cell culture flasks (Greiner Bio-One, Kremsmünster, Austria) with 4.5 g/L Glutamax Dulbecco's Modified Eagle Medium (Gibco, Grand Island, NY, USA) supplemented with 10% Fetal Calf Serum (Greiner Bio-One), 100 U/ml penicillin and 100 µg/ml streptomycin (Gibco). Recombinant BMP4 was purchased from R&D Systems (Minneapolis, MN) and puromycin from Invitrogen (Carlsbad, CA, USA). 2'-*O*-methyl (2OMe) RNA phosphorothioate (PS) AONs were designed using the method described by Aartsma-Rus [52] and produced at Prosensa BV (Leiden, The Netherlands) (sequences in Table 1 and 2 and Figure 1). Gapmers (AON 9 and 10) were designed to include a middle section without 2OMe backbone modification. The PS backbone in this section is capable of inducing RNase H cleavage, while the 2OMe modification increases affinity and reduces breakdown by nucleases including RNase H [53, 54].

Table 1. Sequences of AONs targeted to *SOST*.

Name	Chemistry	Sequence	Target
AON 1	2OMePS	GGUCACGUAGCGGGUGAAGU	Exon 2
AON 2	2OMePS	GCUCGGUGACCGGCUUGGC	Exon 2
AON 3	2OMePS	UGAAGUGCAGCUCGCGGCA	Exon 2
AON 4	2OMePS	CACUGGCCGGAGCACACCAG	Exon 2
AON 5	2OMePS	CGGACACGUCUGUGGAGAGA	Intron/exon boundary exon 2
AON 6	2OMePS	CCAUACCUUUGGUCUCAAG	Intron/exon boundary exon 1
AON 7	2OMePS	CUGCAUGGUACCAGCCAGA	Exon 1
AON 8	2OMePS	CUCCAGCUCCGGUGGAGGCU	Exon 1
AON 9	RNA/dna gapmer	CUGCAtggtaccagCCAGA	Exon 1 (as hAON7)
AON 10	RNA/dna gapmer	CACUGgccggagcacACCAG	Exon 2 (as hAON4)

**Figure 1.** Location of AONs targeted to *SOST*.

AON transfection

For AON transfection, SaOS-2 cells and RAW264.7 cells were seeded in 24-well plates (Greiner Bio-One) at a density of 45,000 cells/well and $1.2\text{--}1.5 \times 10^5$ cells/well respectively. After overnight incubation, cells were washed with Hank's balanced salt solution (HBSS, Gibco) and 1 ml transfection medium containing 2% FCS was added to the wells. Transfection complexes were produced in 0.15 M NaCl with 1 μg AON per 100 μl NaCl solution. The transfection reagent polyethyleneimine (PEI) (Prosensa) was added at an equivalent of 3.65 for SaOS-2 cells and 6.5 for RAW264.7 cells. The amount of PEI was calculated with a method based on the protocol for ExGen500 (Fermentas, Burlington, Canada): $\mu\text{l PEI} = (\text{equivalent} \times \mu\text{g AON} \times 3) / 5.47$. Upon adding PEI, the transfection mix was vortexed and incubated for 10 minutes at room temperature. Per well, 100 μl transfection mix was added to the

Table 2. Sequences of AONs targeted to *Rank*.

Name	Chemistry	Sequence	Target
PS362	2OMePS	ACAGAGAUGAAGAGGAGCAG	Exon 7 Transmembrane domain
PS363	2OMePS	CUUCCUGUAGUAAACGCCGA	Exon 7 Transmembrane domain
PS419	2OMePS	GGCCUCUGUGUCAGAAGAA	Exon 7 Transmembrane domain
PS420	2OMePS	AAGGUUUGCAUUUGUCUGUGG	Exon 5 Out-of-frame
PS421	2OMePS	GUGCUCUAGCUUCCAAGG	Exon 6 Out-of-frame
PS422	2OMePS	GCAGACCACAUCUGAUUCCG	Exon 6 Out-of-frame
PS423	2OMePS	GGUGGUCUCCUCAGUGUCAU	Exon 6 Out-of-frame

cells and medium was changed after 24 hours of incubation. Transfection efficiency was monitored by fluorescence microscopy in each experiment using the fluorescent 5' fluorescein label attached to control AON A and B.

(q)RT-PCR and primers

Total RNA was isolated using TriPure Isolation Reagent (Roche Diagnostics GmbH, Mannheim, Germany) 48 hours after AON transfection. cDNA was synthesized using M-MLV reverse transcriptase (Promega, Madison, WI, USA) according to the manufacturer's instructions. PCR was performed using GoTaq® DNA Polymerase (Promega) with a MyCycler PCR cyler (Bio-Rad, Hercules, CA, USA) and real-time quantitative PCR (qRT-PCR) was performed using the Quantitect SYBRgreen PCR kit (Qiagen, Hilden, Germany) with an iQ5 PCR cyler (Bio-Rad). Primers (Eurogentec, Seraing, Belgium) were designed for *SOST*, the house-keeping gene $\beta 2$ microglobulin and different exons of *Rank* (Table 3). *SOST* qRT-PCR measurements were performed in triplicate and analyzed using the $2^{-\Delta\Delta C_t}$ method [55]. For *Rank*, PCR products were analyzed by agarose gel electrophoresis on a 1-2% agarose gel. In addition, several samples were selected for further analysis and quantification of skipping percentage using an Agilent DNA 1000 chip (Agilent Technologies, Santa Clara, CA, USA) according to the manufacturer's instructions.

Table 3. Sequences of primers used in PCR

Target	Sequence
<i>SOST</i> Fw	TGCTGGTACACACAGCCTTC
<i>SOST</i> Rev	GTCACGTAGCGGGTGAAGTG
β 2 microglobulin Fw	TGCTGTCTCCATGTTTGATGTATCT
β 2 microglobulin Rev	TCTCTGCTCCCCACCTCTAAGT
<i>RANK</i> exon 4 Fw	AGTGTGCACCTGGCTTCG
<i>RANK</i> exon 5 Fw	TGCAGCTCAACAAGGATACG
<i>RANK</i> exon 7 Rev	ATGAGACTGGGCAGGTAAGC
<i>RANK</i> exon 9 Rev	ACCATCTTCTCCTCCCGAGT

Sclerostin measurement in medium

Medium was collected from SaOS-2 cells 48 hours after transfection with AONs. Sclerostin concentration was measured with 96-well MULTI-ARRAY[®] Human Sclerostin Assay (Meso Scale Discovery (MSD), Gaithersburg, MD, USA) according to manufacturer's instructions. Briefly, the MULTI-SPOT 96-well plate was blocked for 1 hour with blocker buffer. Calibrators and samples were added to the wells and incubated for 2 hours. Wells were incubated with detection antibody for 1 hour. Plates were read directly after addition of MSD Read buffer on the Sector Imager 2400 (MSD).

Statistical analysis

Values represent means \pm SD. Differences in experiments with $n > 2$ were tested by One-way Analysis of Variance (ANOVA) followed by Tukey's post hoc test using Graphpad Prism 5 software. Results were considered significant at $p < 0.05$.

Results *SOST*

AONs decrease *SOST* expression compared to control AON

Two AONs were tested for their ability to decrease *SOST* expression in SaOS-2 cells. qRT-PCR results of *SOST* expression after transfection with these AONs were compared with samples that were transfected with a non-targeting control AON. *SOST* expression was decreased by almost 90% with both AONs (Figure 2A), as well

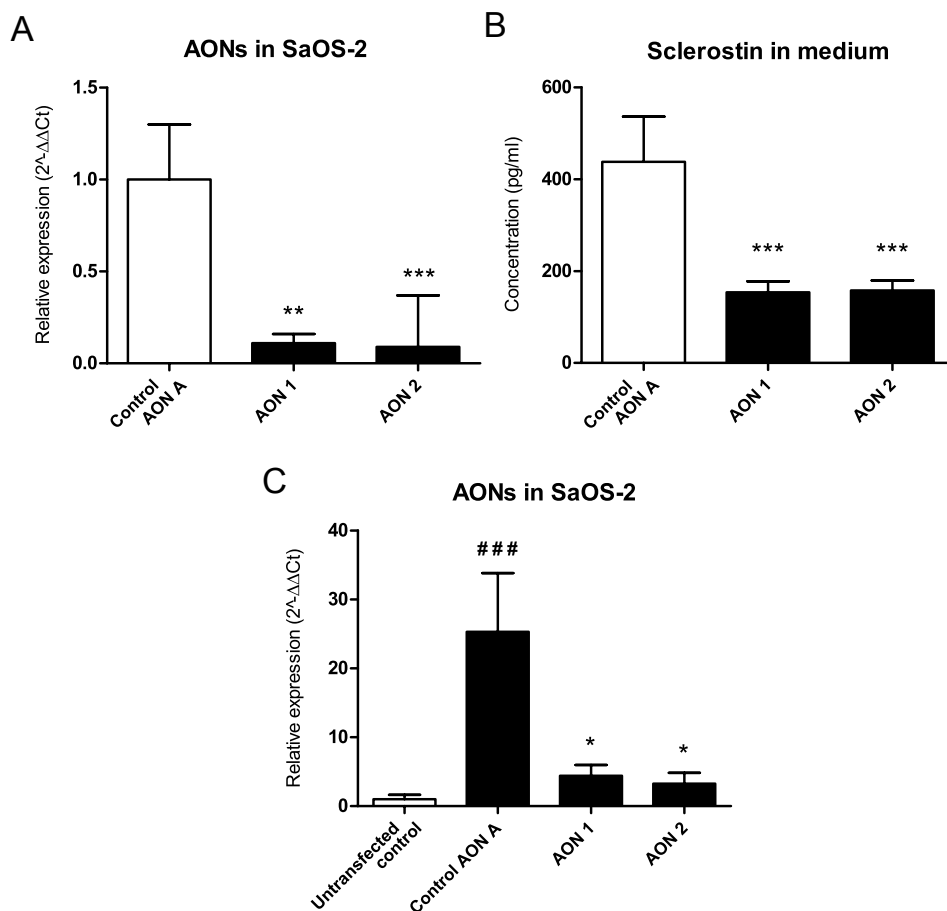


Figure 2. The effect of AONs targeted to *SOST* in SaOS-2 cells. A) SaOS-2 cells were transfected with AON 1 and 2 or Control AON A (n = 6). RNA was isolated 48 hours after transfection. *SOST* expression was decreased by about 90% compared to cells that were transfected with control AON A. B) Sclerostin was measured in medium of cells that were transfected with AONs using the Meso Scale Discovery 96-well MULTI-ARRAY[®] Human Sclerostin Assay (n = 6). Measurements confirmed the decrease in sclerostin compared to cells that were transfected with control AON A. C) *SOST* expression of AON treated wells was compared with *SOST* expression in untransfected control cells (n = 3). Control AON A increased *SOST* expression 48 hours after transfection. There was no difference in *SOST* expression after transfection with AON 1 and 2 compared to untransfected control cells. Compared to Control AON A: * p < 0.05; ** p < 0.01; *** p < 0.001; Compared to untransfected control: ### p < 0.001.

as sclerostin protein concentration in conditioned medium (Figure 2B). However, when *SOST* expression after AON transfection was compared to expression in untransfected cells, there was no decrease. In fact, transfection with the control AON increased *SOST* expression (Figure 2C). This was not due to the transfection reagent or low serum concentration as these conditions did not change *SOST* expression (data not shown). In subsequent experiments, *SOST* expression after

AON transfection was compared to untransfected control cells that were treated like the transfected cells but without addition of transfection reagent or AON. Compared to the untransfected control cells, AONs targeted to *SOST* did not change *SOST* expression (Figure 2C).

Effects of non-targeting control AONs on *SOST* expression

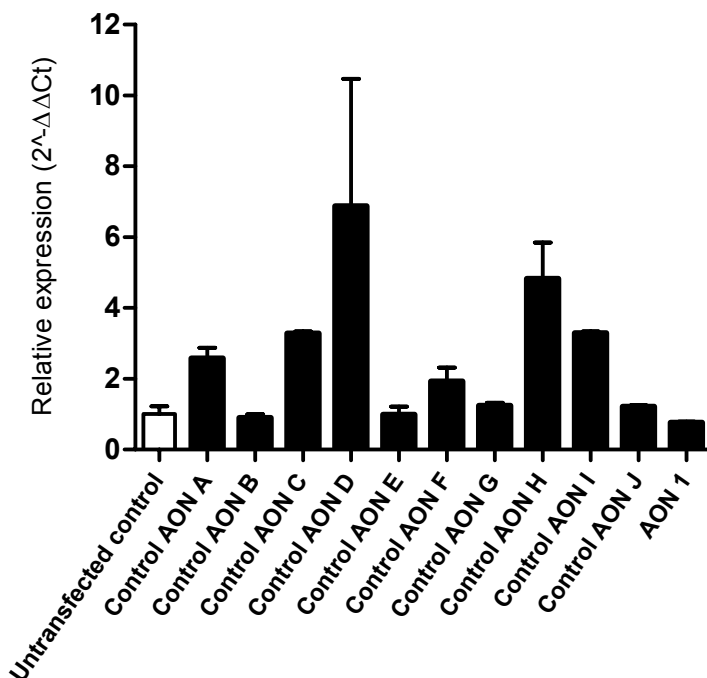
To examine the increase of *SOST* expression after transfection with control AONs, we tested 10 different control AONs for their effect on *SOST* mRNA levels (Table 4). These AONs were designed to target the DMD gene and checked for specificity by Basic Local Alignment Search Tool (BLAST) to exclude partial overlap with the *SOST* gene. As they were ineffective for their target DMD exons and were not expected to have any effect on other targets, these AONs were considered good control AONs. However, the effect of the control AONs on *SOST* expression varied between no effect and a 6.5 fold increase compared to the untransfected control (Figure 3). Results were consistent between two separate experiments and were therefore considered to be AON-specific. The sequences of the AONs that increased *SOST* expression were compared to those that did not, to detect any consensus sequences or motives that might explain the differences in effect. However, no similarities were found.

Effects of *SOST*-targeted AONs on *SOST* expression

Since we were not able to show a decrease in *SOST* expression with the first two AONs directed against *SOST*, another 8 AONs were designed and expression was compared to the untransfected control. While the first AONs were targeted to Exonic Splicing Enhancer (ESE) sites in the second (and last) exon, several AONs in the second series were designed to target ESE sites in the first exon or the intron/exon boundaries. In addition, two gapmers were designed to induce RNase H cleavage of the pre-mRNA (sequences in Table 1). Like the control AONs, the AONs targeting *SOST* had varying effects on *SOST* expression (Figure 4). Several AONs increased *SOST* expression (up to 22-fold compared to untransfected cells), while none of the AONs decreased *SOST* expression. In addition, four out of ten of the AONs that were tested induced widespread cell death after transfection (indicated by † in Figure 4). As before, comparison of the AON sequences did not reveal any consensus sequences that could explain the results.

Table 4. Sequences of control AONs

Name	Chemistry	Sequence
Control AON A	2OMePS + FAM-label	UUUUUCUGUCUGACAGCUG
Control AON B	2OMePS + FAM-label	UGCUGCUGUCUUCUUGCU
Control AON C	2OMePS	AUUUUUCCUGUAGAAUACUGG
Control AON D	2OMePS	CGCUGCCCAAUGCCAUCCU
Control AON E	2OMePS	GUGCUGAGGUUAUACGGUG
Control AON F	2OMePS	GUCCUGUGGGGCUUCAUG
Control AON G	2OMePS	GGGCACUUUGUUUGGCG
Control AON H	2OMePS	UCCUAUAAGCUGAGAAUCUG
Control AON I	2OMePS	GCCUUCUGCAGUCUUCGG
Control AON J	2OMePS	GAGAGGUAGAAGGAGAGGA

**Figure 3.** *SOST* expression in SaOS-2 cells after transfection with control AONs.

SaOS-2 cells were transfected with different control AONs (n = 2). These AONs were specifically designed to target dystrophin, but were ineffective for this purpose. *SOST* expression was increased after transfection with several control AONs. This expression profile was seen in two separate experiments.

Increasing *SOST* expression with BMP₄

Very few cell lines express *SOST*, and those that do (such as the SaOS-2 cells), express very low quantities. With low expression, it might be difficult to detect a further decrease after transfection with AONs. *SOST* expression was therefore increased by stimulating the cells with BMP₄ during AON transfection. As shown in Figure 5, *SOST* expression in cells stimulated with BMP₄ is indeed increased over 40-fold compared to the unstimulated control. However, transfection with AONs targeted to *SOST* did not decrease expression. The control AONs that were chosen for this experiment had the same effect as shown in Figure 3: control AON J did not change expression, while control AON H markedly increased *SOST* expression (Figure 5).

Results RANK

RAW264.7 cells were transfected with different AONs targeted to exon 5, 6 or 7 or combinations of AONs targeting one or more exons. In this case, the aim was to induce an exon skip that produced a soluble and non-functional protein (exon 7 skip), or produce a truncated and non-functional protein (exon 5 and 6 skip). PCR was performed with primers amplifying exon 4-9, showing skips of all targeted exons (Figure 6A). AONs targeting exon 6 resulted in a clearly visible skip product. No additional bands were visible on agarose gel, indicating that no double skips had occurred after targeting multiple exons. In Figure 6B, PCR results are shown that were performed with primers in exon 5 and 7, thus showing only skips of exon 6. Skipped products were excised and sequenced, proving that indeed exon 6 was skipped in all samples targeting exon 6 (data not shown). In addition, several samples were selected for analysis on an Agilent DNA 1000 chip for quantification of skip percentages. The percent of successful exon 6 skip ranged between 6.7 and 10.5% (Figure 6). RT-PCR analysis of samples that were transfected with an AON targeting exon 7 confirmed the absence of a skipped product (data not shown).

Skipping exon 5 or 6 of *Rank* would result in a frameshift and premature stopcodon, which may induce a nonsense-mediated decay mechanism. To inhibit nonsense-mediated decay, 1 µg/ml puromycin was added after AON transfection for 4 hours or overnight. PCR was performed with primers amplifying exon 6 (Figure 7). No apparent increase in the ratio between skipped and unskipped product was seen after addition of puromycin.

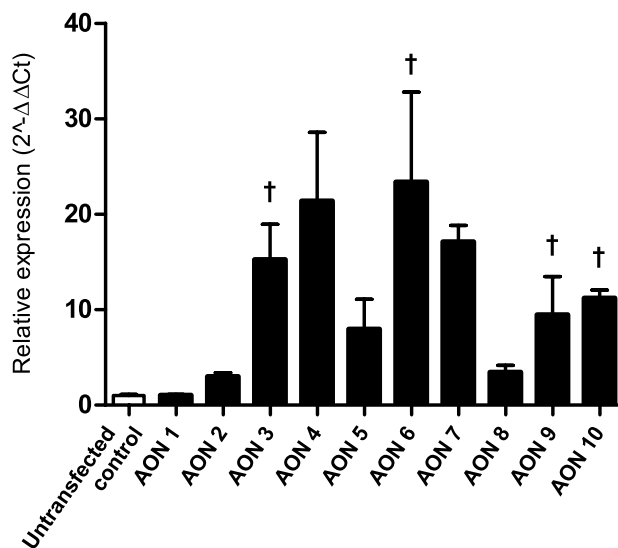


Figure 4. *SOST* expression in SaOS-2 cells after transfection with *SOST*-targeting AONs. SaOS-2 cells were transfected with AONs designed to target *SOST* ($n = 2$). None of the AONs was able to decrease *SOST* expression compared to the untransfected control, while several AONs increased *SOST* expression. AONs 3, 6, 9 and 10 induced cell death after transfection (indicated by †).

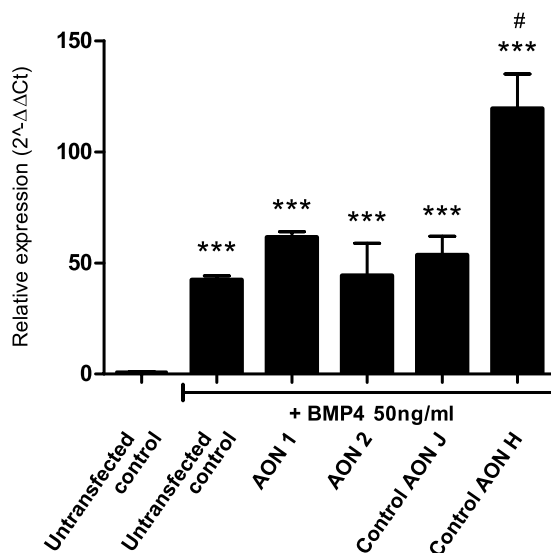


Figure 5. Effect of AON transfection on *SOST* expression in SaOS-2 cells after stimulation with BMP4. Because *SOST* expression in SaOS-2 cells is low, it might be difficult to detect a decrease after transfection with AONs. *SOST* expression was therefore increased with BMP4 during AON transfection. RNA was isolated 48 hours after transfection and stimulation ($n = 2$). *SOST* expression in cells stimulated with BMP4 is increased more than 40-fold compared to the unstimulated control, but transfection with AONs targeted to *SOST* did not decrease expression. As before, control AON J did not change expression, while control AON H increased *SOST* expression approximately 3-fold. *** $p < 0.001$ vs. untransfected and unstimulated control. # $p < 0.05$ vs. untransfected control + BMP4

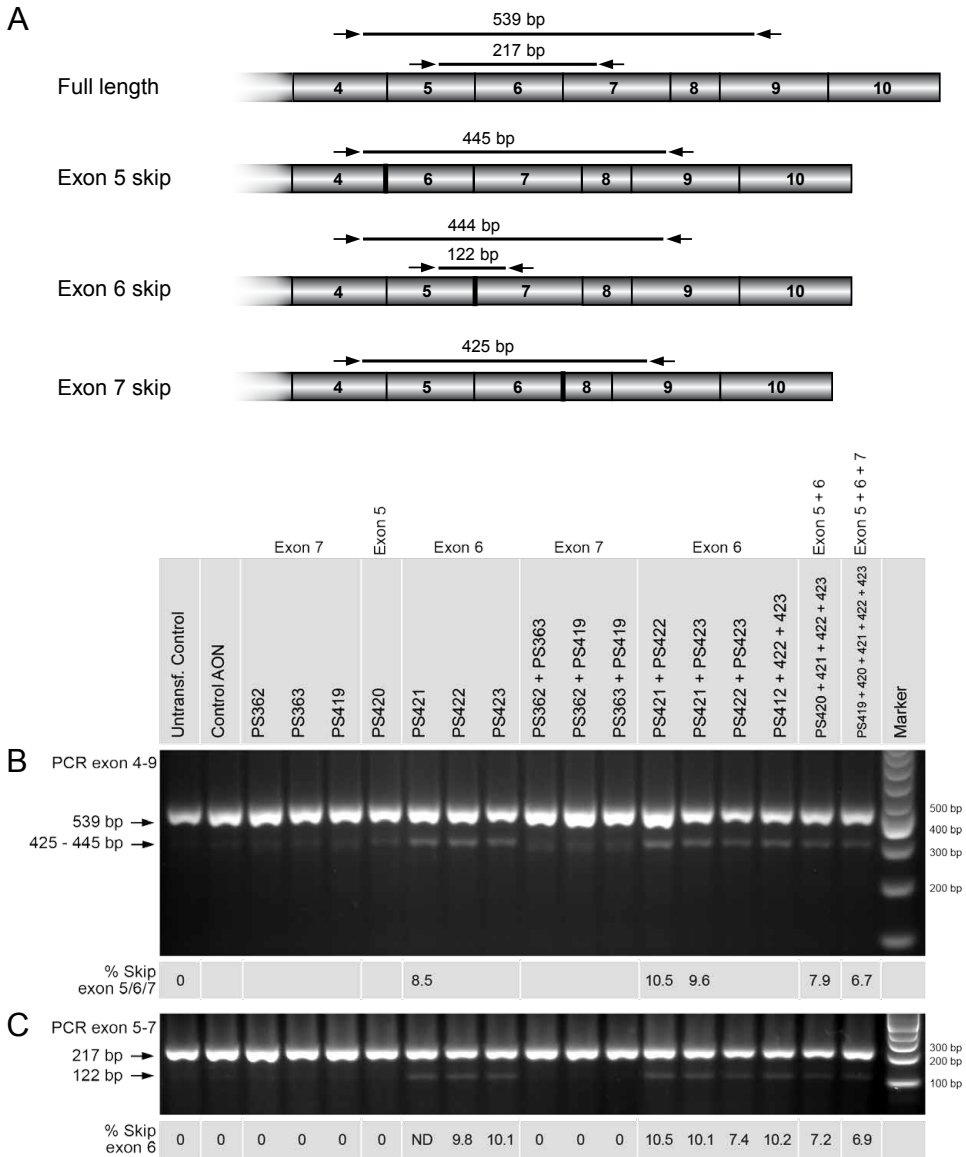


Figure 6. Schematic representation and gel electrophoresis results of *Rank* PCR products after transfection with the AONs and combinations of AONs indicated above the lanes. Targeted exon is also indicated. A) Schematic representation of *Rank* cDNA with primers in exon 4 and 9 or exon 5 and 7 showing product length before and after exon skips. B) PCR was performed with primers in exon 4 and 9, showing skips of all targeted exons. Skips of exon 5 and 7 were very faint. No additional fragments were found, indicating that multiple skips did not occur. Skipped product lengths: exon 5 skip 445 bp, exon 6 skip 444 bp, exon 7 skip 425 bp. C) PCR products are shown with primers in exon 5 and 7, showing only exon 6 skips. Several samples were selected and run on an Agilent DNA 1000 chip and the skipped product percentage of the total product was calculated by the Agilent 2100 software. Skipped product length: exon 6 skip 122 bp.

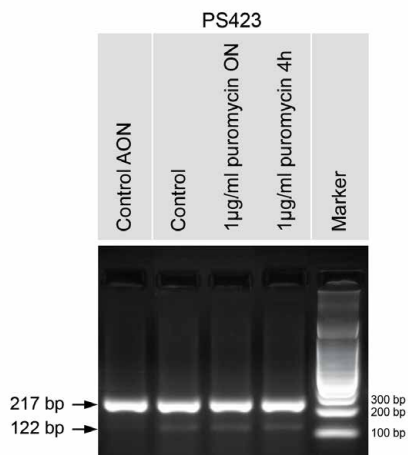


Figure 7. Gel electrophoresis of *Rank* PCR products after transfection with AON PS423 targeting exon 6, and treated with 1 µg/ml puromycin for 4 hours or overnight (ON). The control AON does not show any skipped product, while samples transfected with PS423 display weak bands at the predicted height. The ratio of full length versus skipped product does not markedly change after addition of puromycin.

Discussion

Osteoporosis is a growing problem in the aging society, and there is a need for better therapies. The discovery of important regulatory pathways in bone metabolism has revealed interesting new targets for treatment of this disease. Here we investigated AONs as a means of modulating expression of two of these targets by exon skipping, a technique that is very promising for the treatment of Duchenne muscular dystrophy (DMD). We showed that *SOST* expression was not decreased with any of the tested AONs compared to untransfected control cells, and that changes in *SOST* expression after transfection with different targeting and non-targeting AONs varied widely. Exon skipping of *Rank* was achieved but with low efficiency.

Even with the extensive knowledge of AON design criteria that has been accumulated in DMD research [52], none of the 10 AONs that were examined was able to decrease *SOST* expression. In fact, several AONs increased expression. This effect was consistently seen in two separate experiments and seemed to be unrelated to the target, since several control AONs also increased *SOST* expression. In the described experiments control AONs were used that were targeted to dystrophin, but proved ineffective. These AONs were considered to be good controls, as they were ineffective for their target and were not expected to have any off-target effects. However, we showed that *SOST* expression was consistently influenced by some of these AONs.

It is not clear what the mechanism behind the increased *SOST* expression is. A component of stress in the cells that was caused by the transfection may induce expression of *SOST*. We have tested several stressors like the transfection reagent without AON, oxidative stress, low serum conditions, pH changes and mechanical stress, and none increased *SOST* expression to the levels seen with the AONs (data not shown). Also, as the increases in *SOST* expression were consistent between experiments, they seem to be AON- or sequence-specific and are probably caused by some other factor than transfection-induced stress. The most likely explanation lies in the fact that phosphorothioate AONs bind to serum proteins, in particular heparin-binding proteins and albumin [56, 57]. This binding is aspecific but appears to be influenced by AON length and sequence [58]. *In vivo*, binding to proteins inhibits excretion through the kidney and thereby increases half-life [59, 60]. While the 2OMe modification that was used here in combination with phosphorothioate increases stability and sequence specificity of the AON, it does not abrogate protein binding. As sclerostin is known to interact with heparin [61], the AONs may bind to sclerostin in the growth medium and render it inactive. This could trigger a compensation mechanism leading to increased *SOST* transcription.

The low level of *SOST* expression in SaOS-2 cells may make it difficult to detect downregulation of this gene and show an effect of the AONs. However, when basal *SOST* expression was increased with BMP4 stimulation no decrease of *SOST* expression could be seen with AONs. The two control AONs that were chosen for the subsequent experiment showed the same results before and after BMP4 stimulation; control AON H increased expression and control AON J did not change expression. This validated that *SOST* expression could be modulated in the same way with and without BMP4 stimulation. In addition, basal expression and BMP-stimulated expression can be decreased by other factors such as the Wnt signaling stimulator GIN (Chapter 5), indicating that the lack of downregulation by AONs was not a technical limitation of the experimental model.

To our knowledge, exon skipping has not been attempted on a two-exon gene before. Unlike exon skipping in larger genes like *Rank* and *DMD* where internal exons are targeted, it is not possible to demonstrate an exon skip in *SOST* by fragment analysis by gel electrophoresis. Instead, qRT-PCR was performed using intron-spanning primers to detect a decrease in the full-length RNA. With this method it is

more difficult to detect differences in expression due to exon skipping (or in this case inhibition of splicing), whereas one would usually detect the appearance of a new fragment. This is especially true when the AONs result in a variable expression. It is therefore conceivable that some or even all AONs did have an effect on splicing of *SOST*, but that small decreases in expression could not be detected. We can therefore not conclude that exon skipping is unattainable in two-exon genes and this needs to be investigated in other genes, but the detection method remains challenging.

While exon skipping of *SOST* has not been done before, some experience has been gained in exon skipping of proteins that are involved in inflammatory diseases such as rheumatoid arthritis. Exon skipping of the Tumor necrosis factor alpha (TNF- α) receptor resulted in a soluble protein that was able to reduce inflammation in mouse models for hepatitis and arthritis [62]. In addition, work is ongoing on several other inflammatory mediators such as interleukin-1 receptor accessory protein (IL-1RAcP), IL-5 receptor and complement factor 5 [63]. Even though RANK is a member of the TNF receptor family and therefore shares a similar structure, we were not able to achieve the levels of exon skipping in *Rank* that were shown for the TNF- α receptor. Options for the design of AONs targeting exon 7 in *Rank* were limited as the exon does not contain many ESE sites predicted by ESEFinder (<http://rulai.cshl.edu/cgi-bin/tools/ESE3/ese finder.cgi?process=home>), and the splice sites contain many CCC or GGG motifs that make AONs vulnerable for aggregation. We therefore also targeted exon 5 and 6 of *Rank*. While skipping of exon 7 would produce a soluble protein that could have dual actions – inhibiting signal transduction and competing with membrane-bound molecules – skipping of exon 5 or 6 would produce a reading frame shift and therefore a truncated protein. The maximum of 10.5% skipping efficiency in the exon 6 targeted samples was expected to be too low for a biological effect, and AONs targeting exon 5 or 7 resulted in even lower percentages. It has been reported that proteins undergo nonsense-mediated decay when a premature stop codon is introduced [64], which could lead to underestimation of results. Still, this does not appear to play a large role in this case as inhibition of nonsense-mediated decay with puromycin did not change results. The observed low skipping percentages could partly be due to the cell type that was used, as RAW264.7 cells are difficult to transfect and result in a maximum of ~50% transfection efficiency (data not shown). However, skipping of the IL-1RAcP in these cells was much more

efficient than RANK (data not shown), excluding the cells as the main cause for the observed low skipping efficiency. Nevertheless, skipping efficiency may be optimized by designing and testing more AONs or further optimizing transfection.

In conclusion, exon skipping of *SOST* or *Rank* was unsuccessful with the AONs here described. It has been shown that the sclerosteosis phenotype in some patients is caused by mutations in the 3' splice site of the first exon of *SOST* and these mutations inactivate sclerostin [16, 50, 51]. Even though this proves interference in the process of splicing a two-exon gene is possible, an AON targeting this region (AON6) did not decrease *SOST* expression in our experiments. We were therefore not able to provide a proof-of-principle for splicing modulation of two-exon genes using AONs, but because of the limits to our detection method, it is too early to exclude this possibility. Exon skipping of *Rank* was not efficient enough to anticipate biological effects at this point, but transfection and design may be optimized to increase efficiency.

References

1. Consensus Development Conference: Diagnosis, prophylaxis, and treatment of osteoporosis. *Am.J.Med.* 94, 646-650. (1993).
2. Khosla S, Melton LJ III, Riggs BL. The unitary model for estrogen deficiency and the pathogenesis of osteoporosis: is a revision needed? *J Bone Miner Res* 2011;26:441-51.
3. Harvey N, Dennison E, Cooper C. Osteoporosis: impact on health and economics. *Nat Rev Rheumatol* 2010;6:99-105.
4. Baron R, Hesse E. Update on bone anabolics in osteoporosis treatment: rationale, current status, and perspectives. *J Clin Endocrinol Metab* 2012;97:311-25.
5. McCombs JS, Thiebaud P, Laughlin-Miley C, Shi J. Compliance with drug therapies for the treatment and prevention of osteoporosis. *Maturitas* 2004;48:271-87.
6. Huas D, Debiais F, Blotman F, Cortet B, Mercier F, Rousseaux C *et al.* Compliance and treatment satisfaction of post menopausal women treated for osteoporosis. Compliance with osteoporosis treatment. *BMC Womens Health* 2010;10:26.
7. Cadigan KM, Nusse R. Wnt signaling: a common theme in animal development. *Genes Dev* 1997;11:3286-305.
8. Yang Y. Wnts and wing: Wnt signaling in vertebrate limb development and musculoskeletal morphogenesis. *Birth Defects Res C Embryo Today* 2003;69:305-17.
9. Johnson ML, Kamel MA. The Wnt signaling pathway and bone metabolism. *Curr Opin Rheumatol* 2007;19:376-82.
10. Logan CY, Nusse R. The Wnt signaling pathway in development and disease. *Annu Rev Cell Dev Biol* 2004;20:781-810.
11. Nusse R, Varmus H. Three decades of Wnts: a personal perspective on how a scientific field developed. *EMBO J* 2012;31:2670-84.
12. Li X, Zhang Y, Kang H, Liu W, Liu P, Zhang J *et al.* Sclerostin binds to LRP5/6 and antagonizes canonical Wnt signaling. *J Biol Chem* 2005;280:19883-7.
13. van Bezooijen RL, Roelen BA, Visser A, van der Wee-Pals L, de Wilt E, Karperien M *et al.* Sclerostin is an osteocyte-expressed negative regulator of bone formation, but not a classical BMP antagonist. *J Exp Med* 2004;199:805-14.
14. Van Buchem FS, Hadders HN, Ubbens R. An uncommon familial systemic disease of the skeleton: hyperostosis corticalis generalisata familiaris. *Acta radiol* 1955;44:109-20.
15. Hamersma H, Gardner J, Beighton P. The natural history of sclerosteosis. *Clin Genet* 2003;63:192-7.
16. Balemans W, Ebeling M, Patel N, Van Hul E, Olson P, Dioszegi M *et al.* Increased bone density in sclerosteosis is due to the deficiency of a novel secreted protein (*SOST*). *Hum Mol Genet* 2001;10:537-43.
17. Staehling-Hampton K, Proll S, Paeper BW, Zhao L, Charmley P, Brown A *et al.* A 52-kb deletion in the *SOST*-*MEOX1* intergenic region on 17q12-q21 is associated with Van Buchem disease in the Dutch population. *Am J Med Genet* 2002;110:144-52.

18. van Lierop AH, Hamdy NA, Hamersma H, van Bezooijen RL, Power J, Loveridge N *et al.* Patients with sclerosteosis and disease carriers: human models of the effect of sclerostin on bone turnover. *J Bone Miner Res* 2011;26:2804-11.
19. van Lierop AH, Hamdy NA, van Egmond ME, Bakker E, Dijkers FG, Papapoulos SE. Van Buchem disease: Clinical, biochemical and densitometric features of patients and disease carriers. *J Bone Miner Res* 2012.
20. Costa AG, Bilezikian JP. Sclerostin: therapeutic horizons based upon its actions. *Curr Osteoporos Rep* 2012;10:64-72.
21. Leupin O, Kramer I, Collette NM, Loots GG, Natt F, Kneissel M *et al.* Control of the *SOST* bone enhancer by PTH using MEF2 transcription factors. *J Bone Miner Res* 2007;22:1957-67.
22. Kramer I, Loots GG, Studer A, Keller H, Kneissel M. Parathyroid hormone (PTH)-induced bone gain is blunted in *SOST* overexpressing and deficient mice. *J Bone Miner Res* 2010;25:178-89.
23. Kramer I, Keller H, Leupin O, Kneissel M. Does osteocytic *SOST* suppression mediate PTH bone anabolism? *Trends Endocrinol Metab* 2010;21:237-44.
24. Beighton P, Hamersma H, Brunkow ME. *SOST*-Related Sclerosing Bone Dysplasias. In: Pagon RA, Bird TD, Dolan CR, Stephens K, Adam MP, editors. *GeneReviews™*. Seattle (WA): University of Washington; 2002.
25. Gardner JC, van Bezooijen RL, Mervis B, Hamdy NA, Löwik CW, Hamersma H *et al.* Bone mineral density in sclerosteosis; affected individuals and gene carriers. *J Clin Endocrinol Metab* 2005;90:6392-5.
26. Li X, Ominsky MS, Niu QT, Sun N, Daugherty B, D'Agostin D *et al.* Targeted deletion of the sclerostin gene in mice results in increased bone formation and bone strength. *J Bone Miner Res* 2008;23:860-9.
27. Gooi J, Kramer I, Halleux C, Kneissel M. *Lrp5* is Required for *Sost* Deficiency Induced Mineral Apposition Rate Increases. *J Bone Miner Res* 25[Suppl 1]. (2010).
28. Wada T, Nakashima T, Hiroshi N, Penninger JM. RANKL-RANK signaling in osteoclastogenesis and bone disease. *Trends Mol Med* 2006;12:17-25.
29. Lacey DL, Timms E, Tan HL, Kelley MJ, Dunstan CR, Burgess T *et al.* Osteoprotegerin ligand is a cytokine that regulates osteoclast differentiation and activation. *Cell* 1998;93:165-76.
30. Chambers TJ. Regulation of the differentiation and function of osteoclasts. *J Pathol* 2000;192:4-13.
31. Leibbrandt A, Penninger JM. RANK/RANKL: regulators of immune responses and bone physiology. *Ann N Y Acad Sci* 2008;1143:123-50.
32. Burgess TL, Qian Y, Kaufman S, Ring BD, Van G, Capparelli C *et al.* The ligand for osteoprotegerin (OPGL) directly activates mature osteoclasts. *J Cell Biol* 1999;145:527-38.
33. Wright HL, McCarthy HS, Middleton J, Marshall MJ. RANK, RANKL and osteoprotegerin in bone biology and disease. *Curr Rev Musculoskelet Med* 2009;2:56-64.
34. Dougall WC, Glaccum M, Charrier K, Rohrbach K, Brasel K, de Smedt T *et al.* RANK is essential for osteoclast and lymph node development. *Genes Dev* 1999;13:2412-24.
35. Kong YY, Yoshida H, Sarosi I, Tan HL, Timms E, Capparelli C *et al.* OPGL is a key regulator of osteoclastogenesis, lymphocyte development and lymph-node organogenesis. *Nature* 1999;397:315-23.

36. Bucay N, Sarosi I, Dunstan CR, Morony S, Tarpley J, Capparelli C *et al.* osteoprotegerin-deficient mice develop early onset osteoporosis and arterial calcification. *Genes Dev* 1998;12:1260-8.
37. Amizuka N, Shimomura J, Li M, Seki Y, Oda K, Henderson JE *et al.* Defective bone remodelling in osteoprotegerin-deficient mice. *J Electron Microsc (Tokyo)* 2003;52:503-13.
38. Hughes AE, Ralston SH, Marken J, Bell C, MacPherson H, Wallace RG *et al.* Mutations in TNFRSF11A, affecting the signal peptide of RANK, cause familial expansile osteolysis. *Nat Genet* 2000;24:45-8.
39. Sobacchi C, Frattini A, Guerrini MM, Abinun M, Pangrazio A, Susani L *et al.* Osteoclast-poor human osteopetrosis due to mutations in the gene encoding RANKL. *Nat Genet* 2007;39:960-2.
40. Whyte MP, Hughes AE. Expansile skeletal hyperphosphatasia is caused by a 15-base pair tandem duplication in TNFRSF11A encoding RANK and is allelic to familial expansile osteolysis. *J Bone Miner Res* 2002;17:26-9.
41. Rivadeneira F, Styrkarsdottir U, Estrada K, Halldorsson BV, Hsu YH, Richards JB *et al.* Twenty bone-mineral-density loci identified by large-scale meta-analysis of genome-wide association studies. *Nat Genet* 2009;41:1199-206.
42. Richards JB, Kavvoura FK, Rivadeneira F, Styrkarsdottir U, Estrada K, Halldorsson BV *et al.* Collaborative meta-analysis: associations of 150 candidate genes with osteoporosis and osteoporotic fracture. *Ann Intern Med* 2009;151:528-37.
43. Eghbali-Fatourehchi G, Khosla S, Sanyal A, Boyle WJ, Lacey DL, Riggs BL. Role of RANK ligand in mediating increased bone resorption in early postmenopausal women. *J Clin Invest* 2003;111:1221-30.
44. Syed F, Khosla S. Mechanisms of sex steroid effects on bone. *Biochem Biophys Res Commun* 2005;328:688-96.
45. Pageau SC. Denosumab. *MAbs* 2009;1:210-5.
46. Baron R, Ferrari S, Russell RG. Denosumab and bisphosphonates: different mechanisms of action and effects. *Bone* 2011;48:677-92.
47. Kole R, Krainer AR, Altman S. RNA therapeutics: beyond RNA interference and antisense oligonucleotides. *Nat Rev Drug Discov* 2012;11:125-40.
48. Aartsma-Rus A, van Ommen GJ. Antisense-mediated exon skipping: a versatile tool with therapeutic and research applications. *RNA* 2007;13:1609-24.
49. van Roon-Mom WMC, Aartsma-Rus A. Overview on applications of antisense-mediated exon skipping. In: Aartsma-Rus A, editor. *Exon Skipping: Methods and Protocols*: Humana Press; 2012; p. 79-96.
50. Brunkow ME, Gardner JC, Van NJ, Paepfer BW, Kovacevich BR, Proll S *et al.* Bone dysplasia sclerosteosis results from loss of the *SOST* gene product, a novel cystine knot-containing protein. *Am J Hum Genet* 2001;68:577-89.
51. Balemans W, Cleiren E, Siebers U, Horst J, van HW. A generalized skeletal hyperostosis in two siblings caused by a novel mutation in the *SOST* gene. *Bone* 2005;36:943-7.
52. Aartsma-Rus A. Overview on AON design. In: Aartsma-Rus A, editor. *Exon Skipping: Methods and Protocols*: Humana Press; 2012; p. 117-29.

53. Agrawal S, Jiang Z, Zhao Q, Shaw D, Cai Q, Roskey A *et al*. Mixed-backbone oligonucleotides as second generation antisense oligonucleotides: *in vitro* and *in vivo* studies. *Proc Natl Acad Sci U S A* 1997;94:2620-5.
54. Shen LX, Kandimalla ER, Agrawal S. Impact of mixed-backbone oligonucleotides on target binding affinity and target cleaving specificity and selectivity by *Escherichia coli* RNase H. *Bioorg Med Chem* 1998;6:1695-705.
55. Pfaffl MW. A new mathematical model for relative quantification in real-time RT-PCR. *Nucleic Acids Res* 2001;29:e45.
56. Kurreck J. Antisense technologies. Improvement through novel chemical modifications. *Eur J Biochem* 2003;270:1628-44.
57. Srinivasan SK, Tewary HK, Iversen PL. Characterization of binding sites, extent of binding, and drug interactions of oligonucleotides with albumin. *Antisense Res Dev* 1995;5:131-9.
58. Watanabe TA, Geary RS, Levin AA. Plasma protein binding of an antisense oligonucleotide targeting human ICAM-1 (ISIS 2302). *Oligonucleotides* 2006;16:169-80.
59. Heemskerk H, de Winter C, van Kuik P, Heuvelmans N, Sabatelli P, Rimessi P *et al*. Preclinical PK and PD studies on 2'-*O*-methyl-phosphorothioate RNA antisense oligonucleotides in the mdx mouse model. *Mol Ther* 2010;18:1210-7.
60. Arechavala-Gomez V, Anthony K, Morgan J, Muntoni F. Antisense oligonucleotide-mediated exon skipping for Duchenne muscular dystrophy: progress and challenges. *Curr Gene Ther* 2012;12:152-60.
61. Veverka V, Henry AJ, Slocombe PM, Ventom A, Mulloy B, Muskett FW *et al*. Characterization of the structural features and interactions of sclerostin: molecular insight into a key regulator of Wnt-mediated bone formation. *J Biol Chem* 2009;284:10890-900.
62. Graziewicz MA, Tarrant TK, Buckley B, Roberts J, Fulton L, Hansen H *et al*. An endogenous TNF-alpha antagonist induced by splice-switching oligonucleotides reduces inflammation in hepatitis and arthritis mouse models. *Mol Ther* 2008;16:1316-22.
63. Yilmaz-Elis S, Aartsma-Rus A, Vroon A, van Deutekom J, de Kimpe S, 't Hoen PA *et al*. Antisense oligonucleotide mediated exon skipping as a potential strategy for the treatment of a variety of inflammatory diseases such as rheumatoid arthritis. *Ann Rheum Dis* 2012;71 Suppl 2:i75-i77.
64. Chang YF, Imam JS, Wilkinson MF. The nonsense-mediated decay RNA surveillance pathway. *Annu Rev Biochem* 2007;76:51-74.

A vertical strip on the left side of the page contains a grayscale microscopic image of bone tissue, showing a complex, porous, and fibrous structure. The text 'Chapter 7' is overlaid on this image.

Chapter 7

Validation of a simple and fast method to quantify in vitro mineralization with fluorescent probes used in molecular imaging of bone

M.J.C. Moester
M.A.E. Schoeman
I.B. Oudshoorn
M.M. van Beusekom
I.M. Mol
E.L. Kaijzel
C.W.G.M. Löwik
K.E. de Rooij

Biochem Biophys Res Commun.
2014 Jan 3;443(1):80-5

Abstract

Alizarin Red S staining is the standard method to indicate and quantify matrix mineralization during differentiation of osteoblast cultures. KS483 cells are multipotent mouse mesenchymal progenitor cells that can differentiate into chondrocytes, adipocytes and osteoblasts and are a well-characterized model for the study of bone formation. Matrix mineralization is the last step of differentiation of bone cells and is therefore a very important outcome measure in bone research. Fluorescently labelled calcium chelating agents, e.g. BoneTag and OsteoSense, are currently used for *in vivo* imaging of bone. The aim of the present study was to validate these probes for fast and simple detection and quantification of *in vitro* matrix mineralization by KS483 cells and thus enabling high-throughput screening experiments.

KS483 cells were cultured under osteogenic conditions in the presence of compounds that either stimulate or inhibit osteoblast differentiation and thereby matrix mineralization. After 21 days of differentiation, fluorescence of stained cultures was quantified with a near-infrared imager and compared to Alizarin Red S quantification. Fluorescence of both probes closely correlated to Alizarin Red S staining in both inhibiting and stimulating conditions. In addition, both compounds displayed specificity for mineralized nodules. We therefore conclude that this method of quantification of bone mineralization using fluorescent compounds is a good alternative for the Alizarin Red S staining.

Introduction

During osteoblast differentiation collagen is deposited in the extracellular space. When Ca^{2+} and inorganic phosphate accumulate to form hydroxyapatite crystals, the matrix mineralizes to form bone [1-3]. *In vitro*, primary bone cells or bone marrow derived cells can be induced to form a mineralized matrix when cultured in osteogenic medium [4]. KS483 cells, a murine mesenchymal progenitor cell line, can differentiate into chondrocytes, adipocytes and osteoblasts and are a well-characterized model for bone formation [5, 6]. These cells are used for the study of many aspects of bone biology, as well as new drug targets for bone-related diseases [7-9].

The quantification of matrix mineralization in cell cultures is one of the most important indicators for successful differentiation. Currently, the most common method for the quantification of mineralization is the Alizarin Red S staining [10]. This staining can be quantified by extraction with hexadecylpyridinium chloride and spectrophotometric analysis [3].

IRDye® 800CW BoneTag™ and OsteoSense® 800 are fluorescently labelled probes with high affinity for bone currently used for *in vivo* imaging. BoneTag is a tetracycline derivate coupled to IRDye 800CW [11], while OsteoSense is based on the bisphosphonate pamidronate with an IRDye78 label [12]. Both compounds have an emission wavelength of 800 nm, reducing auto-fluorescence both *in vivo* and *in vitro* [13].

We now describe a simple and fast method for the quantification of matrix mineralization in cell cultures using BoneTag and OsteoSense. To validate this method, results obtained with these compounds were compared to the well-established method of Alizarin Red S staining in different culture conditions. BoneTag and OsteoSense fluorescence correlated with Alizarin Red S staining quantifications in cultures after incubation with compounds that either stimulate or inhibit osteoblast differentiation and/or matrix mineralization. We therefore show the wide range of possibilities for use of these fluorescent probes for *in vitro* bone research.

Materials and methods

Cell culture and differentiation

KS483 cells were cultured as described previously [6]. Briefly, cells were cultured routinely in α -MEM (Gibco, Life Technologies, Carlsbad, CA, USA) supplemented with penicillin/streptomycin (Sigma-Aldrich, St. Louis, MO, USA), Glutamax (Gibco) and 10% fetal calf serum (FCS; Greiner Bio-One, Frickenhausen, Germany). For differentiation assays, KS483 cells were seeded at a density of 9,200 cells/cm² in 12-wells plates (Greiner Bio-One). Every 3-4 days the medium was replaced. At confluence (from day 4 of culture onward) 50 μ g/ml ascorbic acid (BDH Prolabo, VWR International, Radnor, PA, USA) and when nodules appeared (from day 11 of culture onward) 5 mM glycerol 2-phosphate disodium salt (β GP; Sigma-Aldrich, St. Louis, MO, USA) was added to the culture medium. When applicable, bone morphogenetic protein 6 (BMP-6; kindly provided by prof. S. Vukicevic, Department of Anatomy, School of Medicine, Zagreb, Croatia) was added at day 4 of culture or parathyroid hormone related protein (PTHrP; Bachem, Bubendorf, Switzerland) was added from day 4 onward.

Alkaline phosphatase measurements

Medium samples were taken every 3-4 days before medium change. Alkaline phosphatase (ALP) activity was measured by adding 200 μ l of 120 nM p-nitrophenylphosphate (PNPP, Thermo-Scientific, Waltham, MA, USA) in 100 mM glycine/1 mM MgCl₂/0.1 mM ZnCl₂ buffer (pH10.5) and measured for 10 min using a VERSAmax Tunable Microplate Reader (Molecular Devices, Sunnyvale, CA, USA) at 405 nm. ALP activity was determined as the slope of the kinetic measurement (mOD/min).

Quantification of mineralization by fluorescence

At 24 hours before analysis, the cell cultures were incubated with the calcium binding agent IRDye[®] 800CW BoneTag[™] (BoneTag, LI-COR Biosciences, Lincoln, NE, USA) or the IRDye78 labeled bisphosphonate pamidronate OsteoSense[®] 800 (Perkin Elmer, Waltham, MA, USA), both at a concentration of 2 pmol/ml (1:10,000 dilution). After incubation the cells were washed with phosphate-buffered saline

(PBS) and fixed with 3.7% buffered formaldehyde. The fixed cells were scanned with the Odyssey Infrared Imaging System (LI-COR) at a resolution of 42 μm , medium quality and intensity 5.0-6.5. Integrated intensity (counts- mm^2) of each well was calculated by the Odyssey software.

Quantification of mineralization by Alizarin Red S

Mineralized nodules were fixed with 3.7% buffered formaldehyde, stained with 2% Alizarin Red S solution for 2 minutes and washed 3 times with H_2O . Pictures were taken using a Powershot A650IS Digital Camera (Canon, Ōta, Tokyo, Japan) through a light microscope at 5x magnification. For quantification, Alizarin was removed from the cell layer by overnight incubation with 10% hexadecylpyridinium chloride in 10 mM PO_4 buffer (pH 7.5), and measured at 550 nm on a VERSAmax Tunable Microplate Reader (Molecular Devices) against a range of Alizarin standards (0.005-0.8 $\mu\text{g}/\text{ml}$).

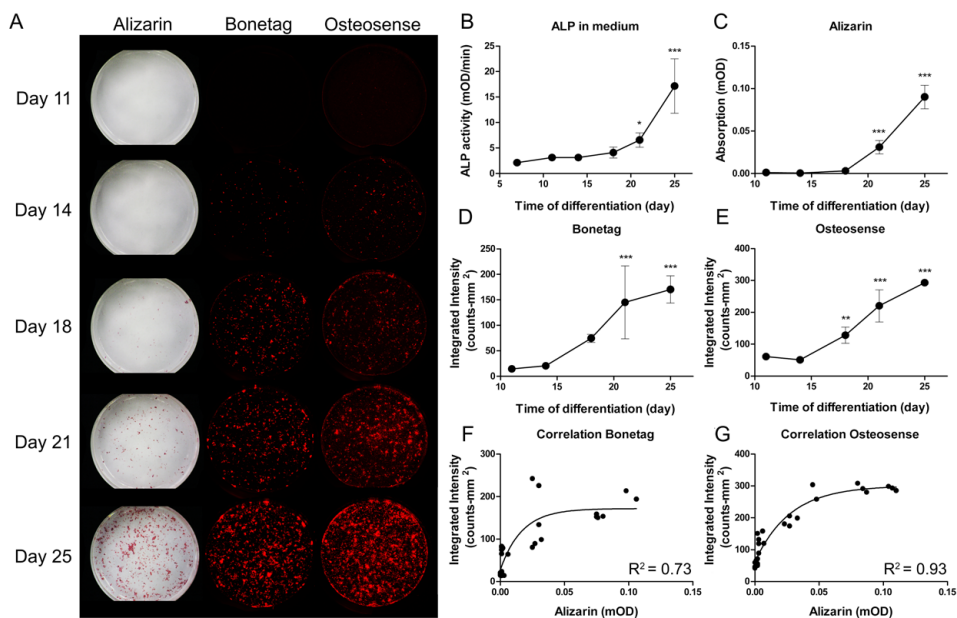


Figure 1. Comparison of Alizarin Red S staining, BoneTag and OsteoSense in KS483 cell cultures during differentiation. A) Representative photos of Alizarin Red S staining and BoneTag and OsteoSense fluorescence; B) measurements of ALP activity; C) quantification of Alizarin Red S staining; D) quantification of BoneTag fluorescence; E) quantification of OsteoSense fluorescence; F) correlation between Alizarin Red S staining and BoneTag fluorescence. $R^2=0.73$ $p<0.0001$; G) correlation between Alizarin Red S staining and OsteoSense fluorescence. $R^2=0.93$ $p<0.0001$.

* $p<0.05$, ** $p<0.01$, *** $p<0.001$ vs. day 11 or for ALP measurements vs. day 4.

Statistics

Values represent means \pm SD. Differences were tested by two-way (ALP measurements) or one-way analysis of variance (ANOVA) followed by Tukey's post hoc test using Graphpad Prism 5 software (La Jolla, CA, USA). Nonlinear regression was performed for the correlation between Alizarin Red S staining and fluorescent markers. Results were considered significant at $p < 0.05$.

Results

Alizarin Red S staining and BoneTag or OsteoSense fluorescence increase over time during differentiation

To validate the quantification of *in vitro* matrix mineralization using the fluorescent compounds BoneTag and OsteoSense, readouts of these compounds were compared to the well-established method of Alizarin Red S staining in different culture conditions. First, Alizarin Red S staining and fluorescent images were quantified at different time points during differentiation. Figure 1A shows representative pictures of Alizarin Red S staining, BoneTag and OsteoSense fluorescence at each time point. ALP activity was measured in medium as a measure for osteoblast differentiation and increased over time (Figure 1B). As shown in Figure 1C-E, signals from all three readouts increased in intensity as the matrix becomes more mineralized over time. Both BoneTag and OsteoSense displayed slight background fluorescence. However, a significant correlation was observed between Alizarin Red S staining and both BoneTag ($R^2 = 0.73$ $p < 0.0001$; Figure 1F) and OsteoSense ($R^2 = 0.93$ $p < 0.0001$; Figure 1G). In addition, both fluorescent readouts appear to be more sensitive for small changes in matrix mineralization than Alizarin Red S, as shown by the non-linear correlation. Indeed, at day 18 of differentiation both BoneTag and OsteoSense were able to identify an increase in matrix mineralization, while this was only apparent from day 21 with Alizarin Red S staining.

Correlation between Alizarin staining and fluorescence after modulation of differentiation

To validate BoneTag and OsteoSense quantification further, we examined whether

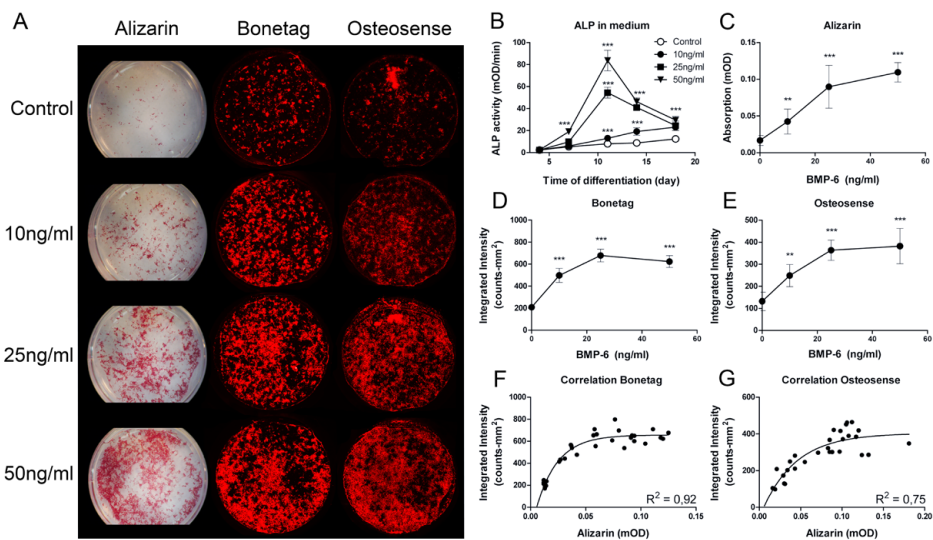


Figure 2. Comparison of Alizarin Red S staining, BoneTag and OsteoSense in differentiated KS483 cell cultures after stimulation with different concentrations of BMP-6. A) Representative photos of Alizarin Red S staining and BoneTag and OsteoSense fluorescence; B) measurements of ALP activity; C) quantification of Alizarin Red S staining; D) quantification of BoneTag fluorescence; E) quantification of OsteoSense fluorescence; F) correlation between Alizarin Red S staining and BoneTag fluorescence. $R^2=0.92$ $p<0.0001$; G) correlation between Alizarin Red S staining and OsteoSense fluorescence. $R^2=0.75$ $p<0.0001$.

ALP: *** $p<0.001$ vs. day 4. Alizarin, Bonetag and Osteosense: ** $p<0.01$ and *** $p<0.001$ vs. control.

the correlation between Alizarin Red S staining and BoneTag or OsteoSense fluorescence is still present after modulation of osteoblast differentiation. Therefore, KS483 cell cultures were stimulated with BMP-6 and inhibited with PTHrP [14]. BMP-6 stimulated ALP activity and increased Alizarin Red S staining and fluorescence dose-dependently (Figure 2A-E). PTHrP dose-dependently decreased ALP activity and both Alizarin Red S staining and fluorescence (Figure 3A-E). Correlation between both BoneTag and OsteoSense and Alizarin Red S staining was significant with $R^2 = 0.92$ and 0.75 ($p < 0.0001$), respectively, for cultures stimulated with BMP-6 (Figure 2F-G) and $R^2 = 0.84$ and 0.92 ($p < 0.0001$), respectively, for cultures with PTHrP (Figure 3F-G).

Specificity of staining for mineralized nodules

Next, we examined the specificity of BoneTag or OsteoSense binding to mineralized matrix by culturing KS483 cells without β GP. Without phosphate, the nodules did not mineralize as shown by the absence of staining in samples without β GP (Figure 4A). ALP activity after stimulation with BMP-6 but without β GP is slightly

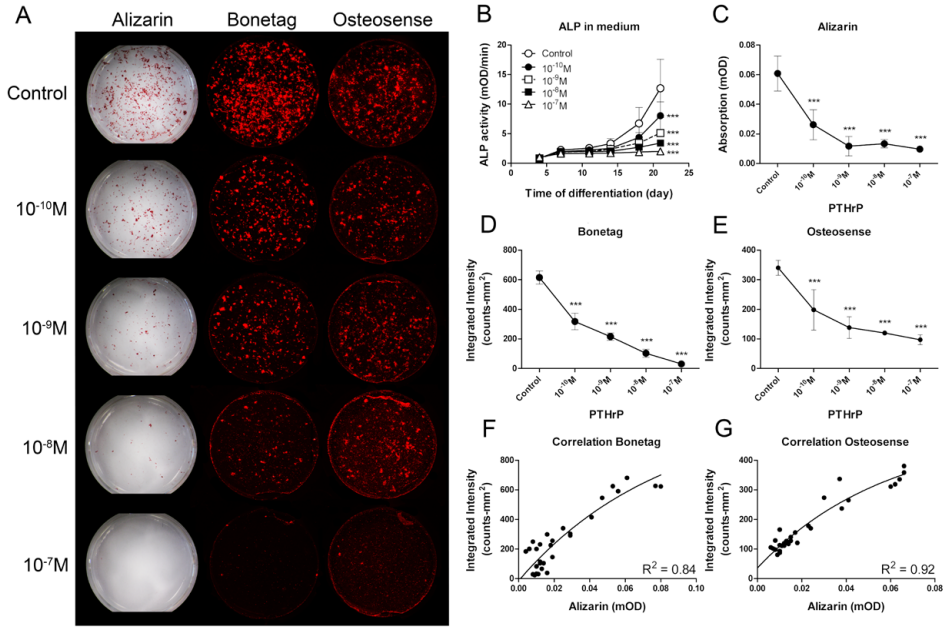


Figure 3. Comparison of Alizarin Red S staining, BoneTag and OsteoSense in differentiated KS483 cell cultures after inhibition with different concentrations of PTHrP. A) Representative photos of Alizarin Red S staining and BoneTag and OsteoSense fluorescence; B) measurements of ALP activity; C) quantification of Alizarin Red S staining; D) quantification of BoneTag fluorescence; E) quantification of OsteoSense fluorescence. F) correlation between Alizarin Red S staining and BoneTag fluorescence. $R^2=0.84$ $p<0.0001$; G) correlation between Alizarin Red S staining and OsteoSense fluorescence. $R^2=0.92$ $p<0.0001$. *** $p<0.001$ vs. Control.

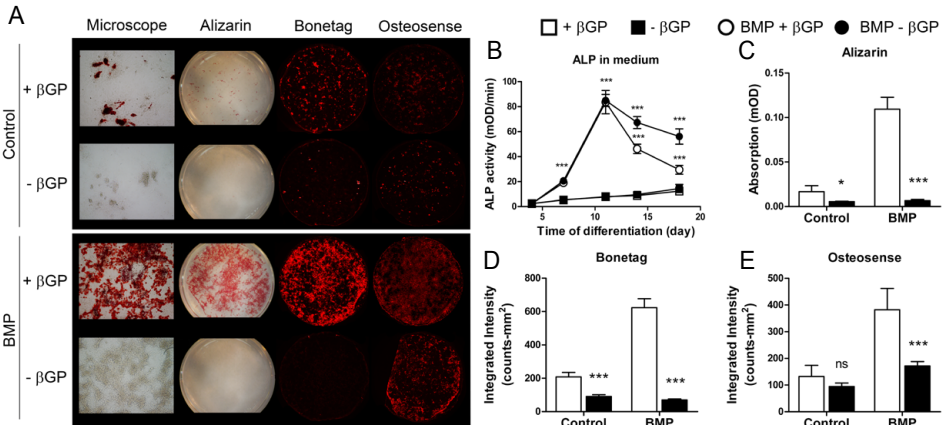


Figure 4. Comparison of Alizarin Red S staining, BoneTag and OsteoSense in KS483 cell cultures differentiated in the presence or absence of β GP and/or stimulated with 50 ng/ml BMP-6 at day 4 of differentiation. A) Representative photos of Alizarin Red S staining, light microscope images of alizarin stained samples at 100x magnification, and BoneTag and OsteoSense fluorescence; B) measurements of ALP activity; C) quantification of Alizarin Red S staining; D) quantification of BoneTag fluorescence; E) quantification of OsteoSense fluorescence. * $p<0.05$; *** $p<0.001$ vs. + β GP

increased compared to BMP+ β GP (Figure 4B). Staining of unmineralized nodules was minimal, even after stimulation with BMP-6 (Figure 4A). Quantification of staining showed a large difference between conditions + β GP and - β GP in both Alizarin and BoneTag-stained samples. OsteoSense showed some background staining in samples without β GP, especially in the control condition (Figure 4C-E). Fluorescence microscopy of stained nodules revealed the localization of fluorescence in the mineralized matrix (Supplementary figure 1).

Discussion

The Near Infrared fluorescent calcium binding agents BoneTag and OsteoSense are currently used for *in vivo* imaging of bone. To validate these agents for quantification of matrix mineralization in cell cultures, we compared the results of quantification with these compounds to the well-established method of Alizarin Red S staining after modulation of differentiation and matrix mineralization. In stimulating and inhibiting conditions both BoneTag and OsteoSense fluorescence correlated with the quantification of matrix mineralization by Alizarin Red S staining. In addition, similar to Alizarin Red S staining, both fluorescent compounds showed selectivity for mineralized nodules.

Differentiation of osteoblasts and matrix mineralization were increased by culturing in the presence of BMP-6. Increased ALP activity with increasing BMP-6 concentrations is evidence of the stimulation of differentiation of osteoblasts [6, 15]. Mineralization of the extracellular matrix increased dose-dependently when the cells were stimulated with BMP-6, which is also reflected by an increase in fluorescent signal of both BoneTag and OsteoSense. On the other hand, PTHrP decreased ALP activity in a dose-dependent manner. Like PTH, PTHrP signals via the PTH receptor and the cyclic AMP pathway to inhibit osteoblast differentiation and thereby matrix mineralization [14, 16-18]. Our results show a good correlation between Alizarin Red S staining and BoneTag or OsteoSense fluorescence after modulation with either BMP-6 or PTHrP. While the fluorescent stains were more sensitive to small changes, Alizarin Red S staining could be used in highly mineralized samples.

Specificity for mineralization was tested by culturing KS483 cells in the presence or absence of β GP. ALP activity dramatically increased after stimulation with BMP-6, and then declined after day 11 of culture. However, ALP activity remained high

when the cells were cultured without β GP. The difference in staining quantification between conditions + β GP and - β GP in both control and BMP-stimulated conditions indicated that the staining was able to distinguish between mineralized and unmineralized nodules and thus indicates specificity. Like Alizarin Red S, BoneTag displayed low background staining in unmineralized nodules, while OsteoSense staining seemed to have a higher background and could not distinguish between + and - β GP without BMP-6 stimulation. This indicates that BoneTag has a higher specificity to the bone mineral compared to OsteoSense.

Bisphosphonates are compounds that bind with high affinity to bone and are used in the clinic for treatment of osteoporosis because of their ability to inhibit bone resorption by osteoclasts [19]. Because of their high affinity, bisphosphonates have a long half-life when bound to a mineralized matrix [19, 20]. OsteoSense is based on the bisphosphonate pamidronate [12], and care must be taken when using this probe in bisphosphonate research, since competition between the administered bisphosphonate and OsteoSense staining may occur. This potential problem is not expected when using BoneTag, which is a tetracylin-based probe [11]. In addition, it is important to note that in our experience OsteoSense is stable for a limited period of time (up to 8 weeks), even when stored at -80°C (data not shown), while BoneTag storage could be extended to over a year without loss of specificity.

Alizarin Red S is the standard staining for mineralized matrix in bone research. It can be dissolved and quantified by spectrophotometry. There are several advantages of using BoneTag and OsteoSense compared to Alizarin Red S staining:

- 1) They are added in the culture medium prior to fixation of the cells, and require no additional washing or staining procedures.
- 2) Both BoneTag and OsteoSense are available with fluorescence at 800nm and 680nm. The long wavelength of these probes makes them ideal for use with mineralized matrix as this greatly reduces autofluorescence.
- 3) These probes are universal in use for *in vivo* and *in vitro* bone research as they can also be used for *in vivo* imaging of bone formation. They are commercially available as quality controlled validated batches, reducing variability.
- 4) They can be quantified with great sensitivity using the dedicated Odyssey near-infrared imaging system.

- 5) Because small amounts of dye are needed for staining, the dyes are very cost-effective; up to 12,000 samples can be stained with a single vial of 24 pmol.

Other options for fluorescent detection of *in vitro* mineralization may be xylenol orange or calcein blue. Wang *et al.* [21] have for example used these substances to evaluate mineralized nodule formation in living osteoblastic cultures. However, this method was used to count the number of positive nodules, and not to quantify mineralization. Furthermore, these fluorescent dyes emit blue or red light, which is sensitive to autofluorescence of the mineralized matrix.

In conclusion, BoneTag and OsteoSense are good substitutes with many advantages over Alizarin Red S staining. The results of both fluorescent compounds provide good correlation with Alizarin Red S staining in a range of different experiments stimulating and inhibiting differentiation and mineralization. BoneTag is more specific in conditions of low mineralization and can be stored for extended periods of time. The long emission wavelength in the near-infrared range reduces autofluorescence during detection. For both compounds numerous possibilities exist for combination with other fluorescent markers at different wavelengths, such as DNA stains. This opens up many possibilities for quantitative and high-throughput experiments in bone research.

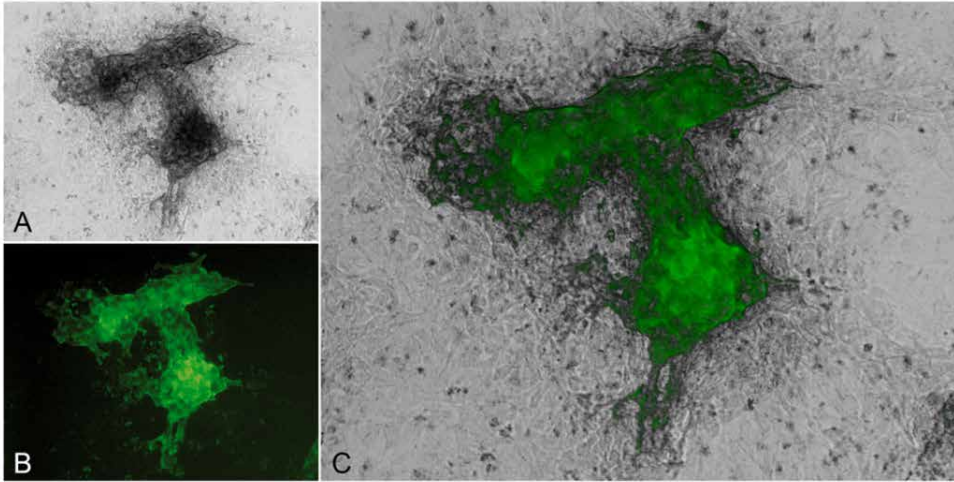
Acknowledgments

This work was supported by grants from NL Agency/IOP Genomics (IGE07001A), the Netherlands Institute for Regenerative Medicine (NIRM, FES0908) and the Dutch Arthritis Foundation (Reumafonds LLP-13). The authors acknowledge prof. S. Vukicevic for generously providing BMP-6 and dr. A.B. Chan for critically reading the manuscript.

References

1. Thyberg J. Electron microscopic studies on the initial phases of calcification in guinea pig epiphyseal cartilage. *J Ultrastruct Res* 1974;46:206-18.
2. Wu LN, Ishikawa Y, Sauer GR, Genge BR, Mwale F, Mishima H *et al.* Morphological and biochemical characterization of mineralizing primary cultures of avian growth plate chondrocytes: evidence for cellular processing of Ca²⁺ and Pi prior to matrix mineralization. *J Cell Biochem* 1995;57:218-37.
3. Gregory CA, Gunn WG, Peister A, Prockop DJ. An Alizarin red-based assay of mineralization by adherent cells in culture: comparison with cetylpyridinium chloride extraction. *Anal Biochem* 2004;329:77-84.
4. Lian JB, Stein GS. Development of the osteoblast phenotype: molecular mechanisms mediating osteoblast growth and differentiation. *Iowa Orthop J* 1995;15:118-40.
5. Yamashita T, Ishii H, Shimoda K, Sampath TK, Katagiri T, Wada M *et al.* Subcloning of three osteoblastic cell lines with distinct differentiation phenotypes from the mouse osteoblastic cell line KS-4. *Bone* 1996;19:429-36.
6. van der Horst G, van Bezooijen RL, Deckers MM, Hoogendam J, Visser A, Löwik CW *et al.* Differentiation of murine preosteoblastic KS483 cells depends on autocrine bone morphogenetic protein signaling during all phases of osteoblast formation. *Bone* 2002;31:661-9.
7. Deckers MM, van Bezooijen RL, van der Horst G, Hoogendam J, van der Bent C, Papapoulos SE *et al.* Bone morphogenetic proteins stimulate angiogenesis through osteoblast-derived vascular endothelial growth factor A. *Endocrinology* 2002;143:1545-53.
8. Miclea RL, van der Horst G, Robanus-Maandag EC, Löwik CW, Oostdijk W, Wit JM *et al.* Apc bridges Wnt/beta-catenin and BMP signaling during osteoblast differentiation of KS483 cells. *Exp Cell Res* 2011;317:1411-21.
9. 't Hoen PA, Jirka SM, Broeke BRt, Schultes EA, Aguilera B, Pang KH *et al.* Phage display screening without repetitious selection rounds. *Anal Biochem* 2012;421:622-31.
10. Puchtler H, Meloan SN, Terry MS. On the history and mechanism of alizarin and alizarin red S stains for calcium. *J Histochem Cytochem* 1969;17:110-24.
11. Kovar JL, Xu X, Draney D, Cupp A, Simpson MA, Olive DM. Near-infrared-labeled tetracycline derivative is an effective marker of bone deposition in mice. *Anal Biochem* 2011;416:167-73.
12. Zaheer A, Lenkinski RE, Mahmood A, Jones AG, Cantley LC, Frangioni JV. *In vivo* near-infrared fluorescence imaging of osteoblastic activity. *Nat Biotechnol* 2001;19:1148-54.
13. Weissleder R, Ntziachristos V. Shedding light onto live molecular targets. *Nat Med* 2003;9:123-8.
14. van der Horst G, Farih-Sips H, Löwik CW, Karperien M. Multiple mechanisms are involved in inhibition of osteoblast differentiation by PTHrP and PTH in KS483 Cells. *J Bone Miner Res* 2005;20:2233-44.
15. Takawa Y, Ohse C, Wang EA, Wozney JM, Yamashita K. Bone morphogenetic protein-2 stimulates alkaline phosphatase activity and collagen synthesis in cultured osteoblastic cells, MC3T3-E1. *Biochem Biophys Res Commun* 1991;174:96-101.
16. Du P, Ye Y, Seitz PK, Bi LG, Li H, Wang C *et al.* Endogenous parathyroid hormone-related peptide enhances proliferation and inhibits differentiation in the osteoblast-like cell line ROS 17/2.8. *Bone* 2000;26:429-36.

17. Martínez ME, García-Ocaña A, Sánchez M, Medina S, del Campo T, Valin A *et al.* C-terminal parathyroid hormone-related protein inhibits proliferation and differentiation of human osteoblast-like cells. *J Bone Miner Res* 1997;12:778-85.
18. Zerega B, Cermelli S, Bianco P, Cancedda R, Cancedda FD. Parathyroid hormone [PTH(1-34)] and parathyroid hormone-related protein [PTHrP(1-34)] promote reversion of hypertrophic chondrocytes to a prehypertrophic proliferating phenotype and prevent terminal differentiation of osteoblast-like cells. *J Bone Miner Res* 1999;14:1281-9.
19. Papapoulos SE. The role of bisphosphonates in the prevention and treatment of osteoporosis. *Am J Med* 1993;95:48S-52S.
20. Shinkai I, Ohta Y. New drugs--reports of new drugs recently approved by the FDA. Alendronate. *Bioorg Med Chem* 1996;4:3-4.
21. Wang YH, Liu Y, Maye P, Rowe DW. Examination of mineralized nodule formation in living osteoblastic cultures using fluorescent dyes. *Biotechnol Prog* 2006;22:1697-701.



Supplementary figure 1. Mineralized nodule in a differentiated KS483 culture stained with BoneTag (LI-COR) and photographed by a Nuance 2.8 camera mounted on a Leica DM IRE2 fluorescence microscope (Leica). Magnification 400x. A) Brightfield image, B) Fluorescence image with BoneTag in green (800 nm), C) Composite of brightfield and fluorescence images. Fluorescence overlaps the mineralized area.

A vertical strip on the left side of the page contains a grayscale microscopic image of biological tissue. The image shows various cellular structures, including what appears to be a cross-section of a vessel or duct with a lumen, and surrounding cellular layers with distinct textures and patterns.

Chapter 8

General discussion

General Discussion

Osteoporosis is a growing problem in the aging society. While several therapies are available, none of these are able to persistently increase bone formation and return bone mass to a more favorable quantity that is strong enough to resist breaking. Research is therefore needed to discover new targets and develop drugs for the treatment of osteoporosis in the future.

Clinical importance

Sclerostin, a natural inhibitor of bone formation that is expressed by osteocytes, was discovered in mutation analyses of patients with sclerosteosis [1, 2]. These patients present with severe bone overgrowth and a bone mass that can be up to 11 standard deviations above normal [3]. Interestingly, the bone of these individuals is of very good quality and no affected person has been reported to have suffered a fracture [4]. Even heterozygous carriers of mutations in the gene coding for sclerostin (SOST) have consistently higher bone mass than control subjects and are relatively resistant to fracture, suggesting a gene-dose effect. The restricted expression pattern of sclerostin adds to the view of sclerostin as one of the most interesting targets for new treatment options for osteoporosis. Knowledge of the mechanism of action and regulation of sclerostin expression are essential to optimally benefit from its characteristics in future therapies. **Chapter 2** therefore gives an overview of the current knowledge on sclerostin function, expression and regulation. Even though much is known about the expression pattern and effect of sclerostin, the exact mechanism of action and pathways by which it is regulated remain to be elucidated.

A lot can be learned from mutation studies, especially in naturally occurring human diseases. In **Chapter 3** we found that Dickkopf 1 (DKK1), a protein that like sclerostin inhibits Wnt signaling through binding to Low-density lipoprotein receptor-related protein 5/6 (LRP5/6), was increased in serum samples from patients with sclerosteosis and Van Buchem disease. DKK1 may be increased in an effort to compensate for the lack of sclerostin in these patients. However, their increased bone mass indicates that the increase in DKK1 expression is insufficient to protect against excessive bone formation. While sclerostin is facilitated by LRP4 [5], DKK1 employs Kremen as a co-receptor [6, 7]. In addition, sclerostin is expressed almost exclusively in osteocytes in mineralized matrix, whereas DKK1 is expressed in many cell types

throughout the body and is implicated in tumorigenesis [8]. The proteins seem to have different roles during development. SOST knockout mice show increased bone mass without gross developmental abnormalities while mice deficient in DKK1 are embryonic lethal displaying fore- and hindlimb malformations and lacking anterior head structures [9, 10]. Therefore, even though both proteins bind to LRP5/6 they have a different mechanism of action, a different expression pattern and may act on osteoblasts at different developmental stages. This may explain the finding that DKK1 was not able to fully compensate for the lack of sclerostin.

The populations of patients with sclerosteosis and Van Buchem disease are quite isolated in South Africa and a small town in the Netherlands, respectively. After the discovery of the causative mutations for sclerosteosis and Van Buchem disease, other sclerostin mutations were found in phenotypically identical patients from Brazil, USA and Senegal [11, 12]. These mutations include several different nonsense mutations leading to a premature stop codon, and a splice site mutation interfering with correct splicing of the gene. In **Chapter 4** we described a novel missense mutation in two siblings from Turkey with classic sclerosteosis characteristics like enlarged skull and jaw, facial nerve palsy, hearing loss, headaches and highly increased bone mineral density (BMD). This mutation causes a cysteine to arginine amino acid substitution at position 167. The affected cysteine residue is the last of six cysteines forming a cystine knot and is highly conserved in multiple species. Recent data have emphasized the importance of the cystine knot motive for sclerostin function [13, 14]. The structure of sclerostin contains two fingers and a loop, emanating from the central cystine knot resembling many other cystine knot proteins [15]. This structure is highly dependent on the folding of the cystine knot. Because of the important function of the cysteine residues in protein folding, the mutation in sclerostin was predicted to disrupt the cystine knot motif and require conformational changes of the loop segment to accommodate the larger arginine side chain. These changes would lead to a global misfolding of the protein and retention in the endoplasmatic reticulum. In addition, we showed that the binding affinity of mutated sclerostin for LRP5 was decreased and its function was impaired. In the patients, this led to a phenotype comparable to that of patients with sclerosteosis. Together, these data highlight the importance of sclerostin structure and correct protein folding for its function in inhibiting Wnt signaling and bone formation.

Modulating sclerostin expression and investigating effects

As sclerostin is a negative regulator of bone formation that acts by inhibiting the Wnt signaling pathway, inhibiting the expression of this protein in patients with osteoporosis would lead to increased bone formation. By understanding the endogenous regulatory mechanisms that control *SOST* expression, we may eventually be able to specifically target and modulate these mechanisms in patients with osteoporosis to increase bone formation with minimal side-effects. In **Chapter 5** we investigated the regulation of *SOST* by modulating the activity of the Wnt signaling pathway. *SOST* expression appeared to be downregulated by increased Wnt signaling activity, and was strongly decreased by the GSK3 β inhibitor GIN. However, several Wnt signaling inhibitors that work at different stages in the pathway could not abrogate the decrease in *SOST* expression. A compound that blocked the binding of β -catenin to the TCF/LEF transcription complex and thereby directly inhibited downstream target gene transcription, had no effect on the expression of *SOST* after treatment with GIN. It seems therefore that the decrease in *SOST* expression is not mediated by Wnt/ β -catenin signaling, but via a different effect of GSK3 β .

The importance of GSK3 β in bone has been shown by inactivation and overexpression studies in mice. Global deletions of GSK3 β are lethal in late embryonic or perinatal stages with various skeletal abnormalities [16-18]. Heterozygous deletions result in increased bone mass (both trabecular and cortical), and increased bone formation parameters without skeletal malformations [18, 19]. In addition to its role in Wnt/ β -catenin signaling, GSK3 β is also involved in insulin signaling through PKB/AKT [20]. While both pathways have been reported to induce bone formation [21, 22], GSK3 β appears to be differentially regulated through the phosphorylation of different amino acids [23]. This may facilitate different downstream actions. Further research will need to identify the mechanism that GSK3 β employs in the regulation of *SOST*.

While interfering with endogenous regulation of sclerostin expression is an interesting therapeutic option, other methods are being investigated to block the effect of the protein. New therapeutic strategies focus on increasing bone formation by inhibiting sclerostin with either antibodies or small molecules. Alternatively, interfering with transcription using antisense methods has become a common method in cell biological experiments, and efforts are being made to develop

these methods for use in the clinic. Antisense technology could therefore also be interesting in the regulation of sclerostin expression. In **Chapter 6** we investigated a novel method for the inhibition of *SOST* expression using antisense oligonucleotides (AONs). As described in detail in **Chapter 1**, AONs interfere with the splicing of a gene, leading to exclusion (skipping) of an exon from the mRNA. Depending on the exon that is skipped and its reading frame, this produces a truncated protein (out-of-frame skip) or a protein with a missing fragment (in-frame skip). As *SOST* contains only two exons, skipping of one of the exons would lead to a nonsense mRNA and obstruction of protein production. Examining 20 different AONs (both targeting *SOST* and control) did not reveal decreased *SOST* expression with any of them. In fact, several AONs increased *SOST* expression. The mechanism behind this increase is not clear, but we hypothesize that this might be due to binding of the AONs to sclerostin, triggering a compensational mechanism. Investigating the mechanism that increases *SOST* expression further may be of therapeutical interest, not to patients with osteoporosis, but instead to those with high bone mass diseases.

As bone mass is a balance between formation and resorption, therapeutic efforts could focus on either or both of these. Most available therapeutics are anti-resorptive and prevent further loss of bone mass. A relatively new anti-resorptive drug, Denosumab, targets RANKL in the RANK/RANKL/OPG pathway. This pathway is critical in the development of osteoclasts, and the anti-RANKL antibody therefore leads to a decrease in osteoclast differentiation and resorption. Denosumab showed substantial improvements in BMD and fracture risk in postmenopausal women with osteoporosis [24, 25]. In **Chapter 6** we included exon skipping of *Rank* for the decrease of resorption. Exon skipping of the membrane-binding domain of *Rank* has the added benefit that the resulting protein resembles osteoprotegerin (OPG), a decoy receptor that has an inhibitory effect on bone resorption due to reduced osteoclast differentiation. Therefore not only will *Rank* be inactivated, but a protein is formed that has an extra inhibitory effect. Unfortunately, while exon skipping was shown in several experiments, further research is required to optimize the efficiency. Only then can a biological effect be expected.

Discovering compounds that induce an increase in bone mass and strength in patients with osteoporosis would greatly improve current therapeutic options. High-throughput screening methods for relevant parameters are needed to efficiently

investigate potential candidates. For osteoblast differentiation, alkaline phosphatase (ALP) or Runx2 activity are often used as early differentiation markers. For later differentiation stages osteocalcin or sclerostin expression can be measured by RT-PCR. However, mineralization is the final and probably most fundamental step in bone formation and should therefore be the readout of choice. To provide an easy and scalable method for quantification of *in vitro* mineralization, **Chapter 7** describes a new method using fluorescent compounds Bonetag 800 and Osteosense 800. The results obtained with this method have been compared to the commonly used Alizarin Red S staining [26], and were confirmed to correlate with this method. In addition, fluorescence was specific for mineralized nodules and even seemed to be more sensitive to small changes in mineralization. Other advantages of this fluorescent method include a fast analysis, few handling or washing steps, and a readily quantifiable result.

Future perspectives of therapeutic strategies

A number of therapies have been approved for treatment of osteoporosis. Most therapies involve a decrease in bone resorption, and in this class bisphosphonates are most frequently prescribed. New therapeutic strategies that aim to increase bone formation and thereby restore bone mass, mainly focus on sclerostin as a target because of the favorable characteristics, such as its restricted expression pattern. Neutralizing antibodies against sclerostin have been shown effective in prevention of osteoporotic fractures and are in late stage clinical trials ([27] for results of the phase II trial; phase III trials NCT01575834 and NCT01631214 on www.clinicaltrials.gov), and small molecule inhibitors of sclerostin are in pre-clinical stages (www.osteogenex.com). The aim of this thesis was to increase knowledge of this interesting target and explore other therapeutic options. We therefore investigated the regulation of sclerostin expression in patients and *in vitro*, and the modulation of splicing using AONs. Modified AONs are a promising class of therapeutics, and many insights have been gained from the AONs used for exon skipping in patients with Duchenne muscular dystrophy (DMD). In DMD, affected muscle cells are often damaged and have leaky membranes through which AONs can easily pass [28-30]. Bone cells in patients with osteoporosis do not have this advantage. In addition, bone cells are already more difficult to reach for any compound since bone tissues

have less vasculature than muscle. Coupling AONs to specific peptides may enhance cellular uptake and targeting to certain tissues or cells [31]. Local delivery would also decrease potential systemic side effects. However, peptides may have effects of their own, leading to unexpected results or even toxicity. Indeed, clinical development of a peptide-coupled phosphorodiamidate morpholino oligomer (PMO) AON for treatment of DMD (AVI-5038) was discontinued after unexpected toxic effects were seen when high doses were administered to primates [32]. For osteoporosis, the class of bisphosphonates would be a good candidate for targeting of AONs. Bisphosphonates bind strongly to the hydroxyapatite in bone, and are therefore quickly cleared from the circulation after administration [33]. Even so, this does not automatically result in a high uptake of the AON by bone cells, as the AON would be bound to the bone matrix. By coupling bisphosphonates to AONs with a cleavable link, the AONs could be released locally by enzymatic cleavage, for example during the bone resorption process. The bisphosphonates would in this case provide a dual effect as they would also retain the antiresorptive action for which they are already used in the clinic now.

Current therapies like bisphosphonates treat osteoporosis by arresting bone resorption, but do not restore bone mass to a healthy and strong level. Drugs that stimulate bone formation would therefore be a valuable addition. This may be achieved by inhibiting sclerostin, whether by neutralizing antibodies, small molecules, modulation of gene regulation, or antisense technology. This thesis describes the development of a new quantification method for *in vitro* mineralization, which can facilitate high-throughput screening of new therapeutic compounds, the exploration of a new method of modulating expression of sclerostin, and studies which add to the knowledge of clinical significance and regulation of this protein.

References

1. Balemans W, Ebeling M, Patel N, van Hul E, Olson P, Dioszegi M *et al.* Increased bone density in sclerosteosis is due to the deficiency of a novel secreted protein (SOST). *Hum Mol Genet* 2001;10:537-43.
2. Brunkow ME, Gardner JC, van Ness J, Paeper BW, Kovacevich BR, Proll S *et al.* Bone dysplasia sclerosteosis results from loss of the *SOST* gene product, a novel cystine knot-containing protein. *Am J Hum Genet* 2001;68:577-89.
3. Gardner JC, van Bezooijen RL, Mervis B, Hamdy NA, Löwik CWGM, Hamersma H *et al.* Bone mineral density in sclerosteosis; affected individuals and gene carriers. *J Clin Endocrinol Metab* 2005;90:6392-5.
4. Hamersma H, Gardner J, Beighton P. The natural history of sclerosteosis. *Clin Genet* 2003;63:192-7.
5. Leupin O, Piters E, Halleux C, Hu S, Kramer I, Morvan F *et al.* Bone overgrowth-associated mutations in the *LRP4* gene impair sclerostin facilitator function. *J Biol Chem* 2011;286:19489-500.
6. Bafico A, Liu G, Yaniv A, Gazit A, Aaronson SA. Novel mechanism of Wnt signalling inhibition mediated by Dickkopf-1 interaction with LRP6/Arrow. *Nat Cell Biol* 2001;3:683-6.
7. Mao B, Wu W, Davidson G, Marhold J, Li M, Mechler BM *et al.* Kremen proteins are Dickkopf receptors that regulate Wnt/beta-catenin signalling. *Nature* 2002;417:664-7.
8. Ke HZ, Richards WG, Li X, Ominsky MS. Sclerostin and Dickkopf-1 as therapeutic targets in bone diseases. *Endocr Rev* 2012;33:747-83.
9. Mukhopadhyay M, Shtrom S, Rodriguez-Esteban C, Chen L, Tsukui T, Gomer L *et al.* Dickkopf1 is required for embryonic head induction and limb morphogenesis in the mouse. *Dev Cell* 2001;1:423-34.
10. Li X, Ominsky MS, Niu QT, Sun N, Daugherty B, D'Agostin D *et al.* Targeted deletion of the sclerostin gene in mice results in increased bone formation and bone strength. *J Bone Miner Res* 2008;23:860-9.
11. Balemans W, Ebeling M, Patel N, van Hul E, Olson P, Dioszegi M *et al.* Increased bone density in sclerosteosis is due to the deficiency of a novel secreted protein (SOST). *Hum Mol Genet* 2001;10:537-43.
12. Brunkow ME, Gardner JC, van Ness J, Paeper BW, Kovacevich BR, Proll S *et al.* Bone dysplasia sclerosteosis results from loss of the *SOST* gene product, a novel cystine knot-containing protein. *Am J Hum Genet* 2001;68:577-89.
13. Veverka V, Henry AJ, Slocombe PM, Ventom A, Mulloy B, Muskett FW *et al.* Characterization of the structural features and interactions of sclerostin: molecular insight into a key regulator of Wnt-mediated bone formation. *J Biol Chem* 2009;284:10890-900.
14. Weidauer SE, Schmieder P, Beerbaum M, Schmitz W, Oschkinat H, Mueller TD. NMR structure of the Wnt modulator protein Sclerostin. *Biochem Biophys Res Commun* 2009;380:160-5.
15. Vitt UA, Hsu SY, Hsueh AJ. Evolution and classification of cystine knot-containing hormones and related extracellular signaling molecules. *Mol Endocrinol* 2001;15:681-94.
16. Hoeflich KP, Luo J, Rubie EA, Tsao MS, Jin O, Woodgett JR. Requirement for glycogen synthase kinase-3beta in cell survival and NF-kappaB activation. *Nature* 2000;406:86-90.

17. Liu KJ, Arron JR, Stankunas K, Crabtree GR, Longaker MT. Chemical rescue of cleft palate and midline defects in conditional GSK-3beta mice. *Nature* 2007;446:79-82.
18. Kugimiya F, Kawaguchi H, Ohba S, Kawamura N, Hirata M, Chikuda H *et al.* GSK-3beta controls osteogenesis through regulating Runx2 activity. *PLoS One* 2007;2:e837.
19. Arioka M, Takahashi-Yanaga F, Sasaki M, Yoshihara T, Morimoto S, Takashima A *et al.* Acceleration of bone development and regeneration through the Wnt/beta-catenin signaling pathway in mice heterozygously deficient for GSK-3beta. *Biochem Biophys Res Commun* 2013;440:677-82.
20. Patel S, Doble B, Woodgett JR. Glycogen synthase kinase-3 in insulin and Wnt signalling: a double-edged sword? *Biochem Soc Trans* 2004;32:803-8.
21. Akune T, Ogata N, Hoshi K, Kubota N, Terauchi Y, Tobe K *et al.* Insulin receptor substrate-2 maintains predominance of anabolic function over catabolic function of osteoblasts. *J Cell Biol* 2002;159:147-56.
22. Krishnan V, Bryant HU, MacDougald OA. Regulation of bone mass by Wnt signaling. *J Clin Invest* 2006;116:1202-9.
23. Ding VW, Chen RH, McCormick F. Differential regulation of glycogen synthase kinase 3beta by insulin and Wnt signaling. *J Biol Chem* 2000;275:32475-81.
24. Papapoulos SE, Chapurlat R, Libanati C, Brandi ML, Brown JP, Czerwinski E *et al.* Five years of denosumab exposure in women with postmenopausal osteoporosis: results from the first two years of the FREEDOM extension. *J Bone Miner Res* 2012;27:694-701.
25. Cummings SR, San MJ, McClung MR, Siris ES, Eastell R, Reid IR *et al.* Denosumab for prevention of fractures in postmenopausal women with osteoporosis. *N Engl J Med* 2009;361:756-65.
26. Puchtler H, Meloan SN, Terry MS. On the history and mechanism of alizarin and alizarin red S stains for calcium. *J Histochem Cytochem* 1969;17:110-24.
27. McClung MR, Grauer A, Boonen S, Bolognese MA, Brown JP, Diez-Perez A *et al.* Romosozumab in postmenopausal women with low bone mineral density. *N Engl J Med* 2014;370:412-20.
28. Alter J, Lou F, Rabinowitz A, Yin H, Rosenfeld J, Wilton SD *et al.* Systemic delivery of morpholino oligonucleotide restores dystrophin expression bodywide and improves dystrophic pathology. *Nat Med* 2006;12:175-7.
29. Heemskerk H, de Winter C, van Kuik P, Heuvelmans N, Sabatelli P, Rimessi P *et al.* Preclinical PK and PD studies on 2'-O-methyl-phosphorothioate RNA antisense oligonucleotides in the mdx mouse model. *Mol Ther* 2010;18:1210-7.
30. Heemskerk HA, de Winter CL, de Kimpe SJ, van Kuik-Romeijn P, Heuvelmans N, Platenburg GJ *et al.* *In vivo* comparison of 2'-O-methyl phosphorothioate and morpholino antisense oligonucleotides for Duchenne muscular dystrophy exon skipping. *J Gene Med* 2009;11:257-66.
31. Tung CH, Stein S. Preparation and applications of peptide-oligonucleotide conjugates. *Bioconjug Chem* 2000;11:605-18.
32. Moulton HM, Moulton JD. Morpholinos and their peptide conjugates: therapeutic promise and challenge for Duchenne muscular dystrophy. *Biochim Biophys Acta* 2010;1798:2296-303.
33. Cremers SC, Pillai G, Papapoulos SE. Pharmacokinetics/pharmacodynamics of bisphosphonates: use for optimisation of intermittent therapy for osteoporosis. *Clin Pharmacokinet* 2005;44:551-70.



Summary
Nederlandse samenvatting
Curriculum vitae

Summary

The skeleton has many different functions. It gives structure to the body, provides protection to vital organs and the bone marrow, serves as a reservoir for minerals and facilitates movement by providing anchor points for muscles. Bone is a living tissue that is constantly formed, resorbed and reformed by the bone cells: osteoblasts, osteoclasts and osteocytes. During the process of remodeling, osteoclasts resorb the bone matrix and new matrix is formed by osteoblasts. Some osteoblasts become trapped in the newly formed bone and differentiate into osteocytes. The osteocytes are connected to each other and to the cells on the bone surface by long cellular processes and are therefore in a perfect position to sense changes in the bone, for example loading. The osteocytes secrete factors to signal instructions to the osteoblasts and osteoclasts to react to these changes. In addition, osteoblasts and osteoclasts also produce signals and can react to some systemic hormones, which results in a complicated and not yet fully defined regulatory network that maintains the bone tissue. In **Chapter 1** some important factors in the regulation of bone metabolism are discussed.

Normally, there is a balance between resorption and formation and a constant bone mass. An imbalance can lead to an increase or decrease in bone mass, and diseases such as osteoporosis. Osteoporosis is the most common skeletal disease and is characterized by low bone mass and loss of internal bone structure. This leads to decreased bone strength and increased risk of fracture, particularly in the spine, hip and wrist. Elderly women are most at risk because bone resorption is accelerated after menopause due to the loss of estrogen production. Treatment for osteoporosis usually consists of bisphosphonates that specifically inhibit osteoclasts and therefore slow down bone resorption and disease progression. Unfortunately, bisphosphonates do not rebuild the bone to a healthy bone mass, and life-long treatment is therefore required. Other drugs are available or will probably become available in the coming years, but the ideal therapy has not yet been found and further research into the mechanisms of bone metabolism and possible therapeutic strategies is necessary.

Chapter 2 gives an overview of current knowledge on sclerostin. Sclerostin is a protein that is produced by osteocytes in mineralized bone matrix and inhibits bone formation through inhibiting Wnt signaling. It is produced by the *SOST* gene. Mutations in *SOST* or the surrounding regulatory regions and loss of



sclerostin production lead to increased bone formation. Patients with sclerosteosis or Van Buchem disease for example can present with a bone mass that is up to 11 standard deviations above normal with consequent problems such as facial paralysis and hearing loss due to facial nerve entrapment. Interestingly, the bone of these individuals is of very good quality and even heterozygous carriers of mutations in *SOST* have consistently higher bone mass than control subjects. This suggests a gene-dose effect in which a lower sclerostin production is associated with a higher bone mass. Since sclerostin is expressed specifically in osteocytes, targeting this protein in future therapies is expected to result in few side-effects. In addition, the gene-dose effect indicates that even small changes in sclerostin production could have a positive effect in patients with osteoporosis. Sclerostin is therefore one of the most interesting targets for new treatment options for osteoporosis.

Sclerostin can be measured in serum samples, and many studies have investigated serum levels in normal individuals and patients with different diseases. In patients with sclerosteosis, who have an inactivating mutation in the *SOST* gene, no sclerostin was found. Van Buchem disease is caused by a mutation in a regulatory region downstream of *SOST* and the disease is usually less severe than sclerosteosis. In accordance with this, small amounts of sclerostin were found in patients with Van Buchem disease. Dickkopf 1 (DKK1) is a protein that, like sclerostin, inhibits Wnt signaling. In **Chapter 3** we found that DKK1 was increased in serum samples from patients with sclerosteosis and Van Buchem disease. DKK1 may be increased in an effort to compensate for the lack of sclerostin in these patients. However, the increase seems to be insufficient to protect against excessive bone formation.

New mutations that result in bone phenotypes can increase knowledge on the physiological actions of the involved protein. In **Chapter 4** we described a novel mutation in sclerostin after analysis of two siblings from Turkey with classic sclerosteosis characteristics. This cysteine to arginine mutation affected the last cysteine residue of the cystine-knot motif and loss of this residue probably leads to impaired folding of the protein and retention in the endoplasmic reticulum. In addition, the mutation resulted in a significantly reduced ability to bind the Wnt co-receptor LRP5. Together, this caused a complete loss of sclerostin function and a sclerosteosis phenotype.

By understanding the endogenous regulatory mechanisms that control *SOST*

expression, we may eventually be able to specifically target and modulate these mechanisms in patients with osteoporosis to increase bone formation with minimal side-effects. In **Chapter 5** we investigated the regulation of *SOST* by modulating the activity of the Wnt signaling pathway. *SOST* appeared to be downregulated by increased Wnt signaling activity. It was strongly decreased by GIN, which inhibits the downstream glycogen synthase kinase 3 beta (GSK3 β) enzyme and thereby increases Wnt signaling activity. However, several Wnt signaling inhibitors that work at different stages in the pathway could not abrogate the decrease in *SOST* expression. In addition, directly blocking Wnt target gene transcription had no effect on the expression of *SOST* after treatment with GIN. It seems therefore that the decrease in *SOST* expression is not mediated by Wnt/ β -catenin signaling, but via a different effect of GSK3 β .

While interfering with endogenous regulation of sclerostin expression is an interesting therapeutic option, other methods are being investigated to block the effect of the protein. In **Chapter 6** we investigated a novel method for the inhibition of *SOST* expression using antisense oligonucleotides (AONs). As described in detail in **Chapter 1**, AONs interfere with the splicing of a gene, leading to exclusion (skipping) of an exon from the messenger RNA (mRNA). As *SOST* contains only two exons, skipping of one of the exons would lead to a nonsense mRNA and obstruction of protein production. Unfortunately, examining 20 different AONs (both targeting *SOST* and control) did not reveal decreased *SOST* expression with one of them. A second target that was investigated in **Chapter 6** is *Rank*, which is essential in the differentiation of osteoclasts. Exon skipping of the membrane-binding domain of *Rank* has the added benefit that the resulting protein is a protein that resembles osteoprotegerin, a decoy receptor that has an inhibitory effect on bone resorption due to reduced osteoclast differentiation. Therefore not only will *Rank* be inactivated, but a protein is formed that has an extra inhibitory effect. While exon skipping was shown in several experiments, further research is required to optimize the efficiency. Only then can a biological effect be expected.

Discovering compounds that induce an increase in bone mass and strength in patients with osteoporosis would greatly improve current therapeutic options. High-throughput screening methods for relevant parameters are needed to efficiently investigate potential candidates. Mineralization is the final and probably most

fundamental step in bone formation and should therefore be the readout of choice. To provide an easy and scalable method for quantification of *in vitro* mineralization, **Chapter 7** describes a new method using fluorescent compounds Bonetag 800 and Osteosense 800. The results obtained with this method have been compared to the commonly used Alizarin Red S staining, and were confirmed to correlate with this method.

Current therapies like bisphosphonates treat osteoporosis by arresting bone resorption, but do not restore bone mass to a healthy and strong level. Drugs that stimulate bone formation would therefore be a valuable addition. In **Chapter 8** the results of this thesis are discussed in relation to current knowledge on bone metabolism and therapeutic strategies for the treatment of osteoporosis.

Samenvatting

Het skelet heeft verschillende functies. Zo geeft het vorm aan het lichaam, beschermt het vitale organen en het beenmerg, is een reservoir voor mineralen en geeft een aanknopingspunt voor spieren zodat bewegen mogelijk wordt. Het bot is een levend weefsel dat voortdurend wordt aangemaakt en afgebroken (geresorbeerd) door botcellen: de osteoblasten, osteoclasten en osteocyten. Osteoclasten resorberen het bot, waarna osteoblasten nieuwe botmatrix vormen. Sommige osteoblasten blijven tijdens het vormen van bot in de matrix zitten, waar ze differentiëren tot osteocyten. Osteocyten zijn met elkaar en de cellen op het oppervlak verbonden via kanaaltjes, waardoor ze veranderingen in het bot (zoals belasting) goed kunnen voelen. Als gevolg hiervan scheiden osteocyten factoren uit waarop de osteoblasten en osteoclasten reageren. Deze worden daarnaast ook beïnvloed door sommige hormonen. Bij elkaar resulteert dit in een ingewikkeld en nog niet volledig begrepen systeem dat het botmetabolisme regelt. In **Hoofdstuk 1** wordt een aantal belangrijke factoren besproken.

In gezonde personen is er een balans tussen aanmaak en afbraak van bot, zodat de botmassa gelijk blijft. Een verstoring van deze balans kan leiden tot een hogere of lagere botmassa, en ziekten zoals osteoporose. Osteoporose is de meest voorkomende ziekte van het skelet en wordt gekenmerkt door een lage botmassa en verlies van stevigheid en interne structuur. Hierdoor breken mensen met osteoporose sneller botten, vooral in de pols, heup en wervels. Oudere vrouwen hebben het hoogste risico op osteoporose omdat tijdens de menopauze de productie van oestrogeen vermindert en hierdoor de botafbraak snel toeneemt. Behandeling van osteoporose gebeurt meestal met bisfosfonaten. Deze medicijnen onderdrukken de botafbraak doordat ze specifiek de activiteit van osteoclasten remmen. Hierdoor remmen ze de progressie van de ziekte en brengen lichte verbetering, maar bisfosfonaten kunnen de botmassa niet terugbrengen naar een gezonde sterkte. Daarom moeten patiënten vaak levenslang behandeld worden. Er zijn andere medicijnen op de markt, en enkele andere komen hoogstwaarschijnlijk in de komende jaren beschikbaar, maar de ideale therapie is nog niet gevonden. Meer kennis over botmetabolisme en mogelijke nieuwe therapieën is daarom nodig.

Hoofdstuk 2 geeft een overzicht van de huidige kennis over sclerostin. Sclerostin is een eiwit dat de botvorming remt en gemaakt wordt door osteocyten in

gemineraliseerde botmatrix. Dit doet het door het remmen van de Wnt signalering, een signaleringsroute die belangrijk is voor botvorming en differentiatie van osteoblasten. Het gen dat codeert voor sclerostin is *SOST*. Mutaties in *SOST* of in de regio's rond het gen die de expressie reguleren kunnen leiden tot verminderde of ontbrekende productie van sclerostin en een verhoogde botmassa. Patiënten met sclerosteose of de ziekte van Van Buchem hebben een zeer sterk verhoogde botmassa. Zij hebben daardoor problemen zoals verlamming van de gezichtsspieren of doofheid door beknelling van de gezichtszenerven. Draggers van deze ziekten hebben geen complicaties, maar wel een verhoogde botmassa vergeleken met controlepersonen. Het bot is van goede kwaliteit en structuur, en zowel patiënten als dragers lijken dan ook goed bestand tegen botbreuken. Dit wijst op een dosis-afhankelijk effect waarbij een lagere productie van sclerostin verband houdt met een hogere botmassa. Omdat sclerostin specifiek gemaakt wordt in osteocyten, worden bij medicijnen die zich richten op dit eiwit weinig bijwerkingen in andere organen verwacht. Bovendien betekent een dosis-afhankelijk effect dat kleine veranderingen in sclerostin productie al een positief effect kunnen hebben bij patiënten met osteoporose. Sclerostin is daarom een van de meest aantrekkelijke aanknopingspunten voor nieuwe therapieën voor osteoporose.

Sclerostin kan worden gemeten in serum, en er zijn veel studies gedaan naar de concentraties in serum van zowel controlepersonen als patiënten met verschillende ziekten. Patiënten met sclerosteose hebben een inactiverende mutatie in *SOST*, en in hun serum is dan ook geen sclerostin gevonden. In patiënten met Van Buchem ziekte werden kleine hoeveelheden sclerostin gevonden. Van Buchem ziekte wordt veroorzaakt door een mutatie in een regulerende regio buiten het coderende deel van *SOST* en de symptomen zijn meestal minder ernstig dan bij sclerosteose. Dickkopf 1 (*DKK1*) is een eiwit dat, net als sclerostin, de Wnt signalering remt. In **Hoofdstuk 3** vonden we dat *DKK1* in serum monsters van mensen met sclerosteose en Van Buchem ziekte verhoogd is. Mogelijk gebeurt dit om te compenseren voor het tekort aan sclerostin. De sterk verhoogde botmassa in deze patiënten suggereert echter dat de verhoging van *DKK1* niet voldoende is om sclerostin te compenseren.

Nieuwe mutaties die botfenotypes tot gevolg hebben kunnen de kennis van de fysiologische werking van het gemuteerde eiwit vergroten. In **Hoofdstuk 4** beschrijven we een nieuwe mutatie in sclerostin na onderzoek van een broer en zus

met klassieke sclerosteose kenmerken. Deze mutatie heeft een aminozuurverandering tot gevolg waardoor een belangrijk onderdeel van de structuur van sclerostin, de cystine-knoop, niet goed gevormd wordt. Het eiwit wordt daardoor vastgehouden in het endoplasmatisch reticulum en niet uitgescheiden. Daarnaast laten we zien dat het gemuteerde eiwit niet goed kan binden aan de Wnt co-receptor LRP5, en dus zijn functie niet goed kan uitoefenen. Samen leiden deze veranderingen tot een totaal verlies van de functie van sclerostin en het sclerosteose fenotype.

Door het ontrafelen van de normale werking van regulatiemechanismen die *SOST* expressie controleren, hopen we uiteindelijk dit gen specifiek te kunnen aangrijpen en daardoor in patiënten met osteoporose de botmassa te verhogen met minimale bijwerkingen. In **Hoofdstuk 5** hebben we de regulatie van *SOST* onderzocht door de activiteit van de Wnt signaleringsroute te variëren. *SOST* expressie leek te worden verlaagd door verhoogde Wnt signalering activiteit, en sterk verlaagd door GIN. Dit is een remmer van glycogen synthase kinase 3 beta ($GSK3\beta$), en daarmee een activator van de Wnt signaleringsroute. Verschillende remmers van de Wnt signalering konden echter de verlaging in *SOST* expressie door GIN niet opheffen. Bovendien had het rechtstreeks blokkeren van transcriptie van de Wnt signalerings targetgenen geen effect op *SOST* expressie. De verlaging van *SOST* expressie lijkt daarom niet veroorzaakt door Wnt signalering, maar door een ander effect van $GSK3\beta$.

Naast het moduleren van de endogene regulatie van sclerostin expressie worden andere methoden onderzocht om het effect van het eiwit te blokkeren. In **Hoofdstuk 6** hebben we een nieuwe methode voor het remmen van *SOST* expressie onderzocht met antisense oligonucleotiden (AONs). Zoals uitgebreid beschreven in **Hoofdstuk 1** verstoren AONs de zogenaamde splicing van een gen. Een gen bestaat uit exonen (coderende stukken) en intronen (niet-coderend), en tijdens splicing worden de exonen aan elkaar geplakt en de intronen weggegooid, waarbij het messenger RNA (mRNA) gevormd wordt. AONs kunnen ervoor zorgen dat een exon niet herkend wordt, en dus overgeslagen tijdens het vormen van mRNA (een exon skip). Omdat *SOST* maar twee exonen heeft, betekent het skippen van een van deze exonen dat er geen eiwitproductie plaats zal vinden. Van de 20 onderzochte AONs (zowel controle als specifiek gemaakt voor *SOST*) bleek helaas geen enkele de *SOST* expressie te verlagen. Een tweede gen waarop exon skipping in **Hoofdstuk 6** onderzocht werd

is *Rank*. Het eiwit dat door dit gen gemaakt wordt is essentieel voor de differentiatie van osteoclasten. Exon skipping van het membraangebonden deel van *Rank* heeft als extra voordeel dat een eiwit gevormd wordt dat lijkt op osteoprotegerin (OPG), een soort dummy-receptor die de osteoclastdifferentiatie en daardoor de botafbraak remt. Hierdoor wordt niet alleen de functie van *Rank* geïnactiveerd, maar wordt gelijktijdig een eiwit gevormd dat een extra positief effect heeft. Hoewel we in enkele experimenten exon skipping hebben aangetoond, is verder onderzoek nodig om de efficiëntie te optimaliseren. Pas dan kan een biologisch effect verwacht worden.

Het ontdekken van stoffen die een verhoging van de botmassa en –sterkte kunnen veroorzaken in patiënten met osteoporose zou een enorme vooruitgang voor de huidige therapie betekenen. Voor het onderzoeken van potentiële kandidaten zijn nieuwe screeningsmethoden voor relevante parameters en met een grote capaciteit nodig. Mineralisatie is de laatste en waarschijnlijk meest belangrijke stap in de botformatie en heeft daarom de voorkeur als uitleesparameter. **Hoofdstuk 7** beschrijft de ontwikkeling van een makkelijke en opschaalbare methode voor het kwantificeren van de mineralisatie in *in vitro* celkweken. Hierbij worden de fluorescente stoffen Bonetag 800 en Osteosense 800 gebruikt. De resultaten van deze methode zijn vergeleken met de veelgebruikte Alizarine Rood S kleuring en we hebben aangetoond dat de nieuwe methode hiermee correleert.

De huidige medicijnen voor osteoporose zoals bisfosfonaten werken door het remmen van de botafbraak, maar kunnen het bot niet herstellen naar een gezond niveau. Geneesmiddelen die de botvorming stimuleren zouden een waardevolle toevoeging zijn aan de huidige behandelmogelijkheden. In **Hoofdstuk 8** worden de resultaten van dit proefschrift bediscussieerd in relatie tot de huidige kennis van botmetabolisme en strategieën voor behandeling van osteoporose.

Curriculum vitae

Martiene Moester werd geboren op 28 juli 1983 in Leidschendam. Na het *cum laude* behalen van haar Gymnasium diploma aan de Dalton Scholengemeenschap in Voorburg in 2001, startte zij in datzelfde jaar met de studie Biomedische Wetenschappen aan de Universiteit van Leiden. Na het behalen van haar propedeuse studeerde zij in 2003 een semester aan het Karolinska Institutet in Stockholm, Zweden. Tijdens een bestuursjaar bij het studentenkoor en -orkest Collegium Musicum in 2004 behaalde zij haar Bachelordiploma *cum laude*. Hiervoor liep zij stage bij dr. D. Stepniak en prof. dr. F. Koning op de afdeling Immunohematologie van het Leids Universitair Medisch Centrum (LUMC) en deed onderzoek naar afbraakproducten van gluten.

Tijdens de onderzoeksmaster van Biomedische Wetenschappen in Leiden deed zij tevens een onderzoekstage bij dr. A.A.F. de Vries op de afdeling Moleculaire Celbiologie van het LUMC. Dit onderzoek was gericht op het produceren van lentivirussen voor het induceren van celdood in specifieke celtypes. Na haar afstudeeronderzoek bij Solvay Pharmaceuticals (het huidige Abbott) in Weesp op het gebied van biomarkers in traumatische hersenschade, behaalde zij in november 2007 haar Masterdiploma.

In januari 2008 begon zij als promovenda met haar promotieonderzoek bij de afdeling Endocrinologie van het LUMC onder supervisie van prof. dr. C.W.G.M. Löwik. Het promotieonderzoek waarvan de resultaten zijn beschreven in dit proefschrift werd afgerond in december 2012. Sinds 1 juli 2013 werkt Martiene als designer van onderzoeksdatabases in ProMISe bij Curium-LUMC en de sectie Advanced Datamanagement, onderdeel van de afdeling Medische Statistiek van het LUMC.